Title
Molecular Insights into the Structure and Function of the Telomerase Holoenzyme in Tetrahymena thermophila

Author
Upton, Heather

Publication Date
2016

Peer reviewed|Thesis/dissertation

Molecular Insights into the Structure and Function of the Telomerase Holoenzyme in *Tetrahymena thermophila*

By

Heather Upton

A dissertation submitted in partial satisfaction of the

requirements for the degree of

Doctor of Philosophy

in

Molecular and Cell Biology

in the

Graduate Division

of the

University of California, Berkeley

Committee in charge:

Professor Kathleen Collins, Chair
Professor Susan Marqusee
Professor Donald Rio
Professor Danica Chen

Spring 2016

ABSTRACT

Molecular Insights into the Structure and Function of the Telomerase Holoenzyme in *Tetrahymena thermophila*

By

Heather Upton

Doctor of Philosophy in Molecular and Cell Biology

University of California, Berkeley

Professor Kathleen Collins, Chair

Telomeres are specialized, G-rich simple-sequence repeats that cap the ends of linear chromosomes to prevent genome instability. These tandem DNA repeats are bound by sequence-specific proteins to create a protective structure that marks the chromosome end thereby preventing aberrant chromosomal recombination, resection, degradation, and fusion. Due to inherent limitations of genome replication and chromosome end processing, telomeres shorten over time leading to potential loss of genetic information if not restored or maintained. The ribonucleoprotein (RNP) telomerase functions in this regard by using an integral RNA template (TER) to synthesize single stranded telomeric repeats at the chromosome end. *In vitro* minimal catalytic activity can be reconstituted from the telomerase protein component TERT and TER; however, *in vivo* biologically active holoenzyme requires further protein components for repeat addition synthesis, enzyme recruitment, and regulation in the cell. The ciliate *Tetrahymena thermophila* serves as an experimentally favorable model system for the study of telomerase due high levels of constitutively active enzyme and robust molecular and genetic techniques. Furthermore, our understanding of the holoenzyme is arguably best characterized from the *Tetrahymena* enzyme, which consists of nine protein components and the RNA (TERT, TER, p65, p50, Teb1, Teb2, Teb3, p75, p45, and p19). Despite knowledge of the overall architecture, relationships between multiple proteins within the holoenzyme and their specific physiological roles had remained unresolved.

Using a variety of *in vitro* and *in vivo* biochemical techniques, I show that the holoenzyme component p50 functions as a central hub for enzyme assembly, connecting the RNP catalytic core to the RPA-like Teb1-Teb2-Teb3 (TEB) and p75-p45-p19 (CST) subcomplexes. To answer existing questions concerning telomerase recruitment, I employ endogenously tagged holoenzyme proteins to show that all telomerase holoenzyme subunits are subject to coordinate telomere recruitment and release dependent on the cell cycle. Using domain tagging and truncation strategies, I

demonstrate that the high-affinity single-stranded telomeric DNA binding component Teb1 is necessary and sufficient for interaction between telomerase and the telomere. This work supports a model for *Tetrahymena* telomerase-telomere recruitment that breaks the precedent established by studies in yeast and vertebrate cells: Teb1-containing holoenzyme is recruited directly to the telomeric DNA rather than telomerase recruitment by interaction with a telomere-bound protein. Together, along with ongoing studies of the *Tetrahymena* TEB and CST subcomplexes, these results suggest commonalities of telomerase interaction, action, and regulation at telomeres across species.

TABLE OF CONTENTS

LIST OF COMMONLY USED ABBREVIATIONS

dsDNA	Double stranded DNA
ssDNA	Single stranded DNA
A	Adenine
G	Guanine
C	Cytosine
T	Thymine
dGTP	Deoxyguanosine triphosphate
dTTP	Deoxythymidine triphosphate
rDNA	Ribosomal DNA
RAP	Repeat addition processivity
RNP	Ribonucleoprotein
TER	Telomerase RNA
TERT	Telomerase reverse transcriptase
TEN	TERT essential N-terminal domain
TRBD	TERT RNA binding domain
RT	TERT reverse transcriptase domain
CTE	TERT C-terminal extension
IFD	Insertion in fingers domain
CST	Ctc1/Cdc13-Stn1-Ten1
TEB	Teb1-Teb2-Teb3
pol α-primase	DNA polymerase α-primase
RPA	Replication Protein A
ZZ	Tandem Z domains of Staphylococcal protein A
F	3xFLAG sequence
His_6	6x histidine
OB	Oligonucleotide/oligosaccharide-binding
EM	Electron microscopy
RRL	Rabbit reticulocyte lysate
FL	Full-length
WT	Wild-type
ChIP	Chromatin Immunoprecipitation
RC	Reaction control

ACKNOWLEDGEMENTS

No man is an island. This phrase has never rung more true. Countless individuals have contributed to the making of this dissertation and you have my eternal gratitude. Your additions will never be forgotten.

I must mention several individuals by name. I am indebted to my advisor, Kathy Collins, for giving me the opportunity to modify my path in graduate school and try my hand at telomerase biochemistry. Her help, patience, and guidance over the years has been invaluable and she has my utmost respect as a scientist and mentor. Her lab has been a pleasure to work with due in no small part to phenomenal labmates and her charismatic leadership. I need to also offer my profound thanks to my thesis committee for their constructive feedback and support: Don Rio, Susan Marqusee, and Danica Chen. My comrades in the department (and outside it, both on campus and off) who made the unbearable parts of graduate school bearable are owed another heaping debt of gratitude for commisery, advice, and just general greatness. I must thank the members of my family for their unwavering support of my intellectual and academic pursuits - I know this has been a long road. My brother, Sean, and my parents, Adrienne and Bruce, have always encouraged my tenacity and curiosity, without which I doubt I would have made it this far. Finally, I owe so much to David Biswanger, who has been a true friend, understanding partner, and steadfast pillar of support. The things he has done for me - to help, surprise, encourage, and uplift me - go beyond what any person deserves.

CHAPTER ONE

Telomeres, Telomerase, and the Ciliate *Tetrahymena*

Introduction

In the 1930s, approximately twenty years before Watson and Crick described the double helix model for the structure of DNA, the natural ends of chromosomes piqued the interest of Hermann Muller at the University of Edinburgh and Barbara McClintock at the University of Missouri at Columbia. Muller and McClintock independently observed that the DNA at the chromosome end in fruit flies and maize, respectively, possessed an inherent ability to prevent chromosome end-to-end fusions (McClintock, 1931; Müller, 1938). By studying the fragmented chromosomes that resulted from X-ray exposure, both geneticists noted that chromosome breakage sites would frequently 'reattach' to other breakage sites but not the natural ends. In 1938, Muller first described the 'telomere,' derived from the Greek words for 'end' (*telos*) and 'part' (*meros*), as a terminal cap responsible for "sealing the end of the chromosome" (Müller, 1938). A year later, McClintock proposed that new and enduring telomeres can be actively formed at sites of chromosome breakage given a particular set of circumstances thereby hinting at a specialized, highly-regulated process yet to be understood (McClintock, 1939).

Telomeres and the end replication problem

Molecular advancements over the next 40 years established the structure of DNA and chromatin and the mechanism of DNA replication. Unexpectedly, these findings highlighted the rather large liability of linear chromosomes: during each round of DNA replication the chromosome ends are incompletely copied leading to sequence loss over time. This 'end-replication problem' is created by two inherent properties of the DNA-dependent DNA polymerases responsible for copying the genome. First, they are unable to initiate de novo DNA synthesis and consequently depend on the presence of an RNA primer. Second, nucleotide chain growth is unidirectional. Combined, these two shortcomings endanger genome integrity.

Briefly, during semiconservative DNA replication leading and lagging strand DNA synthesis occur in tandem as two distinct and harmonious modes. In leading strand synthesis, daughter strand growth proceeds processively in the direction of replication fork movement (5′ to 3′) (Waga & Stillman, 1998). Conversely, in lagging strand synthesis the new DNA is synthesized in the direction opposite replication fork movement (3′ to 5′) through the formation of discontinuous fragments (Okazaki fragments) that are eventually joined to produce a single strand. Each individual fragment requires the synthesis of a short RNA primer by the DNA polymerase α-primase complex (pol α-primase), which then transitions to DNA primer addition. The

RNA-DNA primer is further elongated by DNA polymerase δ, aided by proliferating-cell nuclear antigen and replication factor C, through the end of the Okazaki fragment. The RNA primers are excised, new DNA is synthesized, and the fragments are ligated to form a continuous daughter strand (Waga & Stillman, 1998). Excision of the 8-12 nucleotide RNA primer from the very 5′ end of the lagging strand leaves a gap that matches the requirements for the short 3′ overhang typically found at telomere ends, while the leading strand shortens with each round of replication resulting in sequence loss (Figure 1.1) (Levy, Allsopp, Futcher, Greider, & Harley, 1992; Soudet, Jolivet, & Teixeira, 2014; Waga & Stillman, 1998).

Several models were proposed to explain how nature solved the end replication problem. In 1972, Watson showed that T7 phage used concatemerization of linear DNA to eliminate ends by annealing short complementary sequences at the terminus of the chromosome followed by gap filling and length processing (Watson, 1972). In 1974, Thomas Cavalier-Smith suggested that the telomere was a string of repeating palindromic sequences that would fold back onto itself at the 3′ end providing the obligatory 3′ hydroxyl for DNA polymerase to fill in the gap on the opposite strand (Cavalier-Smith, 1974). In 1978 Elizabeth Blackburn and Joe Gall found that the telomere consisted of short, repetitive hexanucleotide sequences in the ciliate *Tetrahymena thermophila* (d[TTGGGG]•d[CCCCAA]) (E. H. Blackburn & Gall, 1978). They subsequently demonstrated that an exogenous, linear DNA externally flanked by the ciliate telomeric sequence was retained by budding yeast cells and eventually lengthened with the yeasts own telomeric repeats (Shampay, Szostak, & Blackburn, 1984; Szostak & Blackburn, 1982). This finding suggested a 'terminal transferase-like enzyme' that extended telomeric DNA through repeat addition to compensate for incomplete end replication (Shampay et al., 1984).

Activity from the anticipated enzyme was visualized in late 1984 when Carol Greider, a graduate student in the Blackburn Lab, demonstrated that when given a high concentration of telomeric oligonucleotide $(TTGGGG)_4$ and radiolabeled dGTP, *Tetrahymena* cell extract yielded product with a six-base periodicity when separated on a denaturing gel (Greider & Blackburn, 1985). The question remained whether this was a novel enzyme or a previously identified DNA polymerase with the ability to use the added primer to copy endogenous telomere repeats naturally present in the cell extract. Using an experiment similar to that performed by Blackburn and Gall with yeast telomeres, Greider again added radiolabeled dGTP and a 24-base oligonucleotide comprised of the yeast telomere sequence (unrelated to the *Tetrahymena* telomere sequence) with TGGG at the 3′ end to the *Tetrahymena* cell extract. The results were twofold: (1) the yeast telomere was a suitable substrate for extension in extract and (2) the banding pattern visualized by gel suggested synthesis of the endogenous TTGGGG hexanucleotide repeats by the *Tetrahymena* enzyme. This provided compelling evidence for the presence of a telomere-specific terminal transferase, later called telomerase (Greider & Blackburn, 1985). Shortly thereafter while investigating the question of

enzyme specificity, Greider and Blackburn demonstrated the presence of an essential RNA component critical for telomerase activity (Greider & Blackburn, 1987; Greider & Blackburn, 1989).

We now know that telomerase counterbalances incomplete terminal synthesis during replication as it catalyzes telomeric DNA repeat addition at the chromosome termini (Gilson & Geli, 2007). Moreover, these telomeres serve as protective end 'caps' that differentiate natural chromosome ends from double-stranded DNA (dsDNA) breaks to block chromosomal fusions and evade recognition by the DNA damage machinery (Verdun & Karlseder, 2007). Telomeric DNA in most organisms consists of tandem arrays of short double-stranded repetitive sequences with one guanine-rich strand (the G-strand) and one cytosine-rich strand (the C-strand) synthesized as the leading and lagging strands, respectively. The length of this double-stranded telomeric region varies according to species, from 350 base pairs in yeast to 20 kilobase pairs in humans (Chakhparonian & Wellinger, 2003). The extreme terminus of the G-strand exists as a single-stranded extension up to 200 nucleotides in length, producing a 3' overhang commonly referred to as the G-tail. These overhangs are highly conserved and a characteristic feature of telomeres. Structurally, they have been shown to invade the telomeric dsDNA region, base pairing with the complementary strand to produce a lasso-like structure (known as a telomeric- or T-loop). This structure is thought to help conceal the DNA terminus from the dsDNA break repair machinery in addition to restricting access by telomerase (Chakhparonian & Wellinger, 2003).

As alluded to above, loss of telomere function has a wide range of consequences in the model organisms studied to date including shortening or loss of the G-tail, C-strand resection, altered gene-expression profiles, chromosome fusions, increased recombination at chromosome termini, genome instability, growth arrest and cell death (Verdun & Karlseder, 2007). Many of these cellular changes have been associated with driving tumorigenic processes and are hallmarks of a growing number of impaired telomere maintenance syndromes in humans (known as telomeropathies or telomere disorders), underscoring the importance of broadening our understanding of telomerase and telomere biology (Holohan, Wright, & Shay, 2014). Generally, our understanding of telomerase and telomere structure and function has been expanded from investigations in a wide variety of organisms (the yeasts *Kluyveromyces lactis*, *Schizosaccharomyces pombe*, and *Saccharomyces cerevisiae*; the ciliates *T. thermophila*, *Oxytricha nova*, and *Euplotes crassus*; and human and mouse tumor cell lines) for historical or methodological reasons; however, human embryonic stem cells are becoming an attractive model with the development of reliable genome editing technologies. While the importance of each of these systems to the field cannot be understated, the following discussion of telomerase activity, structure, and the telomere will be limited to knowledge gained from the ciliate *T. thermophila*, the yeasts *S. cerevisiae*, and *S. pombe*, and vertebrate cells.

The telomerase core and its catalytic cycle

The ribonucleoprotein (RNP) telomerase evolved as a specialized RNA-dependent DNA polymerase, ultimately owing its unique ability to extend the 3′ chromosomal ends with short, tandem G-rich repeats to the presence of an integral telomerase RNA (TER) (Greider & Blackburn, 1987). This RNA provides the template for telomeric repeat addition catalyzed by the telomerase reverse transcriptase protein component, TERT, in addition to functioning as a scaffold for TERT folding and enzymatic activity. Together, TERT and TER represent the minimal components required for *in vitro* activity and are known as the minimal recombinant RNP (Blackburn & Collins, 2011; Hengesbach, Akiyama, & Stone, 2011). Biologically active telomerase holoenzymes contain the catalytic core along with a variable number of telomerase-associated proteins that are vital for biogenesis, localization, and regulation but dispensable for telomerase activity (discussed below) (Egan & Collins, 2010; Fu & Collins, 2003; Kiss, Fayet-Lebaron, & Jady, 2010; Venteicher et al., 2009).

Unlike conventional reverse transcriptases where the associated RNA only serves as a template for reverse transcription, TER sustains multiple roles in telomerase activity, stability, biogenesis, and regulation (Egan & Collins, 2012). All known TERs share a set of crucial structural elements implicated in telomerase activity, including a telomere-complementary template, a pseudoknot (PK), and a stem-loop moiety. Vertebrate TERs contain an additional hairpin-hinge-hairpin - ACA (H/ACA) domain with homology to small nucleolar (sno) and small Cajal body-specific (sca) RNAs that bind H/ACA scaRNA proteins to target telomerase to the Cajal bodies. Despite these conserved elements, there is a remarkable degree of divergence in size, sequence, and structure along phylogenetic lineages, which has been linked to a multitude of species-specific TER-binding proteins (Egan & Collins, 2012).

The telomerase protein subunit TERT is conserved among species with telomerase and consists of four structural and functional domains: the TERT essential N-terminal (TEN) domain, the high-affinity TERT RNA-binding domain (TRBD), the reverse transcriptase (RT) domain, and the C-terminal extension (CTE) (Figure 1.2). The RT confers the enzymes capacity for RNA-directed DNA polymerization and is primarily comprised of motifs and subdomains that are common to all RTs (Lingner et al., 1997). Notably, the TERT RT domain differentiates itself from other RTs through a large insertion within the conserved fingers subdomain (insertion in fingers domain or IFD) and motif 3, which influence repeat addition processivity (RAP) (Lue, Lin, & Mian, 2003; Xie, Podlevsky, Qi, Bley, & Chen, 2010). Intramolecular interdomain interactions between the CTE and the TRBD constrain the TERT TRBD-RT-CTE domains into a ring in contrast to the horseshoe shape of conventional RTs (Bley et al., 2011; Gillis, Schuller, & Skordalakes, 2008). Extensive biochemical characterization of the telomerase-specific domains has shown that the TEN domain is indispensible to RAP by increasing use of the DNA-template hybrid in the active site, the TRBD is essential for RNP assembly,

and the CTE influences DNA binding and activity (Hossain, Singh, & Lue, 2002; Huard, Moriarty, & Autexier, 2003; Moriarty, Marie-Egyptienne, & Autexier, 2004; Wu & Collins, 2014).

The specialized process by which telomerase adds multiple repeats to a substrate necessitates a two phase catalytic cycle consisting of single repeat addition to the substrate DNA and recycling of the internal RNA template for processive repeat synthesis. (Brown, Podlevsky, & Chen, 2014). The telomerase catalytic cycle begins when the 5′ end of the telomerase RNA template base-pairs with the 3′ end of a telomeric DNA primer to produce an RNA/DNA hybrid. The active site reverse transcribes the remainder of the template sequence onto the 3′ end of the DNA primer. Once a single repeat has been synthesized at the primer 3′ end, the template must dissociate from the product and be repositioned for another round of repeat synthesis, a process known as translocation. Two coordinated motions are necessary for translocation to occur. First, the start of the template must be repositioned in the active site. Second, telomerase must reposition the 3′ end of the substrate DNA in the active site and promote hybrid formation at the start of the template without completely dissociating during template recycling. This implies that telomerase interacts with the single-stranded DNA (ssDNA) in modes in addition to base pairing; translocation must be coordinated by the handling of more distal regions of products (Brown et al., 2014; Greider, 1991). Through this reiterative process of nucleotide addition and template translocation, a single primer (or telomere) can be extended with multiple repeats by a single enzyme.

Telomere protection

To sequester the chromosome terminus from DNA damage sensors and regulate the accessibility of the ends to telomerase, the telomere is bound by multi-protein complexes that contain DNA duplex and 3′ overhang binding proteins, as well as an assortment of linker subunits (Stewart, Chaiken, Wang, & Price, 2012). Due to the rapid divergence of telomere-associated proteins, identifying homologous proteins between species has been challenging. However, the study of mammalian, budding and fission yeast, and ciliate systems have shown recurrent use of shared structural and functional elements for specific aspects of telomere maintenance. High-resolution structures collected over the past two decades have shown that telomere end-protection proteins consistently bind the G-tail using the structurally conserved oligonucleotide/oligosaccharide-binding (OB) fold. Similarly, the telomere duplex binding proteins have Myb motifs in common within their DNA binding domain (Linger & Price, 2009; Stewart et al., 2012). Throughout the following discussion of telomere proteins, please refer to Figure 1.3 for an illustration of protein-protein interactions at the telomere and in the telomerase holoenzyme.

In vertebrates, the telomere is bound by six specialized proteins, together known as shelterin, that coordinately bind and protect the chromosome end from degradation and the DNA damage response. Shelterin consists of TRF1 and TRF2 (telomeric repeat binding factors 1 and 2), TIN2 (TRF1-interacting nuclear protein 1), RAP1 (repressor and activator protein 1), POT1 (protection of telomeres 1), and TPP1 (POT1-and TIN2-interacting protein) (Palm & de Lange, 2008). The telomeric dsDNA is bound by TRF1 and TRF2, which in turn interact with RAP1 and TIN2. TPP1 interacts with TIN2 and the ssDNA binding protein POT1 thereby bridging the telomere duplex and G-overhang. Multiple lines of evidence suggest that that shelterin is inhibitory to telomerase action at the telomere despite being responsible for enzyme recruitment (inhibition of TRF1, TRF2, TPP1, and POT1 *in vivo* causes telomerase-dependent telomere elongation) (Loayza & De Lange, 2003; van Steensel & de Lange, 1997; Ye et al., 2004). Interestingly, *in vitro* TPP1 has been shown to enhance telomerase processivity and POT1 DNA binding affinity; however, the biological consequences of the *in vitro* activity remains controversial (Nandakumar et al., 2012; Sexton, Youmans, & Collins, 2012; Wang et al., 2007; Zaug, Podell, Nandakumar, & Cech, 2010).

The fission yeast, *S. pombe*, maintains a complex structurally like shelterin that packages the yeast telomere (Stewart et al., 2012). The dsDNA binding protein Taz1 (homolog of TRF1/TRF2) and Pot1 have both been linked to independent recruitment of the other fission yeast shelterin components Rap1, Poz1 (a TIN2 homolog), and Ccq1 to the telomere (Miyoshi, Kanoh, Saito, & Ishikawa, 2008). Like mammalian TPP1, Tpz1 dimerizes with Pot1 and depletion results in loss of telomere protection; however, Ccq1 is responsible for recruitment of telomerase to Tpz1 and Pot1. In contrast, budding yeast has evolved two separate complexes to bind the telomeric repeat duplex DNA (Rif1-Rap1-Rif2) and the ssDNA (Cdc13-Stn1-Ten1). Cdc13 alone is part of the complex formed for telomerase activation at the telomeric DNA end while Cdc13 and Stn1 stimulate C-strand fill-in synthesis by polα-primase (Stewart et al., 2012). Before homologous Cdc13/CTC1-Stn1-Ten1 (CST) complexes were identified in vertebrate and fission yeast systems, budding yeast was thought to have evolved an independent telomere protection complex. We now know that CST is a universal ssDNA binding complex responsible for coordinating telomerase-dependent G-strand synthesis with polα-primase-dependent C-strand synthesis (Stewart et al., 2012).

The 3′ overhangs of *Tetrahymena* telomeres maintain a simpler shelterin-like complex bound by the human POT1 ortholog, Pot1a, which dimerizes with TPP1-like Tpt1 to inhibit activation of the DNA damage response mechanism and negatively regulate telomerase activity (Linger, Morin, & Price, 2011; Premkumar et al., 2014). Tpt1 interacts with Pat1 and Pat2 producing a Pot1a-Tpt1-Pat1-Pat2 four-component complex (Premkumar et al., 2014). While the exact role of Pat1 and Pat2 remain poorly understood, evidence suggests that they are necessary for telomerase to act on the telomere as depletion results in steady telomere shortening without affecting telomerase levels (Premkumar et al., 2014). It remains to be seen whether or not a

double-stranded telomeric DNA binding protein like the vertebrate TRFs will be identified at the *Tetrahymena* telomere. Furthermore, this shelterin-like complex seems to be independent of telomerase as the holoenzyme has evolved a separate mechanism to promote telomerase-telomere interaction (discussed below and in Chapter 4).

Telomerase holoenzyme

Like the telomere-associated proteins, assembly of telomerase and recruitment to the telomere is a complex process with overarching similarities between evolutionarily distant organisms at the level of telomere binding and telomerase function. Shared characteristics of all telomerase holoenzymes examined thus far include TERT, TER, and TER-binding proteins that stabilize the RNA and are essential to assembly of the catalytic core (the H/ACA proteins in vertebrates, p65 in *Tetrahymena*, and the Sm and LSm proteins in yeast). Intriguingly, only the reverse transcriptase domain of TERT maintains high evolutionary conservation while all other components (including the RNA) are highly divergent (Linger & Price, 2009). Our current understanding of the holoenzyme to date is arguably best characterized in the ciliate *T. thermophila* for two primary reasons: 1) a series of unique genomic rearrangements results in thousands of telomeres and an abundance of telomerase, and 2) robust molecular and genetic methods are available for quick and simple strain generation and genome manipulation making the organism an ideal candidate for structural and biochemical studies (Collins, 2012).

Studies over the past decade have identified components of the *Tetrahymena* telomerase holoenzyme by reciprocal affinity pull-down and mass spectrometry. These include nine protein components and an RNA: TERT, TER, p65, p50, p45, p75, p19, Teb1, and more recently, Teb2, and Teb3 (Jiansen Jiang et al., 2015; Miller & Collins, 2000; Min & Collins, 2009; Witkin & Collins, 2004; Witkin, Prathapam, & Collins, 2007). p65 facilitates assembly of TERT with TER, acting as an RNA chaperone and a stable component of the RNP catalytic core (TERT-TER-p65) (Singh et al., 2012). Structural studies of the holoenzyme have shown the p50 protein to function as a central hub, anchoring the TERT-TER-p65 RNP catalytic core to the high-affinity ssDNA binding subcomplex Teb1-Teb3-Teb3 (referred to as TEB) and the p75-p45-p19 subcomplex. Remarkably, the latest high-resolution EM structure and crystallographic studies from collaborations with the Feigon, Zhou, and Lei Labs have revealed that there are two RPA-like heterotrimers found within the holoenzyme: TEB and p75-p45-p19 (Jiang et al., 2015; Wan et al., 2015). We had previously proposed that Teb1, which is paralogous to the large subunit of the Replication Protein A ssDNA binding complex, may form a hetertrimer with as of then unidentified holoenzyme subunits (discussed in Chapter 3). Teb1 had been shown to significantly increase repeat addition processivity of the p50-RNP *in vitro* likely by anchoring telomere DNA; the addition of Teb2 and Teb3 further increases overall activity, consistent with additional stabilization through interaction with the TEN domain of TERT and Teb1 (Jiang et al., 2015; Min & Collins, 2009, 2010).

The second RPA-like heterotrimer is formed by the p75-p45-p19 subcomplex. This heterotrimer had previously been seen in multiple conformations, rotating as an intact substructure hinged on p50 in EM density; however, the biological function of this genetically essential subcomplex had remained elusive (Jiang et al., 2013). Crystal structures of the p45 N-terminal domain in complex with p19 and the p45 C-terminal domain in addition to the high resolution EM map suggested that p75-p45-p19 is CST in *Tetrahymena* (Jiang et al., 2015; Wan et al., 2015). Functional studies confirmed that disruption of the p45-p19 interaction results in uncoupling of G- and C-strand dynamics, lending support to the idea that p75-p45-p19 is a *Tetrahymena* CST that coordinates telomerase extension with polα-primase C-strand synthesis (Wan et al., 2015). This stable assembly of *Tetrahymena* CST into the telomerase holoenzyme may have evolved as a more efficient system to transition from repeat addition to C-strand fill in.

Here I report a body of work that aims to advance our biochemical and structural understanding of *Tetrahymena* telomerase holoenzyme assembly, activation, and recruitment.

Figure 1.1

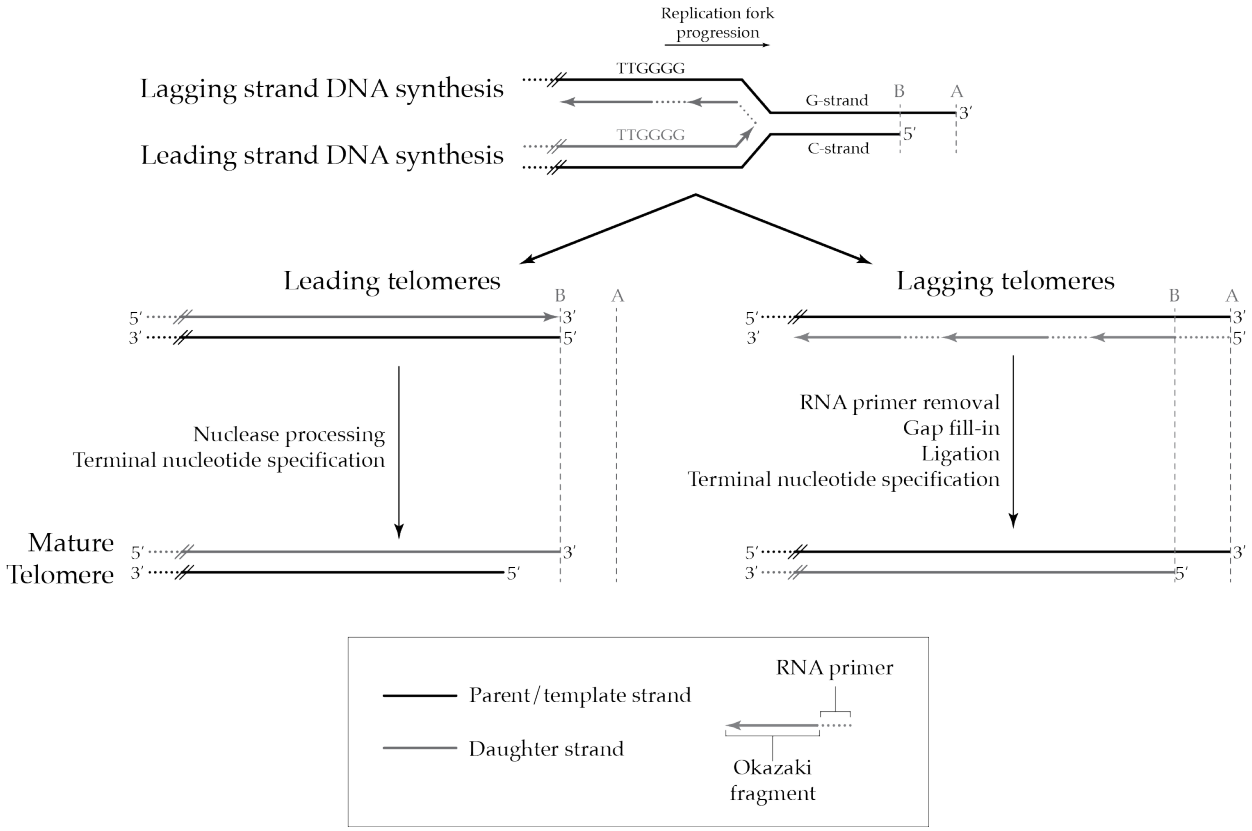

The end-replication problem in the presence of a 3′ overhang. The conserved ssDNA overhang of eukaryotic telomeres must be regenerated following leading- (at left) and lagging-strand (at right) duplication. During leading strand synthesis, DNA polymerase δ copies up to the end of the template strand resulting in a blunt-ended product. The end subsequently undergoes nuclease processing and terminal nucleotide specification to restore the mature 3′ overhang leading to shortening of the daughter chromosome (compare dashed line at A to dashed line at B). During lagging strand synthesis, the terminal primer deposited by DNA polymerase α-primase is removed during processing followed by gap fill in, ligation, and terminal nucleotide specification resulting in little, if any, shortening once the mature telomere has been generated.

Figure 1.2

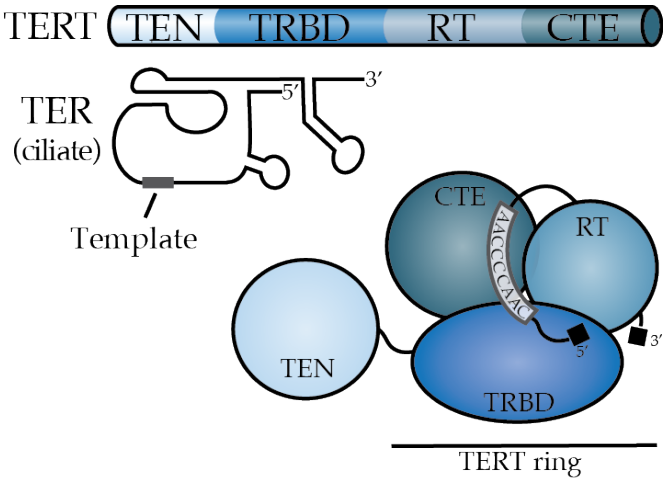

The telomerase protein component (TERT) consists of four domains and an unstructured linker. Top: The TERT essential N-terminal (TEN) domain is separated from the TERT high-affinity RNA-binding domain (TRBD) by an unstructured linker of variable length depending on species. This is followed by the reverse-transcriptase (RT) domain and the TERT C-terminal extension. Assembly of the enzyme requires the presence of an RNA carrying 1.5 copies of template sequence complementary to the telomere. Bottom: A model for tertiary assembly of the minimal RNP showing the TRBD-RT-CTE ring and approximate placement of the RNA template.

Figure 1.3

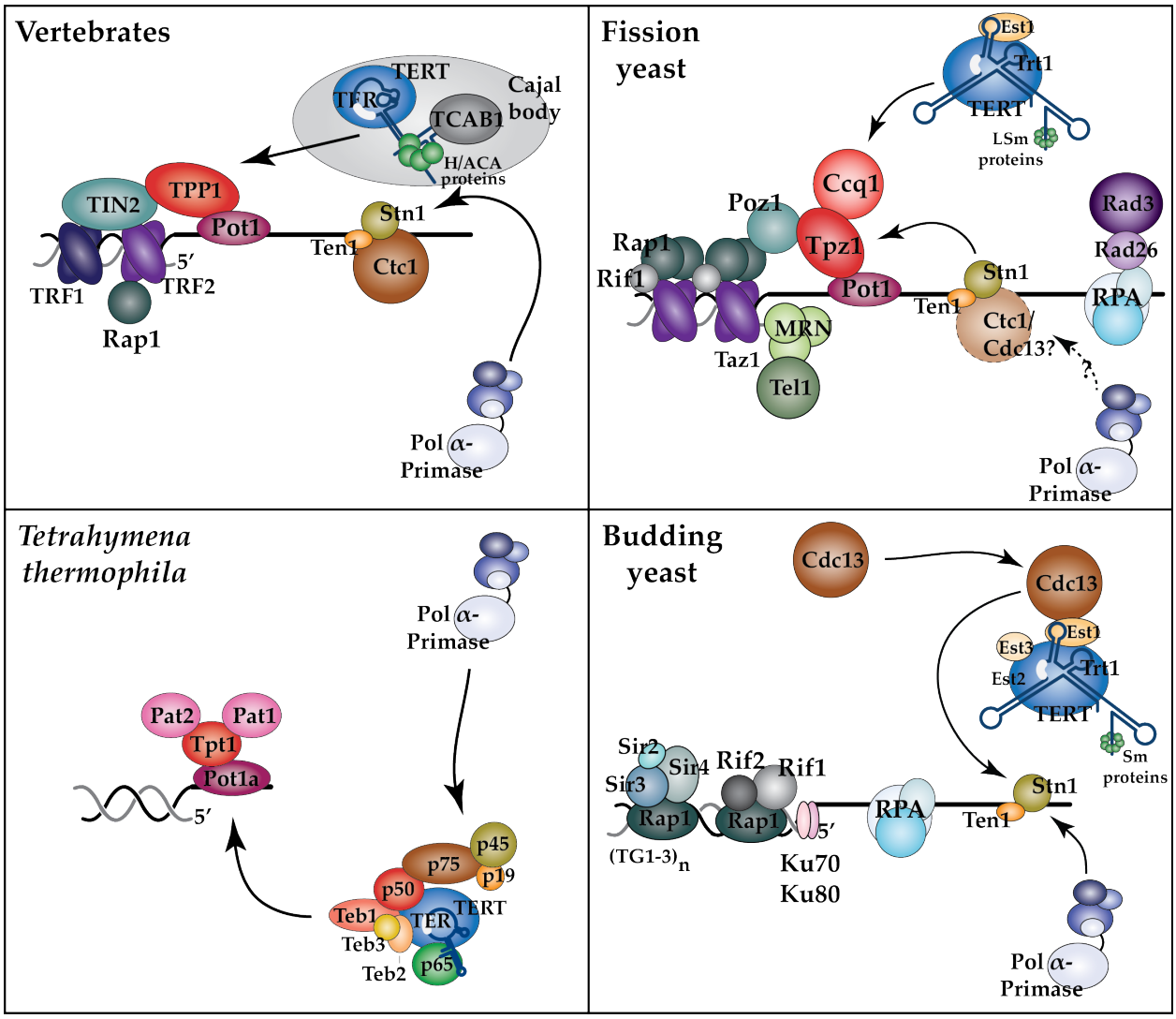

Models of telomere and telomerase holoenzyme protein interaction in vertebrates, yeasts, and the ciliate *T. thermophila*. Functional homologs have been similarly colored.

CHAPTER TWO

Tetrahymena Telomerase Holoenzyme Assembly, Activation, and Inhibition by Domains of the p50 Central Hub

Based on Hong et al., *MCB*, 2013

Abstract

The eukaryotic reverse transcriptase, telomerase, adds tandem telomeric repeats to chromosome ends to promote genome stability. The fully assembled telomerase holoenzyme contains a ribonucleoprotein (RNP) catalytic core and additional proteins that modulate the ability of the RNP catalytic core to elongate telomeres. Electron microscopy (EM) structures of *Tetrahymena* telomerase holoenzyme revealed a central location of the relatively uncharacterized p50 subunit. Here we have investigated the biochemical and structural basis for p50 function. We show that the p50-bound RNP catalytic core has a relatively slow rate of tandem repeat synthesis but high processivity of repeat addition, indicative of high stability of enzyme-product interaction. The rate of tandem repeat synthesis is enhanced by p50-dependent recruitment of the holoenzyme single-stranded DNA binding subunit, Teb1. An N-terminal p50 domain is sufficient to stimulate tandem repeat synthesis and bridge the RNP catalytic core, Teb1, and the p75 subunit of the holoenzyme subcomplex p75-p19-p45. In cells, the N-terminal p50 domain assembles a complete holoenzyme that is functional for telomere maintenance, albeit at shortened telomere lengths. Also, in EM structures of holoenzymes only the N-terminal domain of p50 is visible. Our findings provide new insights about subunit and domain interactions and functions within the *Tetrahymena* telomerase holoenzyme.

Introduction

In most eukaryotic nuclei, chromosomes are capped with an array of tandem simple-sequence DNA repeats. These telomeric repeats, along with bound proteins, create an end-protective structure that distinguishes authentic chromosome ends from unintended double-stranded DNA breaks (O'Sullivan & Karlseder, 2010; Palm & de Lange, 2008; Stewart et al., 2012). Telomere integrity is compromised by the attrition of repeats as an inevitable consequence of genome replication and the many steps of chromosome end processing (Pfeiffer & Lingner, 2013; Sampathi & Chai, 2011; Wu, Takai, & de Lange, 2012). Replication-linked telomere shortening is progressive, leading eventually to one or more telomeres of a length insufficient for end-protective function. Critically short telomeres induce genome instability, proliferative senescence, and tissue renewal failures in human disease (Armanios & Blackburn, 2012; Shay & Wright, 2011).

The telomerase ribonucleoprotein (RNP) can compensate for telomere erosion, using a region within its integral RNA component to template the synthesis of new repeats. Telomerase catalytic activity can be reconstituted from the biologically co-folded subunits of a telomerase RNP catalytic core including telomerase reverse transcriptase (TERT), the template-containing telomerase RNA (TER), and proteins that fold and stabilize TER to promote TERT-TER interaction (Blackburn & Collins, 2011; Hengesbach et al., 2011). Beyond the RNP catalytic core, additional telomerase holoenzyme proteins are required for repeat synthesis at telomeres *in vivo* (Egan & Collins, 2012; Podlevsky & Chen, 2012). Some holoenzyme proteins assemble with telomerase RNP only in the DNA synthesis phase of the cell cycle (Londono-Vallejo & Wellinger, 2012; Nandakumar & Cech, 2013). Differing models have been offered to explain telomerase holoenzyme protein functions at a molecular level, and accordingly many open questions remain to be addressed.

Telomere-rich ciliated protozoa are experimentally favorable organisms for insights about telomerase (Blackburn, Greider, & Szostak, 2006). As a ciliate model organism, *Tetrahymena thermophila* has numerous advantages including large-scale culture growth, a sequenced genome, and methods for genetic manipulation (Collins, 2012). These features enabled endogenously assembled telomerase holoenzyme purification to homogeneity and comprehensive subunit identification at a molecular level (Min & Collins, 2009; Witkin & Collins, 2004; Witkin et al., 2007). The *Tetrahymena* telomerase holoenzyme purified from cell extract contains 8 subunits, each of which is telomerase-specific and essential for telomere maintenance: TERT, TER, the telomerase assembly factor p65, and 5 additional proteins that give p65-TER-TERT (the RNP catalytic core) an ability to elongate telomeres *in vivo* (Miller & K. Collins, 2000; Min & Collins, 2009; Witkin & Collins, 2004; Witkin et al., 2007). These additional subunits are the holoenzyme single-stranded telomeric-repeat DNA binding protein Teb1; one copy each of p75, p45, and p19 assembled as a subcomplex designated 7-1-4; and p50 (Jiang et al., 2013; Min & Collins, 2009). Of these subunits, only Teb1 has domains readily

detectable by sequence homology and fold prediction. The 4 oligonucleotide/oligosaccharide binding (OB)-fold domain architecture of Teb1 is paralogous to that of the large subunit of the general single-stranded DNA binding factor Replication Protein A, with 3 of the predicted Teb1 OB-fold domains confirmed by high-resolution structures (Min & Collins, 2009; Zeng et al., 2011).

Functional associations of recombinant *Tetrahymena* telomerase RNP catalytic core, Teb1, and 7-1-4 require p50 (Jiang et al., 2013). The p50 subunit alone stimulates RNP catalytic core activity, and p50 is required for additional activity stimulation by Teb1 or 7-1-4 (Figure 2.1A, left). The physical arrangement of these *Tetrahymena* telomerase holoenzyme subunits was defined by difference imaging, comparing electron microscopy (EM) 2D image class averages and/or 3D reconstructions of telomerase complexes purified from cell extracts and labeled with Fab antibodies (Jiang et al., 2013). Individual subunits or subunit combinations were fused to tandem Protein A domains (ZZ tag) and/or 3 consecutive FLAG peptides (F tag). Taking advantage of the F tag still present after 2-step affinity purification, binding of anti-FLAG Fab antibody fragment was used to localize individual subunits within the holoenzyme. C-terminal tagging of p65, TERT, p75, p19, or Teb1 preserved telomerase function for each of these subunits *in vivo*. C-terminally tagged p50 also retained biological function but purified a very low holoenzyme yield. Therefore, N-terminally tagged F-p50 telomerase was used to map the location of p50. N-terminal tagging of p50 disrupted holoenzyme association of the Teb1 C-terminal OB-fold domain (Teb1C), which tethers the central Teb1 high-affinity DNA binding domains (Teb1A and Teb1B) to the holoenzyme complex (Jiang et al., 2013; Min & Collins, 2010). By using holoenzyme subcomplexes in addition to differential subunit tagging, a model for holoenzyme architecture was developed that pinpoints p50 as the central hub of telomerase holoenzyme subcomplex coordination (Figure 2.1A, right).

Despite the critical role of p50 in *Tetrahymena* telomerase holoenzyme assembly and repeat synthesis processivity, little is known about this protein at a molecular level. The p50, Teb1, and p65 proteins are particularly sensitive to partial proteolysis in cell extract (Jiang et al., 2013; Min & Collins, 2009). For Teb1 and p65, partial proteolysis releases N-terminal domains of unknown function from the C-terminal domains that mediate holoenzyme assembly and catalytic activation. Unlike Teb1 and p65, p50 does not have a known multi-domain architecture or even any domains predicted by sequence analysis. Here we have investigated the biochemical, biological, and structural roles of N-terminal and C-terminal regions of p50. We identify an N-terminal ~30 kDa domain of p50 that is necessary and sufficient for physical and functional association of the RNP catalytic core, Teb1, and 7-1-4 both *in vitro* and *in vivo*. Our results suggest that the p50 C-terminal region has a regulatory role. Overall our findings bring new insight into the mechanism of processive repeat synthesis, the specificity of subunit interactions, and the overall architectural organization of *Tetrahymena* telomerase holoenzyme.

Materials and Methods

Telomerase reconstitutions in vitro

We used synthetic open reading frames for TERT, p75, p65, p50, p45, and p19 expression in rabbit reticulocyte lysate (RRL) and for Teb1BC expression in *E. coli*. TER was gel-purified following *in vitro* transcription by T7 RNA polymerase. Subunit expression, reconstitution, and affinity purification from RRL protein synthesis reactions was done according to previously optimized protocols (Jiang et al., 2013; Min & Collins, 2010). Unless otherwise indicated, complexes bound to anti-FLAG antibody resin were washed into T2MG (20 mM Tris•HCl pH 8.0, 1 mM $MgCl_2$, 10% glycerol, 2 mM DTT). More extensive washing was performed prior to SDS-PAGE analysis of physical interactions using T2MG with 0.1% Igepal CA-630. Peptide elutions were performed for subunit interaction assays and 2-step affinity purification using 150-200 ng/μl peptide.

Detection of protein, RNA, DNA, and telomerase activity

Protein expression in RRL was monitored by [^{35}S]-methionine incorporation. TER detection was done by blot hybridization using an oligonucleotide [^{32}P]-end-labeled by T4 polynucleotide kinase. Genomic DNA was purified, digested, and hybridized for Southern blot analysis as described (Couvillion & Collins, 2012), using a sequence 3′-flanking the targeted region to detect differentially sized wild-type and recombinant chromosomes. Telomeric restriction fragments were detected following denaturing gel electrophoresis of HindIII-digested genomic DNA using a 5′ end-labeled oligonucleotide probe complementary to the subtelomeric region of the palindromic chromosome encoding ribosomal RNAs (Miller & Collins, 2000). The HindIII-cleaved telomeric restriction fragment has ~350 bp of non-telomeric sequence as well as a variable number of telomeric repeats. Activity assays used a standard *Tetrahymena* telomerase reaction buffer containing 50 mM Tris•acetate pH 8.0, 2 mM $MgCl_2$, and 5 mM β-mercaptoethanol or 2 mM DTT or 1 mM TCEP•HCl. Product synthesis reactions additionally contained 3 mM [a-^{32}P]dGTP, 200 mM dTTP, 100-200 nM primer $(GT_2G_3)_3$, and 50-200 nM Teb1BC and were performed for 10 min at room temperature unless indicated otherwise. A 5′-labeled oligonucleotide DNA recovery control was added to telomerase products before precipitation.

Tetrahymena *strain construction and enzyme purification from cell extracts*

Flanking genomic regions were used for targeting the endogenous *TAP50* locus to express synthetic open reading frames of full-length or truncated p50, with the F and ZZ tag modules separated by a Tobacco Etch Virus protease cleavage site (Min & Collins, 2009). Selection was performed using the bsr2 cassette (Couvillion & Collins,

2012). Cell extract production and affinity purification were done as optimized previously (Jiang et al., 2013; Min & Collins, 2009) using T2EG50 buffer (20 mM Tris•HCl pH 8.0, 1 mM EDTA, 10% glycerol, 50 mM NaCl, 2 mM DTT or 1 mM TCEP•HCl). Prior to an activity assay, the enzyme was washed into T2MG with 50 mM NaCl and 0.1% Igepal CA-630. For EM samples, the 2-step antibody affinity purification (Jiang et al., 2013) was followed by microscale gel filtration over a Sephadex 200 PC 3.2/30 column in 20 mM HEPES•NaOH pH 8.0, 50 mM NaCl, 1 mM $MgCl_2$, and 1 mM TCEP•HCl. Fab labeling was done as described (Jiang et al., 2013).

Electron microscopy and image analysis

Methods used were largely as described previously (Jiang et al., 2013). Briefly, purified holoenzyme was subjected to negative staining using uranyl formate (0.8%) on glow-discharged grids coated with carbon film. Micrographs were recorded on a TIETZ F415MP 16-megapixel CCD camera at 68,027x magnification in an FEI Tecnai F20 electron microscope operated at 200 kV. This study used 19,325 particles of p50N30-F telomerase and 15,427 particles of Fab-labeled p50N30-F telomerase for 2D image classification, and 5,593 particles of p50N30-F telomerase for 3D reconstruction by the random conical tilt (RCT) method (Radermacher, Wagenknecht, Verschoor, & Frank, 1987).

Results

Holoenzyme protein interactions increase the rate of tandem repeat synthesis

The p50 subunit occupies a central position among the *Tetrahymena* telomerase holoenzyme subunits mapped by EM (Jiang et al., 2013). Consistent with its location, p50 is required for stimulation of RNP catalytic core activity by Teb1 or 7-1-4 (Jiang et al., 2013). Compared to the profile of product synthesis by the reconstituted RNP catalytic core alone, product lengths increased with the addition of p50 and increased even more with the addition of both p50 and Teb1 (Jiang et al., 2013). We investigated the mechanism for these increases in product length using a time course of direct telomeric primer elongation with radiolabeled dGTP and dTTP (Figure 2.1B). RNP catalytic core containing TERT C-terminally tagged with a triple FLAG epitope (TERT-F) was assembled in RRL and then combined with separately RRL-expressed p50. Importantly, C-terminal tagging of *Tetrahymena* TERT does not impede telomerase holoenzyme function *in vivo* (Witkin & Collins, 2004). Telomerase complexes were removed from other RRL reaction components by affinity purification with anti-FLAG antibody resin. Direct primer extension assays of purified complexes were then performed with or without the addition of bacterially expressed Teb1BC, which is the C-terminal half of Teb1 sufficient to confer holoenzyme-like high repeat addition processivity (RAP) (Min & Collins, 2010).

Given sufficient reaction time, the *Tetrahymena* telomerase RNP catalytic core assembled with p50 gave substantial high-RAP activity (Figure 2.1B, lanes 2-6), much greater than that of the RNP catalytic core alone (lane 1). As reported previously (Jiang et al., 2013), supplementing the p50-bound RNP catalytic core with Teb1 dramatically increased the overall level of catalytic activity and high-RAP product synthesis (Figure 2.1B, lanes 8-12). Notably, unlike the RNP catalytic core alone (Hardy, Schultz, & Collins, 2001), and with or without Teb1, the p50-bound RNP catalytic core continued to elongate high-RAP products for more than 60 min without reaching an equilibrium distribution of product lengths. We conclude that p50 association with the RNP catalytic core is sufficient to confer a high stability of enzyme-product interaction even without Teb1.

Curiously, addition of Teb1 increased the rate of tandem repeat synthesis: products were longer at each time point in the reaction with Teb1 than the reaction without Teb1 (Figure 2.1B, for example compare lanes 2-3 to lanes 8-9). In addition to increasing the rate of high-RAP product synthesis, Teb1 also enhanced productive association of p50 with the RNP catalytic core: the RNP catalytic core low-RAP product synthesis was almost completely converted to high-RAP product synthesis in the presence but not absence of Teb1 (Figure 2.1B, compare products +4, +10, +16 in lanes 2-6 versus lanes 8-12). This suggests that Teb1 stabilizes a p50 conformation favorable for its assembly with or activation of the RNP catalytic core.

The p75 subunit of 7-1-4 interacts with p50

In addition to bridging the RNP catalytic core and Teb1, p50 also bridges the RNP catalytic core to 7-1-4. Endogenously expressed p75, p45, and p19 form a remarkably tight subcomplex that is resistant to dissociation by micrococcal nuclease treatment of p45-F holoenzyme, a treatment that degrades TER and releases p65, TERT, Teb1, and a large fraction of p50 from intact 7-1-4 (Jiang et al., 2013; Min & Collins, 2009, 2010). The 7-1-4 subcomplex is positionally dynamic relative to the rest of the holoenzyme, hinging as a unit around p50, which suggests a role for this subcomplex in holoenzyme coordination with unknown additional factors involved in telomere synthesis (Jiang et al., 2013). Addition of p75, p45, and p19 co-expressed in RRL stimulated product synthesis by the p50-bound RNP catalytic core with or without Teb1 (Jiang et al., 2013). However, unlike Teb1, 7-1-4 increased the overall level of RNP catalytic activity without increasing product length.

To investigate whether the stimulatory influence of 7-1-4 correlates with direct physical interaction of 7-1-4 subunits and p50, we combined C-terminally triple-FLAG tagged but not radiolabeled p50-F with [^{35}S-Met]-labeled but untagged p75, p45, and/or p19, each synthesized independently in RRL reactions. This radiolabeling strategy resolved the potential overlap in migration of p45 and p50 expression products. Protein-protein interactions were assessed by the amount of radiolabeled protein that copurified with p50-F using anti-FLAG antibody resin. As a negative control, we verified that untagged

p75, p45, and p19 did not bind anti-FLAG antibody resin in the absence of p50-F (Figure 2.2A, lane 8). As expected, the combination of all 3 of the 7-1-4 proteins allowed all 3 to associate with p50 (Figure 2.2A, lane 7). For the 7-1-4 subunits individually, only p75 could copurify with p50 (Figure 2.2A, lanes 1-3). The interaction of p45 with p50 was dependent on the presence of p75, and p19 interaction with p50 was dependent on the presence of both p75 and p45 (Figure 2.2A, lanes 4-7). The simplest explanation for these findings would be that p75 binds to p50, then p45 can bind to p75, and finally p19 can bind to p45 (Figure 2.2A, schematic). However, it remains possible that each 7-1-4 subunit physically contacts each other subunit and/or p50 in a manner dependent on conformational changes induced by subunit interactions.

To confirm that p75 associates with p50 in the context of a catalytically active enzyme, we used p75, p45, or p19 tagged at the protein C-terminus, which preserves subunit function *in vivo* (Min & Collins, 2009). Each subunit was expressed as an F-tagged protein and combined individually, or as 7-1-4, with p50-bound RNP catalytic core. Telomerase complexes assembled on an F-tagged 7-1-4 subunit were then recovered by affinity purification using anti-FLAG antibody resin. In the presence or absence of untagged p45 and p19, p75-F copurified telomerase activity (Figure 2.2B, lanes 1-2). In contrast, p45-F and p19-F copurified telomerase activity only in the presence of other untagged 7-1-4 subunits (Figure 2.2B, lanes 4 and 6). We also tested whether p75 alone could recapitulate the 7-1-4 stimulation of overall telomeric-repeat product synthesis (Jiang et al., 2013). Addition of p75 to the p50-bound RNP catalytic core did induce the same increase in telomerase activity as addition of 7-1-4, whereas addition of p45 or p19 alone did not (Figure 2.2C).

An N-terminal domain mediates p50 biochemical roles in telomerase activation

We next investigated whether the activity stimulation and subunit bridging functions of p50 could be mapped to specific regions of the protein. The RNP catalytic core assembled on TERT-F was combined with full-length or various p50 N- or C-terminal truncations. Full-length p50 stimulated the overall level and RAP of product synthesis (Figure 2.3A, compare lanes 1-2). The same result was observed for C-terminally truncated p50 polypeptides lacking up to half of the protein primary sequence (Figure 2.3A, lanes 3-6). No activity stimulation was detected in assays of N-terminally truncated p50 polypeptides, including modest truncations of only 20-50 amino acids (Figure 2.3A, lanes 9-10). The presence of a structurally autonomous p50 N-terminal domain is supported by partial proteolysis of endogenously expressed p50 during some purifications from *Tetrahymena* cell extract (Figure 2.S1), which generates an ~30 kDa fragment of p50 that would roughly correspond to amino acids 1-252 (hereafter designated p50N30). The C-terminal 170 amino acids of p50 that are absent in p50N30 are not required for processive repeat synthesis (Figure 2.3A, lane 4), and even the slightly shorter p50N25 (amino acids 1-213) could stimulate catalytic activity although to a lesser extent (Figure 2.3A, lane 6).

To complement the definition of p50 domain requirements for biochemical activity described above, we determined which regions of p50 are required for physical interaction with the RNP catalytic core and p75. We [^{35}S-Met]-labeled the variously truncated p50 polypeptides (Figure 2.3B, Input) and assayed for copurification with unlabeled TERT-F RNP catalytic core or unlabeled, untagged TERT RNP catalytic core and p75-F. The TERT-F RNP catalytic core and p75-F copurified full-length p50 and p50 C-terminal truncations up to p50N30 with similar recovery (Figure 2.3B, lanes 1-3). Any additional truncation reduced p50 association with the RNP catalytic core (Figure 2.3B, lane 4), and truncation to p50N25 reduced p50 association with p75 (lane 5). By physical association assay, p50N25 interaction with the RNP catalytic core was reduced more than expected by its copurification of RNP catalytic activity (Figure 2.3A, lane 6; Figure 2.3B, lane 5). This difference is likely due to the higher stringency of washes used in the physical association assay (see Materials and Methods), which was necessary to remove non-specific background protein association with the purification resin.

Additional tests of p50N30 biochemical activities did not detect any loss of function in comparison to full-length p50. For example, we compared the ability of full-length p50 and p50N30 to confer activity stimulation by 7-1-4 and Teb1. For all combinations of telomerase holoenzyme subcomplexes, the profiles of product synthesis were indistinguishable for enzymes with p50N30 or full-length p50 (Figure 2.3C, compare lanes 1-4 and 9-12). In comparison, the C-terminal half of p50 (C25, amino acids 214-422) did not stimulate RNP catalytic core activity with or without 7-1-4 and/or Teb1 (Figure 2.3C, lanes 5-8). Also, no difference from full-length p50 was detected in the p50N30 specificity of activity stimulation by individual 7-1-4 subunits (Figure 2.S2). In these and additional biochemical assays, no loss of function was detected as a consequence of p50 C-terminal truncation to p50N30.

Curiously, in the course of experiments above, we noticed that the overall level of catalytic activity was often higher for enzymes reconstituted using the same volume of RRL expression reaction for p50N30 versus full-length p50. This difference could arise from an expression or folding advantage of the smaller p50N30 protein, or it could reflect the removal of an inhibitory C-terminal domain of p50. To address this distinction, we devised a strategy to compare the specific activity of telomerase complexes containing full-length p50 or p50N30. Because the two polypeptides have different structural environments at their C-terminal ends, and because N-terminal tagging of p50 is disruptive for Teb1 assembly into holoenzyme (Jiang et al., 2013), it was necessary to use untagged versions of the p50 proteins. This was accomplished by capturing p50-bound telomerase complexes using p75-F and anti-FLAG antibody resin, which also eliminated any activity contribution from RNP catalytic core without p50. We normalized the amount of purified RNP using parallel aliquots of the p75-F complexes to detect catalytic activity (Figure 2.3D, top panel) and TER (lower panel). RNP with p50N30 reproducibly had about twice the specific activity of RNP with full-length p50 (Figure 2.3D, lanes 2-3). Only a low level of activity was detected for RNP

assembled by p50N25 (Figure 2.3D, lane 4), consistent with reduced stability of p50N25 interaction with p75 and the RNP catalytic core.

The N-terminal domain of p50 supports physiological telomerase holoenzyme assembly and function

Because the p50 C-terminal ~20 kDa was unnecessary for recombinant telomerase holoenzyme assembly or catalytic activity *in vitro*, we investigated whether this region was required for telomere maintenance *in vivo*. We targeted the *TAP50* locus for replacement with C-terminally tagged full-length p50, p50N30, or p50N25. In each targeting construct, we used the synthetic open reading frame of the p50 RRL expression vector and the FZZ tag developed for holoenzyme affinity purification from *Tetrahymena* cell extracts (see Materials and Methods). Integration of the targeting vector initially replaced only a few of the 45 expressed macronuclear copies of *TAP50* with the modified open reading frame and selectable marker cassette. A standard protocol of additional selection, clonal cell line isolation, and release from selection was used to discriminate whether the recombinant chromosome can genetically substitute for the wild-type chromosome (Chalker, 2012).

We performed genomic DNA Southern blot hybridization to distinguish wild-type and recombinant chromosomes. As expected from previous results, which introduced the FZZ tag in fusion with the endogenous rather than the synthetic p50 open reading frame (Min & Collins, 2009), the newly generated p50-FZZ expression construct could completely replace the wild-type *TAP50* locus (Figure 2.4A, lanes 1-3; the p50-FZZ cell line analyzed in lane 2 was used for subsequent studies). Wild-type chromosomes were also replaced by chromosomes with the p50N30-FZZ expression construct (Figure 2.4A, lanes 4-6; the p50N30-FZZ cell line in lane 4 was used for subsequent studies). The silent micronuclear gene locus not targeted for replacement gives rise to a low wild-type *TAP50* locus signal that does not recover to higher copy number after release from selection. In contrast, all cell lines expressing p50N25-FZZ had a high copy number of wild-type chromosomes (Figure 2.4A, lanes 7-8; the p50N25-FZZ cell line in lane 7 was used for subsequent studies). This abundance of wild-type chromosomes indicates that p50N25 is not able to provide genetically essential p50 function. Southern blot results were confirmed using RT-PCR to verify the absence (in p50-FZZ and p50N30-FZZ cell lines) or presence (in p50N25-FZZ cell lines) of wild-type *TAP50* mRNA (data not shown).

Although p50N30 retained the genetically essential functions of full-length p50, telomeres were shorter in cells expressing p50N30-FZZ than untagged p50 (Figure 2.4B, compare lanes 1 and 3). In contrast, telomeres were longer than wild-type in both the p50-FZZ cell line created here by integration of a complete p50-FZZ synthetic open reading frame (Figure 2.4B, lane 2) and in the p50-FZZ strain created previously (Min & Collins, 2009) by integration of just the FZZ tag (Figure 2.S3). Because p50 knock-down

and overexpression both shorten telomere length (Min & Collins, 2009), the increase in telomere length resulting from p50 C-terminal tagging is unlikely to reflect a simple change in protein abundance. Instead, we suggest that it reflects tag interference with an inhibitory activity of the p50 C-terminal domain (see Discussion).

Single-step affinity purification of p50N30-FZZ or p50N25-FZZ from *Tetrahymena* cell extracts showed that both proteins could coenrich holoenzyme catalytic activity (Figure 2.S4). More stringent 2-step affinity purification coenriched activity in association with p50N30-F but not p50N25-F (Figure 2.4C), consistent with weaker p50N25 interaction with the RNP catalytic core (Figure 2.3B). Only p50N30-FZZ purification recovered associated proteins with the expected SDS-PAGE profile of telomerase holoenzyme subunits (Figure 2.4D). Consistent with complete replacement of endogenous p50 by p50N30-FZZ, the yield of p50N30-F holoenzyme was comparable to the yield of TERT-F holoenzyme and more than the yield of N-terminally tagged F-p50 (Figure 2.4D), which has reduced high-RAP catalytic activity (Figure 2.4C) and does not provide genetically essential p50 function (Jiang et al., 2013). Of note, under standard purification conditions, p50N30-FZZ and p50N25-FZZ coenriched a heterogenous background of proteins not present in purifications of TERT-FZZ (Figure 2.4D; see also Fig 2.5C).

Deletion of the p50 C-terminal domain does not change the holoenzyme structure determined by EM

We exploited the genetically stable substitution of untagged p50 by p50N30-FZZ (Figure 2.4A) and the high yield of holoenzyme obtained from p50N30-FZZ 2-step affinity purification (Figure 2.4D) to investigate whether the holoenzyme structure determined by EM previously (Jiang et al., 2013) encompasses the p50 C-terminal domain as well as the N-terminal domain located by Fab binding to F-p50. Gel filtration was required after p50N30-FZZ 2-step affinity purification (Figure 2.5A) to remove an interfering background of large particles that by EM and image analysis were heterogeneous in size and did not contain consistent structural features (Figure 2.S5). The large particles that fractionated as aggregates had low if any telomerase activity compared to the offset peak of fractionated telomerase holoenzyme (Figure 2.5A,B). A substantial population of aggregate-sized particles was not detected for telomerase holoenzyme purified using TERT-FZZ (Figure 2.5A). SDS-PAGE analysis showed a background of polypeptides in the aggregate-sized p50N30-F Peak A complexes in addition to the expected telomerase holoenzyme subunits, which were selectively enriched in the Peak B samples used for additional studies (Figure 2.5C). Truncation of full-length p50 by partial proteolysis during purification yields an SDS-PAGE profile of holoenzyme subunits with apparently substoichiometric p50 (Min & Collins, 2009). Minimized extract proteolysis of genetically truncated p50N30 allowed visualization of subunit copurification at a much more comparable stoichiometry with other holoenzyme subunits (Figure 2.5C, Peak B).

Difference maps of EM class averages generated from p50N30-F telomerase versus TERT-F telomerase (Jiang et al., 2013) showed no additional density in the complete holoenzyme (Figure 2.6A) or holoenzyme lacking Teb1 (Figure 2.6B). Comparison of 3D EM reconstructions of p50N30-F telomerase to TERT-F telomerase from our previous study (Jiang et al., 2013) showed no difference significant for the 26 Å resolution of the structures (Figure 2.6C,D; Figure 2.S6). Structures from the small subset (~5%) of p50N30-F particles lacking Teb1 allowed the boundary between p50N30 and Teb1 to be more readily visualized (Figure 2.6B,D). Overall the structures suggest that telomerase enzymes containing endogenous p50 are purified without retaining the p50 C-terminal region due to proteolysis and/or that the C-terminal region of p50 is positionally flexible relative to an N-terminal domain.

We used anti-FLAG Fab labeling of p50N30-F telomerase complexes to define the physical location of the p50N30 C-terminus (residue 252 of full-length p50) within the holoenzyme. Our F tag can bind up to 3 Fab, as shown in previous labeling experiments (Jiang et al., 2013). Intriguingly, only a single Fab is seen in the class averages of Fab-labeled p50N30-F telomerase (Figure 2.6E), with its paratope (Figure 2.6F, asterisk) proximal to p45/p75 and ~40 Å from the apparent boundary of p50. Assuming that only the most terminal of the 3 FLAG epitopes was accessible for Fab binding, and that each FLAG epitope extends a maximum of 20 Å based on peptide length, the C-terminus of p50N30 is likely to be near the p50 boundary with p45 and/or p75 (Figure 2.6F, white square). However, because a maximum of only 1 Fab could bind p50N30-F holoenzyme, the location of the p50N30 C-terminus was not possible to determine as precisely as the locations of a tagged protein terminus that bound 2 or 3 Fab.

Discussion

EM structures of *Tetrahymena* telomerase holoenzyme revealed a central location of the p50 subunit (Jiang et al., 2013). Combined with findings from holoenzyme reconstitution *in vitro* (Jiang et al., 2013), p50 was proposed as the structural and functional hub for coordination of the RNP catalytic core, 7-1-4, and Teb1. Here we have biochemically and structurally characterized the roles of p50 in recombinant and endogenously assembled telomerase holoenzymes. We show that a p50 N-terminal domain supports all of the previously identified functions of p50, including physical bridging of other holoenzyme subunits and stimulation of processive repeat synthesis. The p50-bound RNP catalytic core has an unexpectedly slow elongation rate of tandem repeat synthesis but high stability of product interaction and RAP. Although direct p50-DNA interaction could account for the p50-mediated increase in RAP, we suggest that p50 confers high RAP by inducing a conformational change in the RNP catalytic core. In the holoenzyme subunit model based on EM structures (Jiang et al., 2013), p50 is close to the TERT N-terminal (TEN) domain, which is crucial for conferring RAP to the otherwise single-repeat synthesis activity of the remaining TERT domains (Robart & Collins, 2011).

Addition of Teb1 to the p50-bound RNP catalytic core dramatically increased the elongation rate for tandem repeat synthesis. At least under the conditions typical for telomerase assays *in vitro*, product synthesis is rate-limited by dissociation of the thermodynamically favorable product-template hybrid (Collins, 2011; Podlevsky & Chen, 2012). Therefore, we suggest a model in which Teb1C favors hybrid dissociation after synthesis to the template 5′ end, disfavors template-product reassociation in the post-synthesis register (product base-paired to the template 5′ end), and/or favors template-product reassociation for the next repeat synthesis (product base-paired to the template 3′ end). In parallel, direct protein-DNA interactions mediated by Teb1A and Teb1B would enhance retention of the single-stranded DNA product. Given the closely triangulated arrangement of the TERT TEN domain, p50, and Teb1C (Jiang et al., 2013), Teb1C could act by allosteric regulation or by direct DNA or RNA contact. A direct nucleic acid binding activity of Teb1C and/or p50 could escape detection in biochemical assays of the isolated subunits, if holoenzyme protein-protein interactions are necessary for folding or positioning the contact surface. Future studies of the physical path of DNA would be aided by a reconstitution system that recapitulated the high physiological stability of Teb1 interaction with the remainder of the holoenzyme, which is compromised in the current reconstitutions (Jiang et al., 2013; Min & Collins, 2010).

In the structure of *Tetrahymena* telomerase holoenzyme determined by EM, we could distinguish the general locations but not the individual boundaries of p75, p45, and p19 since these subunits were always present as a complete 7-1-4 subcomplex. By differential tagging and individual expression of the 7-1-4 subunits described above, we could separate the requirements of each for assembly with p50 in a manner that was not possible to define biochemically or by EM using endogenously assembled telomerase complexes. We show that the interaction of RRL-expressed p75 and p50 is specific and independent of p45 or p19. In addition, p75 alone influenced the activity of p50-bound RNP catalytic core to a similar extent as the entire 7-1-4 complex. From EM structures, both p75 and p45 were modeled to contact p50 (Jiang et al., 2013). The biochemical results here confirm a direct interaction of p75 with p50 and leave open the possibility that p45 may also contact p50 in a p75-dependent manner. The general location of p45 in the EM structure is unambiguous, and the locations of the p19 and p75 C-termini place these subunits adjacent to each other. Because recombinant p19 binding to p75 and p50 requires p45, p19 likely extends farther from p75 toward p45 than previously modeled. The biochemical stability of the 7-1-4 subcomplex predicts an extensive network of subunit interactions, only some of which we may be able to determine using proteins expressed in RRL.

Because all of the known biochemical functions of p50 are mediated by the p50 N-terminal domain, the function of the C-terminal half of p50 is uncertain. This region of p50 is not detectable in the holoenzyme structures and has a relatively small effect on telomerase function *in vitro* or *in vivo*. One tantalizing speculation is that this domain is

regulatory. Negative regulation is suggested by the higher specific activity of telomerase reconstituted with p50N30 *versus* full-length p50. Negative regulation is also consistent with telomere elongation in cells expressing p50-FZZ versus untagged p50, because C-terminal tagging could interfere with p50 C-terminal domain function. However, there are caveats to interpretation for all of biochemical and biological assays of p50 C-terminal domain function to date, which preclude a firm conclusion about its regulatory role. Considering results from holoenzyme reconstitution *in vitro*, the higher specific activity of telomerase RNP with p50N30 *versus* full-length p50 could derive from an impact of heterologous expression on domain folding. Unfortunately, *in vitro* activity comparison of purified holoenzymes endogenously assembled with p50 *versus* p50N30 is not reliable due to the heterogeneity of full-length p50 partial proteolysis. Finally, considering telomere length as an *in vivo* readout of holoenzyme activity, the shortened telomeres observed in p50N30-FZZ cells could arise from a difference in holoenzyme function but also could be secondary to p50N30-FZZ aggregation or functional interference from its C-terminal tag. Although we have not defined all of its roles, our studies establish that p50 has an N-terminal domain hub for holoenzyme assembly and activation and also a structurally uncharacterized C-terminal domain with potential regulatory function.

Acknowledgements

This work was supported by grants from NIH GM54198 to K.C., NSF MCB1022379 and NIH GM48123 to J.F., NIH GM071940 and AI069015 to Z.H.Z, NSF predoctoral fellowship to H.U., and Ruth L. Kirschstein NRSA postdoctoral fellowship GM101874 to E.J.M. We acknowledge the use of instruments at the Electron Imaging Center for NanoMachines supported by NIH (1S10RR23057 to ZHZ) and CNSI at UCLA.

Figure 2.1

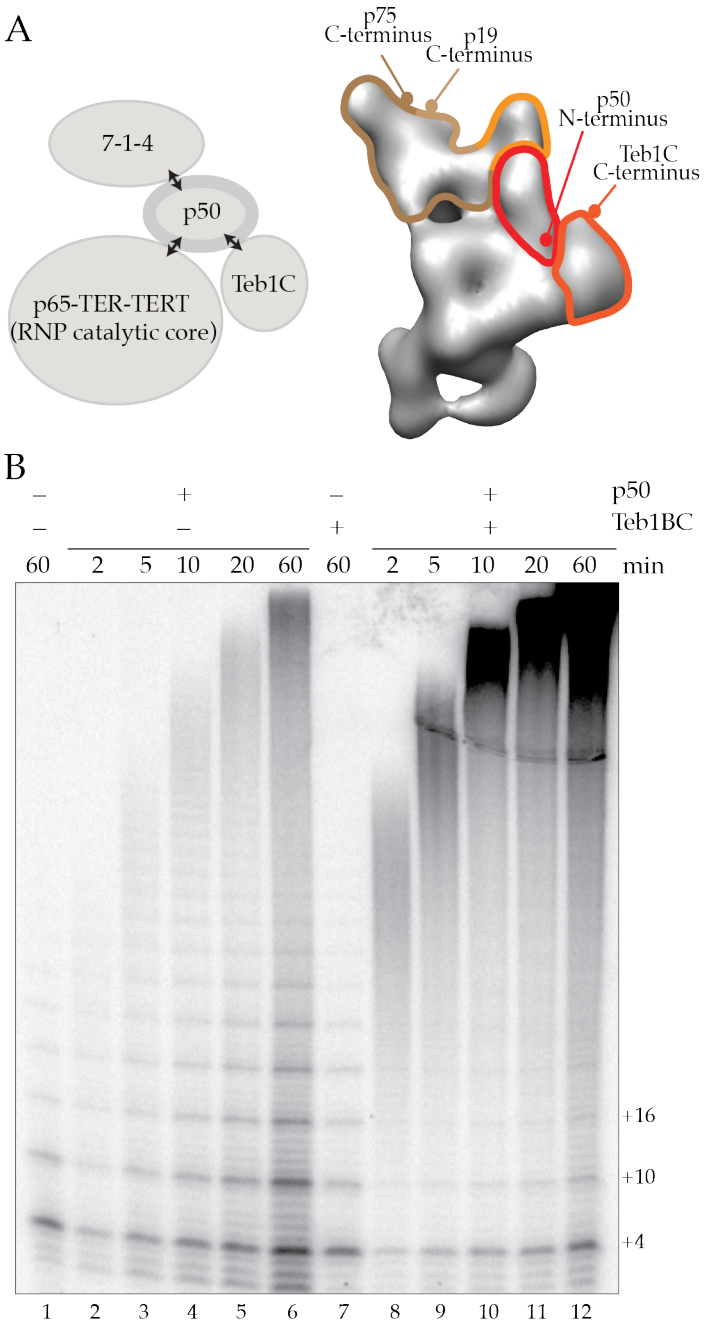

Catalytic activity stimulation by Teb1 involves an increase in the rate of product synthesis. (A) At left, the schematic summarizes the functional dependence of holoenzyme subcomplexes. At right, a 3D reconstruction of Teb1-F holoenzyme is shown with outlined regions assigned to 7-1-4 (brown, beige, and orange edges for p75, p19, and p45, respectively), p50, and Teb1 (Jiang et al., 2013). The protein terminus of these subunits mapped by Fab labeling is indicated. (B) Activity assays were performed for the RNP catalytic core alone (lane 1) or the RNP catalytic core with or without p50 and/or Teb1BC.

Figure 2.2

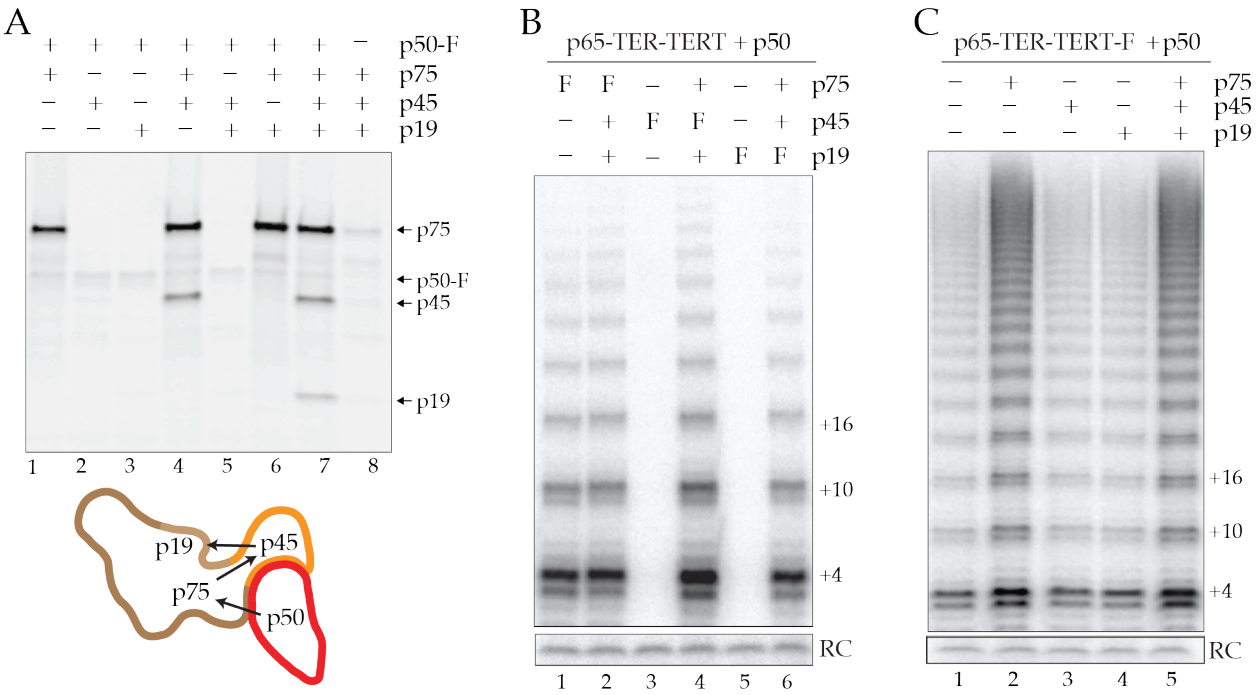

The p75 subunit of 7-1-4 interacts directly with p50. (A) Unlabeled p50-F was combined with RRL synthesis reactions of [^{35}S-Met]-labeled p75, p45, and/or p19, and the mixture was incubated with anti-FLAG antibody resin. Bound proteins were eluted and analyzed by SDS-PAGE. Trace radiolabeling of p50-F derived from protein synthesis after RRL mixing. Below the gel image, using the subunit outlining from Figure 2.1A, arrows indicate assembly dependence. (B and C) Activity assays are shown for telomerase complexes recovered by anti-FLAG antibody purification of the catalytic core, p50, and the indicated 7-1-4 subunit(s). In (B), F indicates the F-tagged subunit. RC is the recovery control added to telomerase products before precipitation. Quantification and normalization for relative methionine content gives a molar ratio of p75: p45: p19 of 1.0: 0.6: 0.2, consistent with the step-wise rather than exclusively cooperative assembly of 7-1-4 by p75 interaction with p45 and subsequent recruitment of p19.

Figure 2.3

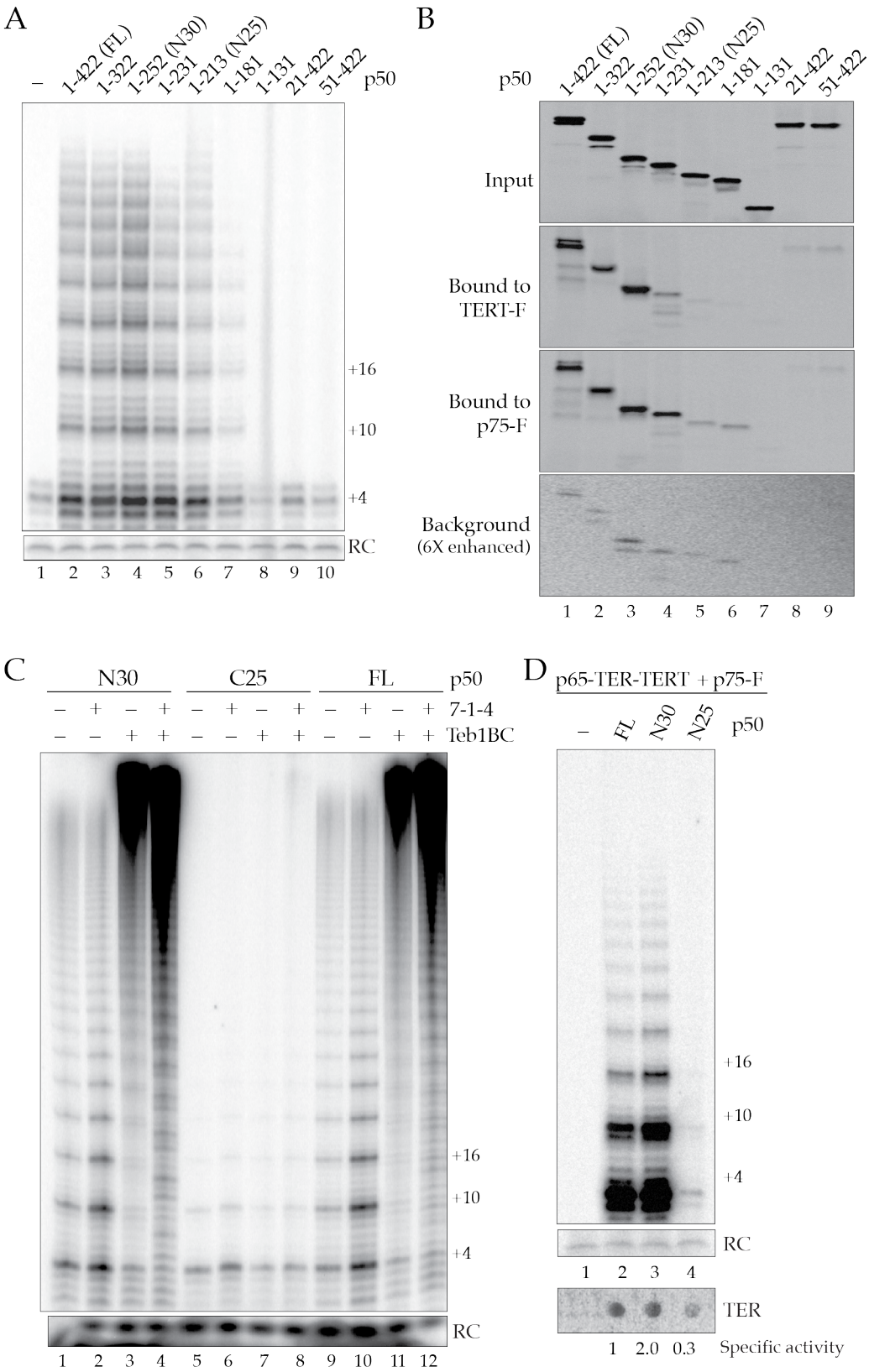
A
– 1-422 (FL) 1-322 1-252 (N30) 1-231 1-213 (N25) 1-181 1-131 21-422 51-422 p50
+16
+10
+4
RC
1 2 3 4 5 6 7 8 9 10
B
p50 1-422 (FL) 1-322 1-252 (N30) 1-231 1-213 (N25) 1-181 1-131 21-422 51-422
Input
Bound to TERT-F
Bound to p75-F
Background (6X enhanced)
1 2 3 4 5 6 7 8 9
C
N30 C25 FL p50
– + – + – + – + – + – + 7-1-4
– – + + – – + + – – + + Teb1BC
+16
+10
+4
RC
1 2 3 4 5 6 7 8 9 10 11 12
D
p65-TER-TERT + p75-F
– FL N30 N25 p50
+16
+10
+4
RC
1 2 3 4
TER
1 2.0 0.3 Specific activity

Figure 2.3 (cont.)

An N-terminal domain of p50 reconstitutes holoenzyme interactions and catalytic activity *in vitro*. (A) Full-length (FL) and truncated p50 polypeptides were combined with RNP catalytic core containing TERT-F, and complexes purified by anti-FLAG antibody resin were assayed for primer extension activity. (B) The same untagged p50 polypeptides were assayed for physical interaction with RNP catalytic core containing TERT-F, or for interaction with p75-F in the presence of untagged RNP catalytic core. The bottom panel is shown with radiolabeled protein signal intensity increased about 6 times relative to the other panels to allow visualization of the weak background of non-specific binding. (C) Activity assays were performed for 20 min using complexes assembled on RNP catalytic core containing TERT-F. (D) Activity assays were performed for complexes purified using p75-F that harbored the indicated untagged p50 polypeptide, with spot-blot hybridization for TER shown in the lower panel. Relative specific activity was calculated as the quantified ratio of product intensity to TER, normalizing full-length p50 to 1. Triplicate independent replicates of protein expression, RNP assembly, purification, and activity assay were performed on separate days with a specific activity increase for p50N30 relative to full-length p50 of 2.1 +/- 0.38 standard error of the mean.

Figure 2.4

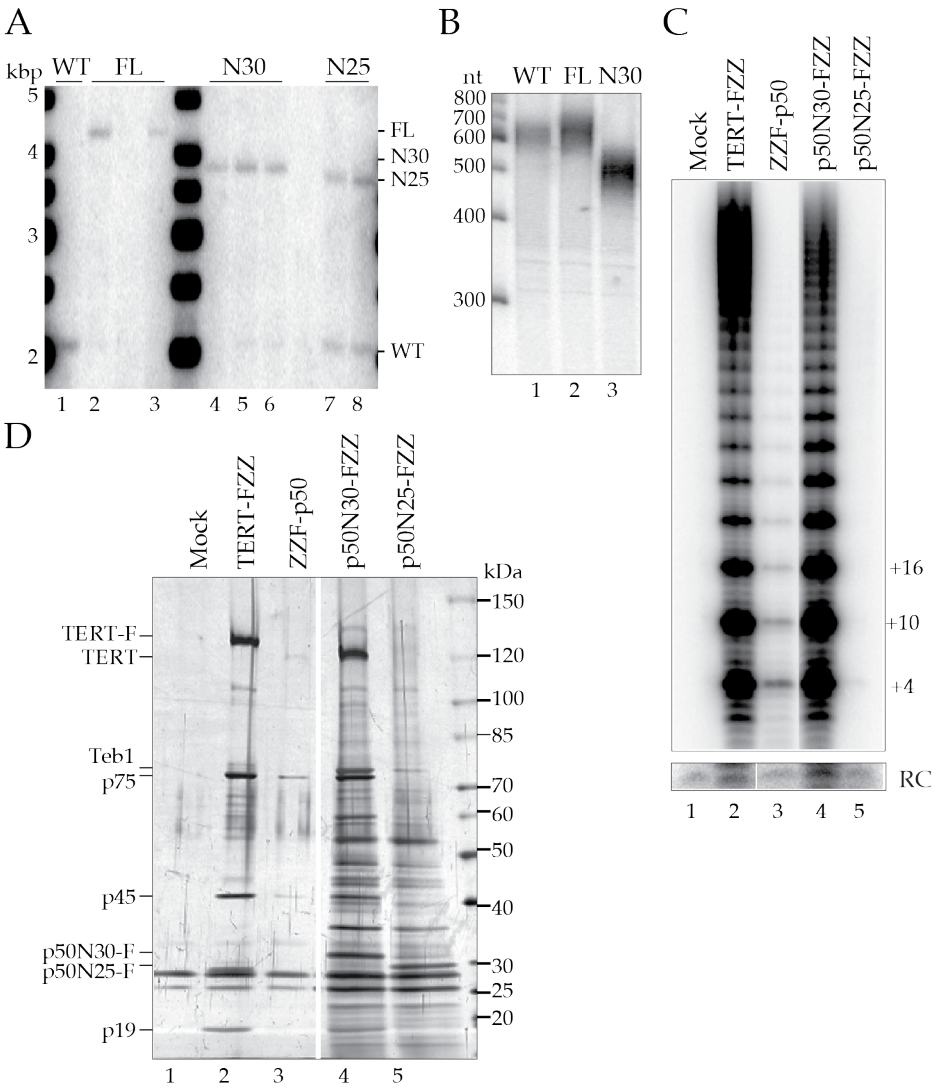

An N-terminal domain of p50 reconstitutes holoenzyme assembly *in vivo*. Cells or cell extracts had no tagged protein (WT) or a C-terminally tagged p50 polypeptide with recombinant open reading frame (full-length, N30, or N25 as indicated). (A) Genomic DNA Southern blots were performed to assess wild-type versus recombinant chromosome content. (B) Telomeric restriction fragment length was assayed after denaturing gel electrophoresis by hybridization with an oligonucleotide probe complementary to the subtelomeric region of the palindromic chromosome encoding ribosomal RNA. (C and D) Two-step affinity purifications from equivalent amounts of cell extract were assayed for telomerase catalytic activity (C) or protein composition (D). The right and left sides of each panel were cropped and aligned from the same gel with the same intensity settings.

Figure 2.5

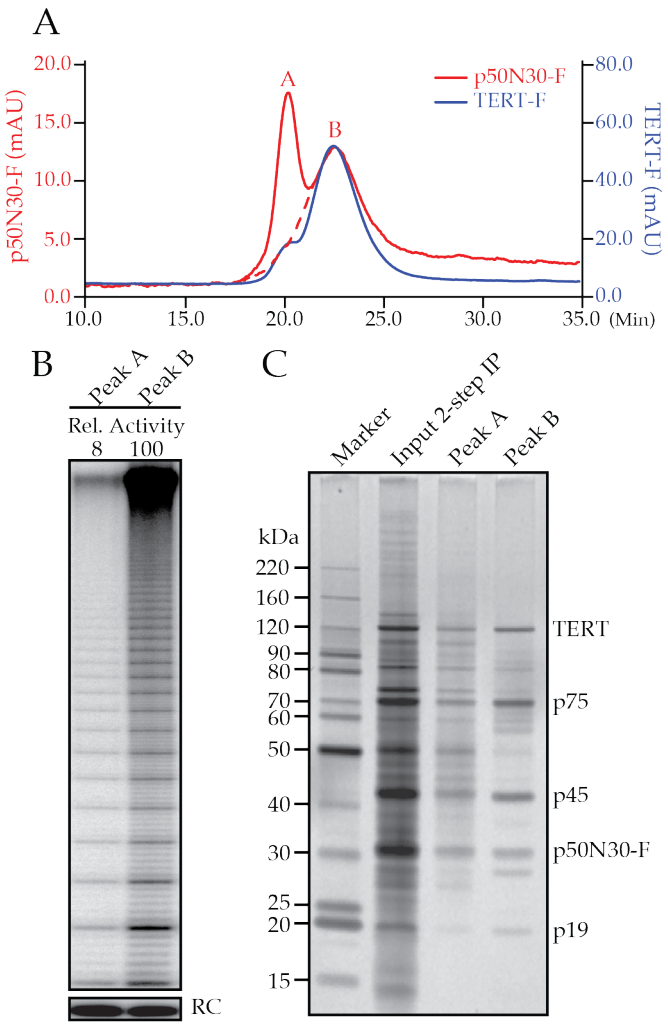

Purification of p50N30-F telomerase for EM. (A) Microscale size-exclusion purification of p50N30-F (red) and TERT-F (blue) after 2-step affinity purification. (B and C) Activity assay (B) or SDS-PAGE and silver staining (C) of p50N30-F telomerase purification by the size-exclusion chromatography shown in (A). In (B), relative (Rel.) activity is total product synthesis quantified for the assays shown, which used peak fractions normalized by absorbance at 280 nm. Note that activity detected in Peak A could derive from overlap with Peak B.

Figure 2.6

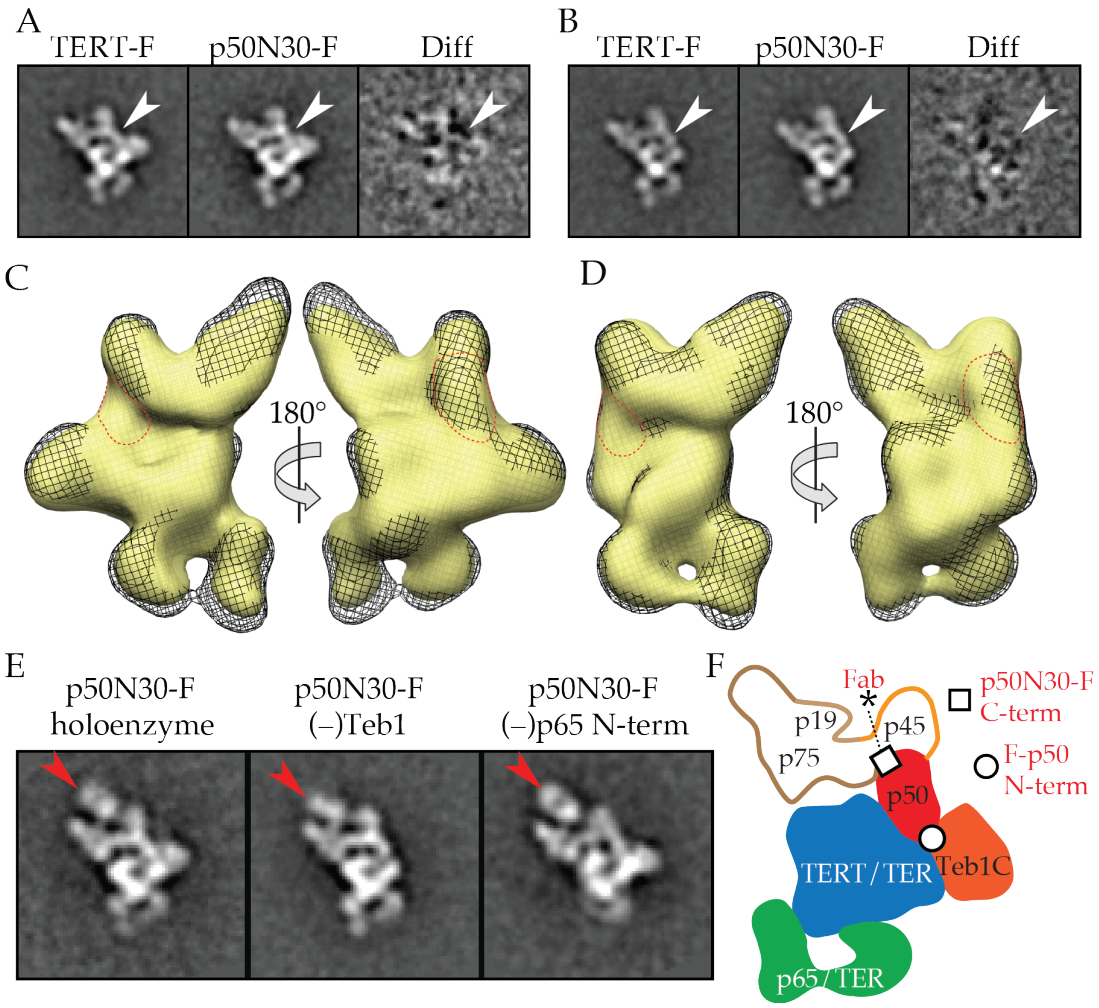

The p50 C-terminal region occupies an unknown location relative to other holoenzyme proteins. (A and B) Class averages of TERT-F, p50N30-F, and difference maps, for holoenzyme (A) or particles lacking Teb1 (B). White arrows indicate p50 location. (C and D) Comparison of RCT 3D reconstructions of TERT-F (black mesh) and p50N30-F (yellow surface) for holoenzyme (C) or particles lacking Teb1 (D), with p50 outlined (red dashes). The structure of p50N30-F telomerase with or without Teb1 was reconstructed using 1,162 or 945 particles, respectively. (E) Class averages of Fab-labeled p50N30-F telomerase. Red arrows indicate Fab density. (F) Model for subunit placement, highlighting the previously defined location of the p50 N-terminus (white circle) and the proposed location of the p50N30 C-terminus (white square) based on the location of the single Fab-bound paratope (asterisk). Box side length of class averages is 350 Å in (A), (B), and (E).

Figure 2.S1

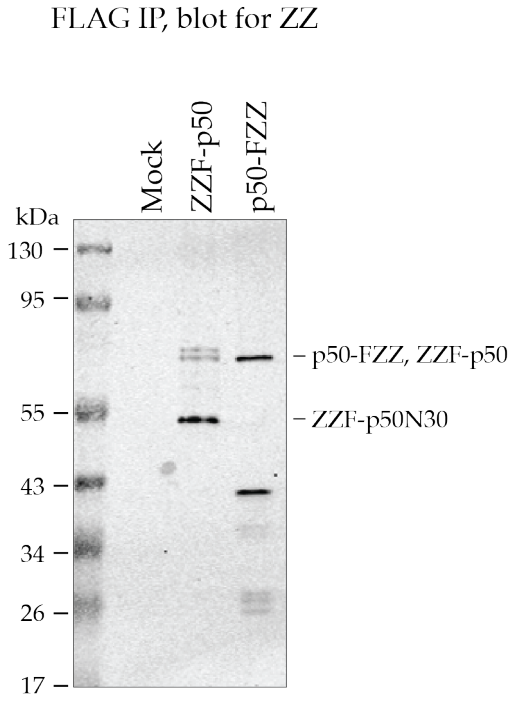

Endogenously expressed ZZF- or FZZ-tagged p50 can be truncated by partial proteolysis. One-step affinity purifications from cell extracts of *Tetrahymena* were performed using anti-FLAG antibody resin. Eluted samples were subject to immunoblot analysis with rabbit IgG as primary antibody to detect the ZZ tag module. Mock indicates purification from a cell extract lacking tagged protein. At right, the suggested annotation of full-length and truncated p50 proteins is based on SDS-PAGE migration.

Figure 2.S2

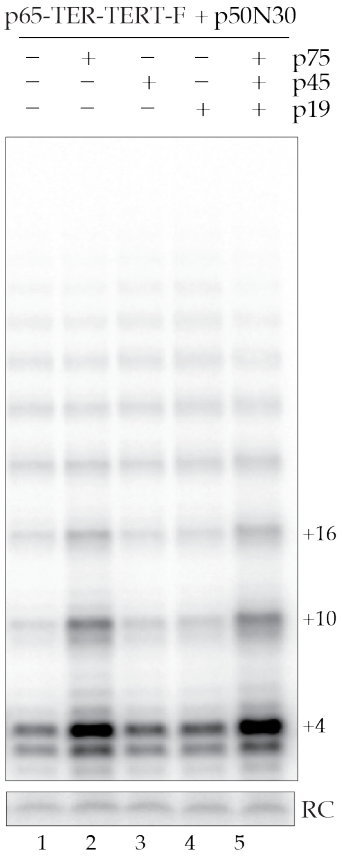

The N-terminal domain of p50 is sufficient for activity stimulation by p75. Activity assays were done as in Figure 2.2C with the substitution of p50N30 for full-length p50.

Figure 2.S3

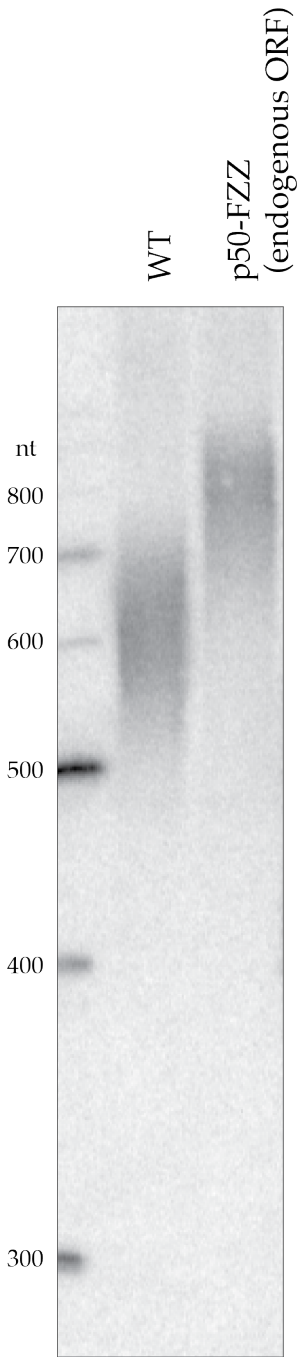

C-terminal tagging of p50 increases telomere length. Telomeric restriction fragment length was assayed after denaturing gel electrophoresis by hybridization with an oligonucleotide probe complementary to the subtelomeric region of the palindromic chromosome encoding ribosomal RNA. Genomic DNA from p50-FZZ cells used a cell line created previously (Min & Collins, 2009) by tag fusion to the endogenous open reading frame sequence.

Figure 2.S4

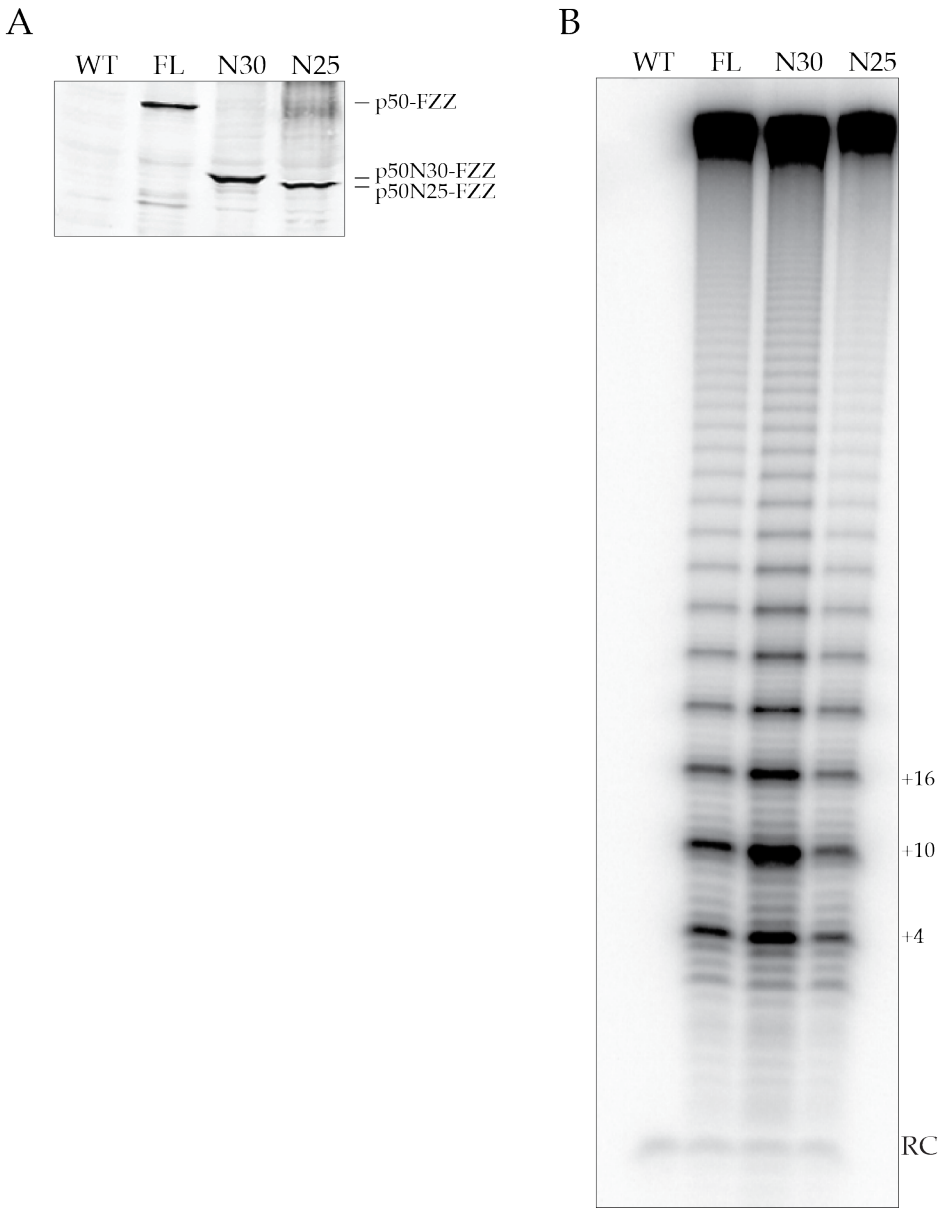

Endogenously expressed p50N30 and p50N25 can copurify telomerase holoenzyme activity. Cell extracts expressed no tagged protein (WT) or a full-length (FL) or truncated C- terminally tagged p50. (A) Cell extract was used for immunoblot analysis with rabbit IgG as primary antibody to detect the ZZ tag module. (B) One-step affinity purifications from *Tetrahymena* cell extract were performed using anti-FLAG antibody resin, with a 20 min activity assay reaction.

Figure 2.S5

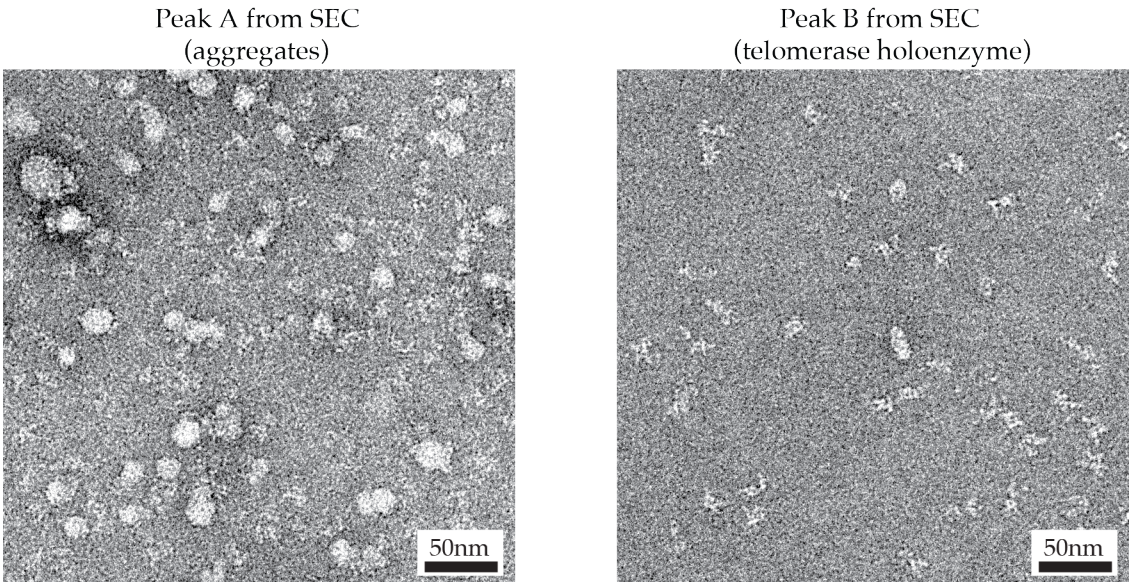

Representative negative staining EM images of p50N30-F telomerase in Peak A (left) and Peak B (right) from size-exclusion chromatography (see Figure 2.5).

Figure 2.S6

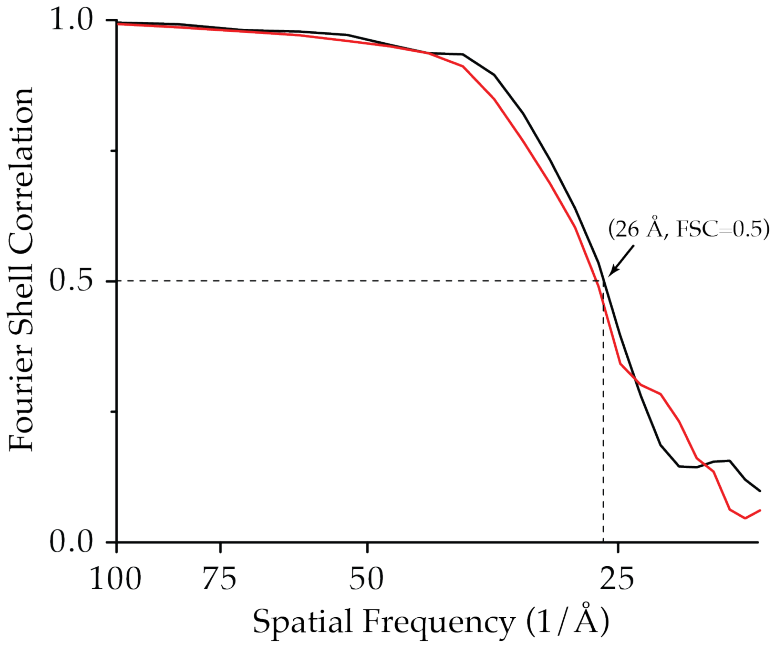

Fourier shell correlation (FSC) of the RCT 3D reconstructions of p50N30-F telomerase holoenzyme (black line) or particles lacking Teb1 (red line). Calculations were performed by splitting the data by odd and even numbers before the final round of 3D reconstruction. Both reconstructions have a resolution of ~26Å based on the FSC=0.5 criterion.

CHAPTER THREE

Direct Single-stranded DNA Binding by Teb1 Mediates the Recruitment of *Tetrahymena* Telomerase to Telomeres

Based on Upton et al., *MCB*, 2014

Abstract

The eukaryotic reverse transcriptase telomerase copies its internal RNA template to synthesize telomeric DNA repeats at chromosome ends to compensate for sequence loss during cell proliferation. Previous work has established several key factors involved in telomerase recruitment in yeast and mammalian cells; however, it remains unclear what determines the dynamically regulated association of telomerase with telomeres in *Tetrahymena thermophila*. Here we investigate the cell cycle dependence of telomere binding by each of the seven *Tetrahymena* telomerase holoenzyme proteins TERT, p65, Teb1, p50, p75, p45, and p19. We observed coordinate cell cycle-regulated recruitment and release of all of the subunits, including the telomeric-repeat DNA binding subunit Teb1. Using domain truncation and mutagenesis approaches we investigated which subunits govern the interaction of telomerase holoenzyme with telomeres. Our results show that Teb1 is critical for telomere interaction of other holoenzyme subunits and demonstrate that high affinity Teb1 DNA binding activity is necessary and sufficient for cell cycle-dependent telomere interaction despite constitutive holoenzyme assembly. Overall these and additional findings indicate that in *Tetrahymena*, telomerase recruitment to telomeres requires direct single-stranded DNA binding in contrast to indirect DNA recognition through telomere-bound proteins in yeast and mammalian cells.

Introduction

The ends of linear chromosomes are subjected to an onslaught of illicitly activated double-stranded DNA (dsDNA) repair mechanisms and sequence loss due to incomplete replication by DNA polymerases (O'Sullivan & Karlseder, 2010). These biological challenges are in part overcome by the presence of tandem telomeric DNA repeats at the termini of eukaryotic nuclear chromosomes (for example the sequence TTAGGG in humans and TTGGGG in the ciliate *Tetrahymena*), which extend to form an overhang on the 3′-OH strand (Blackburn & Gall, 1978; Blackburn et al., 2006; Moyzis et al., 1988). Each terminal repeat array is maintained in a dynamic equilibrium of telomeric DNA attrition from genome replication and *de novo* synthesis by the enzyme telomerase (de Lange, 2009; Greider, 1996; Pfeiffer & Lingner, 2013). The telomerase ribonucleoprotein (RNP) is minimally composed of the catalytic reverse transcriptase (TERT) and an RNA with an internal template (TER) responsible for RNA-dependent extension of the 3′ chromosome end (Blackburn & Collins, 2011; Hengesbach et al., 2011). While *in vitro* DNA synthesis activity can be reconstituted by expression of only TERT and TER, additional subunits of the telomerase complex are required for high activity and processivity *in vitro* and for telomere elongation by telomerase recruitment to telomeres *in vivo* (Egan & Collins, 2012; Podlevsky & Chen, 2012).

Studies in yeasts and mammalian cells have yielded significant insights into how telomere proteins recruit telomerase by protein-protein interactions (Nandakumar & Cech, 2013; Stewart et al., 2012). In mammalian cells, telomere-bound protein complexes termed shelterin (O'Sullivan & Karlseder, 2010; Palm & de Lange, 2008) include the dsDNA telomere binding proteins TRF1 and TRF2 and the single-stranded DNA (ssDNA) telomere binding protein POT1 (Baumann & Cech, 2001; Palm & de Lange, 2008). Together with RAP1 and the TIN2 and TPP1 proteins that bridge TRF1 and TRF2 to POT1, the telomeric DNA binding proteins create a network of complexes that block DNA damage response activation (Palm & de Lange, 2008). Interestingly, TPP1 also interacts with telomerase as an essential step of recruitment in a manner physiologically restricted to S-phase of the cell cycle (Sexton et al., 2012; Xin, Liu, Wan, Safari, Kim, O'Connor, et al., 2007; Zhang et al., 2013; Zhong et al., 2012). In fission yeast the dsDNA binding protein Taz1 takes the place of TRF1 and TRF2, Pot1 binds to the single-stranded DNA overhang, and Rap1, Poz1, and Tpz1 function as bridging proteins that link Taz1 to Pot1 (Miyoshi et al., 2008; Moser & Nakamura, 2009). Like mammalian TPP1, Tpz1 and another telomere protein Ccq1 recruit telomerase to telomeres only in S-phase of the cell cycle (Miyoshi et al., 2008; Tomita & Cooper, 2008).

Ciliates provide yet another model system for studies of telomere and telomerase biology. Their unusual genomic organization of a germline micronucleus and a polyploid, fragmented-chromosome macronucleus obliges tens of thousands of telomeres and an abundance of telomerase (Jahn & Klobutcher, 2002). In the model organism *Tetrahymena*, macronuclear telomeres are bound by a POT1 ortholog, Pot1a,

which associates with the TPP1 ortholog Tpt1 to prevent DNA damage response activation and negatively regulate telomerase access (Jacob, Lescasse, Linger, & Price, 2007; Linger et al., 2011). Two additional proteins, Pat1 and Pat2, interact with Pot1a-Tpt1 but their biological role is not well understood (Linger et al., 2011; Premkumar et al., 2014). While Pat1 and Pat2 are not required for telomere end-protection, they are essential for end elongation by telomerase. The *Tetrahymena* telomerase holoenzyme subunits TERT, TER, and p65 (which form the physiological RNP catalytic core) and Teb1, p75, p50, p45, and p19 (subunits necessary for telomerase function at telomeres) are co-assembled in both dividing and non-dividing cells (Min & Collins, 2009; Witkin & Collins, 2004; Witkin et al., 2007). This potentially constitutive assembly of holoenzyme is different from the paradigm set by yeast telomerase holoenzyme subunit regulation by the cell cycle (Egan & Collins, 2012; Moser, Chang, Kosti, & Nakamura, 2011; Moser & Nakamura, 2009; Nandakumar & Cech, 2013). Nonetheless, constitutive *Tetrahymena* telomerase holoenzyme assembly would be consistent with the dramatic elongation of telomeres in non-dividing cells depleted of the Pot1a-Tpt1-Pat1-Pat2 complex (Jacob et al., 2007).

Reconstitution assays have enabled the dissection of the biochemical roles of individual telomerase holoenzyme subunits, providing an important foundation for investigating the mechanism and regulation of telomere elongation *in vivo*. Extensive studies have demonstrated that within the telomerase catalytic core, both TERT and TER interact with ssDNA. The TERT N-terminal (TEN) domain stimulates active-site use of a short primer-template hybrid while the remainder of TERT provides some functional recognition and physical protection of ssDNA (Wu & Collins, 2014). Within TER the template binds to the ssDNA 3′ end by hybridization, and other RNA motifs contribute to template placement in the active site (Blackburn & Collins, 2011). Additional telomerase holoenzyme proteins augment the activity of the catalytic core *in vitro*, but the relation of these *in vitro* activities to their roles *in vivo* remains unclear.

Among the *Tetrahymena* holoenzyme accessory subunits, the p50 N-terminal 30 kDa region (p50N30) confers high repeat addition processivity (RAP) and is sufficient to bind p75 and the catalytic core *in vitro* with the C-terminal region of p50 possibly acting to restrain holoenzyme activity (Hong et al., 2013; Jiang et al., 2013). Addition of Teb1 to the p50-bound RNP catalytic core increases the elongation rate of tandem repeat synthesis under conditions typical for telomerase assays *in vitro.* Of the accessory subunits, only Teb1 has domains readily detectable by sequence homology, with a composition of four oligonucleotide/oligosaccharide-binding (OB)-fold domains (Min & Collins, 2009, 2010). The domain architecture of Teb1 is paralogous to that of the largest subunit, Rpa1, of the general ssDNA binding factor Replication Protein A (RPA) (Min & Collins, 2009, 2010). Three of the four predicted Teb1 OB-fold domains are confirmed by high-resolution structures, including a co-crystal structure of the highest affinity Teb1 DNA binding domain with telomeric ssDNA (Zeng et al., 2011).

To gain additional insight into how these telomerase holoenzyme subunits are assembled *in vivo* and engaged at the telomere, we utilized chromatin immunoprecipitation (ChIP) assays to investigate cell cycle regulated changes in the association of *Tetrahymena* telomerase holoenzyme subunits with telomeres. Here we show that all of the *Tetrahymena* telomerase proteins have telomere interaction that is restricted in the cell cycle, despite ubiquitous, cell cycle independent assembly of the high-RAP holoenzyme complex. Furthermore, using numerous domain and sequence variants of p50 and Teb1, we define Teb1 as a critical subunit in the recruitment of the telomerase holoenzyme to the telomere. By creating a panel of full-length Teb1 proteins defective specifically in holoenzyme assembly or individual sites of DNA interaction, we show that the affinity of DNA binding influences Teb1 association with telomeres. Together these results suggest a direct DNA interaction mechanism for *Tetrahymena* telomerase recruitment to telomeres that is distinct from the recruitment mechanisms proposed in other organisms. Overall our findings provide new structural insights about the *Tetrahymena* telomerase holoenzyme, contribute to understanding telomerase enzyme mechanism, and illuminate a new level of detail for the cellular process of telomerase recruitment to telomeres.

Materials and Methods

Telomerase reconstitutions

Telomerase reconstitution assays used codon-optimized open reading frames for TERT, p50, and p75 expression in rabbit reticulocyte lysate (RRL) and for Teb1 and p65 expression in *Escherichia coli* as previously described (Jiang et al., 2013; Min & Collins, 2009). For RNP catalytic core assembly, recombinant p65 and *in vitro* transcribed TER were added to the TERT RRL expression reaction during protein synthesis at 25 nM each. Holoenzyme reconstitution and affinity purification from RRL synthesis reactions were performed as described in previously optimized protocols (Hong et al., 2013; Jiang et al., 2013; Min & Collins, 2010). Briefly, telomerase complexes were bound to anti-FLAG M2 affinity resin (Sigma) and washed into T_2MG (20 mM Tris-HCl [pH 8.0], 1 mM $MgCl_2$, 10% glycerol, and 2 mM dithiothreitol [DTT]). Recombinant Teb1 was purified using Ni-NTA agarose and added to a final concentration of 200 nM for 20 min at room temperature prior to the activity assay.

Telomerase activity and DNA binding assays

Activity assays of native and reconstituted holoenzyme were performed at room temperature using a standard *Tetrahymena* telomerase reaction buffer containing 50 mM Tris-acetate (pH 8.0), 2 mM $MgCl_2$, 10 mM spermidine, and 5 mM β-mercaptoethanol. Product synthesis reactions additionally contained 24 nM [α-^{32}P] dGTP, 300 nM unlabeled dGTP, 200 μM unlabeled dTTP, and 200 nM DNA primer $(GT_2G_3)_3$. Reactions were allowed to proceed for 5 min for purified endogenous holoenzyme and 10 min for

recombinant holoenzyme. *Tetrahymena* cell lysate was assayed at a final dilution of 1:200 for 10 min. A 5′-labeled oligonucleotide DNA recovery control (RC) was added to telomerase products before precipitation. Products were resolved by denaturing gel electrophoresis and detected by phosphorimager analysis using a Typhoon Trio.

Expression constructs for sequence-modified Teb1BC and full-length Teb1 were generated using PCR-based mutagenesis. N-terminally 6-histidine (His_6) tagged proteins were bacterially expressed and isolated by single-step nickel agarose purification. Extensive washing and subsequent elution resulted in soluble protein purified to homogeneity as visualized by SDS-PAGE. Electrophoretic mobility shift assays (EMSAs) with recombinant Teb1 were performed as described previously (Min & Collins, 2010) using the ^{32}P 5′ end-labeled oligonucleotide 5′-GTTGGGGTTGGGGTTGGG-3′ as the probe. Binding affinities were calculated based on free probe signal using ImageQuant software.

Tetrahymena *strain construction, cell growth, and enzyme purification from extract*

Tetrahymena endogenous-locus replacement strains TERT-FZZ, Teb1-FZZ, p75-FZZ, p65-FZZ, p50-FZZ, p45-FZZ, and p19-FZZ and transgene strains p50N30-FZZ, p50N25-FZZ, ZZF-p50, Teb1-FZZ, F-Teb1BC, and F-Teb1C were previously described (Hong et al., 2013; Jiang et al., 2013; Min & Collins, 2009). F-Teb1BC and F-Teb1C were expressed in the genetic background of TERT with a C-terminal ZZ-tag (Jiang et al., 2013). New strains Teb1 F590A F648A-FZZ, Teb1 Δ555-581 GSGSG-FZZ (ΔZn), Teb1 Δ660-666 AGSSG-FZZ (ΔL_{45}), Teb1 Δ687-701-FZZ (ΔCTαH), Teb1 F293A-FZZ, Teb1 K300A-FZZ, Teb1 F423A-FZZ, Teb1 Y450A-FZZ, Teb1 F603A-FZZ, and Teb1 K660A-FZZ were made by targeting transgene integration at the β-tubulin 1 locus (*BTU1*) under control of the metallothionein 1 (*MTT1*) promoter using selection for blasticidin resistance conferred by the bsr2 cassette (Couvillion & Collins, 2012). Strains expressing p50N25-FZZ, ZZF-p50, F-Teb1BC, F-Teb1C, and all of the newly generated Teb1-FZZ strains retain endogenous subunit expression for viability. Genotypes were verified by Southern blot and western blot for the transgene-encoded protein.

Cells were grown in modified Neff medium (0.25% proteose peptone, 0.25% yeast extract, 0.5% dextrose, and 30 μM $FeCl_3$) to mid-log phase (3 x 10^5 cells/mL). Cells were starved in 10 mM Tris (pH 8.0) for 16 h and re-fed with modified Neff medium to synchronize the cell cycle at G_1. For transgene expression, transgene induction was achieved by addition of $CdCl_2$ to a final concentration of 0.5 μg/mL upon re-feeding. Cell counts were measured by fixation in 0.4% formaldehyde. Cell counting was completed in triplicate independent growth cultures.

Cell extract preparation and affinity purification were performed as described (Min & Collins, 2009). For western blots, cell pellets were lysed by heating at 95°C for 5 min in 100 μL of 2x SDS loading buffer (4% SDS, 160 mM Tris-HCl [pH 6.8], 20% glycerol,

0.0025% bromophenol blue, 10% β-mercaptoethanol) to avoid sample proteolysis. Protein extracts were separated on a 10% SDS-polyacrylamide gel and transferred to Hybond N-XL nitrocellulose membrane (Amersham Biosciences). Blots were blocked in 5% milk and 1x Tris-buffered saline (TBS; 50 mM Tris-HCl [pH 7.5], 150 mM NaCl) then incubated with anti-FLAG M2 mouse monoclonal antibody (Sigma) and anti-tubulin DM1A mouse monoclonal antibody (EMD Millipore). For TER Northern blot analysis, RNA was spotted onto nitrocellulose membrane, UV-crosslinked, and hybridized using a ^{32}P end-labeled oligonucleotide (5′-AGGTTCAAATAAGTGGTAATGCGGGACAAAA GACTATCG-3′).

ChIP analysis

For each assay 2 x 10^7 cells per immunoprecipitation were fixed with 0.75% formaldehyde at room temperature for 10 min, quenched with 125 mM Tris (pH 7.5), and washed twice with TBS. Nuclei were isolated as described by Jacob *et al* (Jacob, Stout, & Price, 2004). Briefly, pelleted cells were lysed in 10 ml of 1x TMS (10 mM Tris-HCl [pH 7.5], 10 mM $MgCl_2$, 3 mM $CaCl_2$, 250 mM sucrose, and 1 mM DTT), 0.16% Igepal CA-630 for 20 min at 4°C with end-over-end rotation. Sucrose was added to a concentration of 0.816 g/mL and the lysate was centrifuged at 9,000 *x g* for 30 min at 4°C. The pelleted nuclei were washed once with TMS before micrococcal nuclease (MNase) digestion. For MNase digestion, nuclei were resuspended in 500 µL 50 mM Tris-HCl (pH 7.5), 60 mM KCl, 15 mM NaCl, 2 mM $CaCl_2$, 0.05% spermidine phosphate, and 1 mM DTT and treated with 6 U MNase (New England Biolabs) for 30 min on ice (generated fragment size of ~500 bp dsDNA; data not shown). The reaction was stopped by adding ethylenediaminetetraacetic acid (EDTA) to a final concentration of 50 mM and the nuclei were lysed in the presence of 2% Triton X-100, 250 mM NaCl, and protease inhibitors (0.1 mM phenylmethanesulfonyl fluoride and 1x Sigma Protease Inhibitor Cocktail) followed by incubation at room temperature for 30 min.

The lysate was centrifuged at 16,000 *x g* for 5 min at 4°C and the supernatant was immunoprecipitated overnight at 4°C with anti-FLAG M2 affinity resin (Sigma). Precipitates were washed sequentially with 1 mL each Buffer A (50 mM Tris-HCl [pH 7.5], 250 mM NaCl, 2% Triton X-100, and 5 mM EDTA), Buffer B (50 mM Tris-HCl [pH 7.5], 250 mM NaCl, 1.5% Triton X-100, and 5 mM EDTA), CHAPS Buffer (50 mM Tris-HCl [pH 7.5], 250 mM NaCl, 1% Triton X-100, 5 mM EDTA, 0.1% SDS, and 0.05% 3-[(3-cholamidopropyl)dimethylammonio]-1-propanesulfonate), and LiCl Buffer (50 mM Tris-HCl [pH 7.5], 250 mM NaCl, 1% Triton X-100, 5 mM EDTA, and 150 mM LiCl). DNA crosslinks were reversed and the bound material was eluted by resuspending the resin in 400 µL Elution Buffer (50 mM Tris-HCl [pH 7.5], 200 mM NaCl, 1% SDS, and 1 mM EDTA) and incubating at 65°C for 16 hours.

The eluted DNA was purified by phenol:chloroform:isoamyl alcohol (25:24:1) extraction and ethanol precipitation. Resulting product was spotted on nitrocellulose membrane,

UV-crosslinked, and hybridized with 5′-end labeled probe against the telomeric DNA (5′-CCCCAACCCCAACCCCAA-3′) or the sub-telomeric ribosomal DNA (rDNA) (5′-TGATAAATAACCAAAAATCAAAGTATTACATCAATAAATAACTTTTACTCAATG TCAAAGAAATTATTGGGG-3′). Additional hybridization using a probe for an internal rDNA region was also performed to ensure sufficient fragmentation of all ChIP samples. Dot blots were hybridized in 30 mM NaCl, 3 mM $Na_3C_6H_5O_7$, and 0.1% SDS at 55°C for 12-16 h, washed, then quantified by phosphorimager analysis. Relative signal was quantified using ImageQuant software. Resulting data was normalized to input rDNA signal following subtraction of background, to calculate signal from telomerase per chromosome end rather than per length of telomeric repeat DNA tract.

Results

Tetrahymena *telomerase association with telomeres is cell cycle regulated*

To address how telomere interaction by telomerase is coordinated with genome replication in *Tetrahymena*, we exploited a G_1 cell cycle phase enrichment protocol involving nutrient starvation to establish synchrony. Following starvation, cells were re-fed and samples were collected for ChIP as a time course of cell cycle progression. The micronucleus replicates and divides rapidly, but only in subsequent macronuclear replication does the vast majority of telomere synthesis occur. Macronuclear DNA synthesis occurs broadly over an interval from approximately 2 to 4 h post feeding, followed by morphological changes that ultimately pinch apart the macronucleus and the cell (Figure 3.1A). To confirm the synchrony of cell cycle entry, cell counts were taken in triplicate at several time points. There was no major change in cell number over a 6 h period after feeding, but at approximately 8 h the cell count doubled (Figure 3.1B).

The method of choice for detecting and quantifying chromosome association of telomere-recruited factors like telomerase is telomere ChIP. This technique is typically limited by variable affinity and specificity of antibodies against individual telomere-associated proteins. To overcome this hurdle, we combined endogenous-locus tagging of telomerase holoenzyme proteins with FLAG monoclonal antibody ChIP. Previously generated telomerase tagged-subunit strains, each expressing a holoenzyme protein with a C-terminal triple FLAG peptide (F) and tandem protein A domains (ZZ) in substitution of the untagged native protein from the endogenous locus, were used to ensure physiological subunit expression level and biological function. Consistent with their cellular assembly as a holoenzyme complex, comparable levels of tagged TERT-FZZ, Teb1-FZZ, p75-FZZ, p65-FZZ, p50-FZZ, p45-FZZ, and p19-FZZ were detected in whole cell extract by FLAG antibody western blot (Figure 3.1C). The slight reduction in accumulation of p19-FZZ was previously shown to be an artifact of protein tagging at the C-terminus (Min & Collins, 2009).

Telomerase catalytic activity assayed in cell extracts was similar for cells from parental and tagged-subunit expression strains at different stages of the cell cycle (Figure 3.1D). From each strain at each time point, fragmented chromatin was prepared from formaldehyde-crosslinked cells (data not shown) and used for immunoprecipitation of the tagged protein subunit. Because of the relative abundance of endogenous telomerase in *Tetrahymena*, we were able to quantify protein-bound telomeric repeat DNA directly by hybridization of crosslink-reversed DNA with an end-labeled oligonucleotide complementary to the G-rich telomeric repeats (data not shown). To control for input extract variations in the preparation of total chromatin, we normalized telomere ChIP signal to rDNA chromosome signal in the input extract (see Materials and Methods). Only low sub-telomeric rDNA chromosome hybridization signal was detected in bound ChIP samples (data not shown).

We found that all seven telomerase holoenzyme proteins dramatically increased in telomere association with cell cycle progression to S phase, after which telomere association for all proteins except p50-FZZ decreased (Figure 3.1E). Notably, the peripheral holoenzyme subunit Teb1 had a similar telomere ChIP profile compared to the RNP catalytic core subunits TERT and p65 (Figure 3.1E), despite indirect interaction of Teb1 with the RNP catalytic core through p50 (Jiang et al., 2013). The delay in loss of telomere ChIP at 6 h unique to p50-FZZ may be a difference imposed by epitope tagging, since previous studies indicate that C-terminal tagging of p50 affects enzyme catalytic activity and increases the length at which telomeres are maintained in cells (Hong et al., 2013; Min & Collins, 2009). It is also possible that telomerase holoenzyme architecture changes following telomere recruitment in a manner that increases p50 crosslinking efficiency prior to holoenzyme dissociation, possibly by bringing p50 in closer proximity to product DNA. The alternate explanation that prolonged ChIP signal reflects telomere binding by holoenzyme-free as well as holoenzyme-bound p50 is doubtful, because the biological stability of p50 depends on the other holoenzyme subunits and thus p50 is unlikely to be present as a holoenzyme-free protein (Min & Collins, 2009). Overall we conclude that telomerase holoenzyme subunits are not constitutively bound to telomeres and that all holoenzyme proteins show coordinate telomere recruitment in the cell cycle interval of macronuclear genome replication.

Telomere recruitment is independent of the p50 C-terminal domain but requires p50 interaction with Teb1

Previous functional analyses demonstrated that the N-terminal 252 residues of p50 (p50N30) support all biochemically identified roles of p50 (Hong et al., 2013). Removal of an additional 39 residues (p50N25) compromised holoenzyme assembly and stability, but the holoenzyme that did assemble with p50N25 retained normal catalytic activity *in vivo* and *in vitro* (Hong et al., 2013). Furthermore, previous structural analyses indicate that all of the p50 subunit density in the holoenzyme structure determined by electron microscopy (EM) derives from p50N30 (Hong et al., 2013; Jiang et al., 2013). The C-

terminal 20 kDa of p50 appears at least partially disordered in structure, as it is highly sensitive to proteolysis in native cell extract (Hong et al., 2013; Jiang et al., 2013). However, because C-terminal tagging of p50 increases telomere length, the p50 C-terminal domain seems likely to have a biological role in holoenzyme regulation (Hong et al., 2013). In contrast to C-terminal tagging, N-terminal tagging of p50 inhibits the holoenzyme association of Teb1 and disrupts telomerase biological function (Jiang et al., 2013). To investigate how these phenotypes relate to changes in telomerase-telomere interaction, we examined telomere ChIP by N- or C-terminally tagged full-length or truncated p50 proteins (Figure 3.2A) in strains with either complete or partial disruption of the endogenous p50 locus (see Materials and Methods).

We assayed ChIP for C-terminally tagged full-length p50 and p50N30 each expressed in replacement of the endogenous untagged protein, which gave the tagged proteins similar accumulation levels in cells (Figure 3.2B, lanes 1-3). Expression of p50N25 was at a lower cellular level (Figure 3.2B, lane 4) due to incomplete genetic substitution for the endogenous protein (Hong et al., 2013). Because ChIP uses denaturing cell lysis and protein purification conditions, it should reduce the differences in p50 purification recovery imposed by native extract proteolysis between the p50-FZZ C-terminal tag and the N-terminal domain (Jiang et al., 2013). Indeed, ChIP by p50-FZZ and p50N30-FZZ was similarly robust, while ChIP by p50N25-FZZ had reduced signal (Figure 3.2C). Like p50-FZZ, ChIP of p50N30-FZZ showed the same increase in telomeric signal with the onset of macronuclear replication and the same persistence of ChIP signal at 6 h. As described above for p50-FZZ, the p50N30-FZZ increase in ChIP telomere signal from 4 to 6 h could reflect a change in holoenzyme regulation imposed by elimination of the p50 C-terminal domain. Truncation of p50N30 to p50N25 decreased but did not eliminate telomeric signal association (Figure 3.2C), consistent with some p50N25 holoenzyme assembly *in vivo*. In contrast, ChIP signal was minimal if at all detectable for the N-terminally tagged full-length ZZF-p50 (Figure 3.2C). Because Teb1 is the only holoenzyme subunit dissociated by p50 N-terminal tagging (Hong et al., 2013; Jiang et al., 2013), this finding suggests that Teb1 is required for telomere association of the other holoenzyme subunits assayed by ZZF-p50 ChIP.

Single-residue substitutions of OB-fold DNA binding surfaces impose a DNA binding or telomerase activation defect in full-length Teb1

Paralogous to Rpa1, Teb1 has an N-terminal domain and three additional OB-fold domains sequentially designated A, B, and C (Min & Collins, 2010). Rpa1 A, B, and C domains interact with ssDNA with affinity contribution A>B>C (Wold, 1997). Teb1 A and B domains specifically bind the *Tetrahymena* telomeric repeat G-rich ssDNA with affinity A>B (Min & Collins, 2010). Teb1C can enhance Teb1B DNA binding activity, but whether Teb1C interacts with DNA directly is unknown. Teb1C does interact directly with the p50 RNP catalytic core and alone can stimulate its catalytic activity.

These findings provided the groundwork for understanding what biochemical properties of Teb1 are required for telomerase-telomere interaction.

To better characterize the contributions of each Teb1 OB-fold domain to overall Teb1 function, we constructed a panel of full-length Teb1 proteins with single amino acid substitutions on the typical DNA binding surfaces of the A, B, and C domains. Single residue substitutions to alanine were previously assayed in single-domain Teb1A, single-domain Teb1B, or Teb1BC (Zeng et al., 2011). Here we generated two different substitutions in each domain in full-length protein context (Figure 3.3A), using substitutions that eliminated Teb1A-DNA interaction by EMSA (F298A, K300A), reduced Teb1B-DNA interaction ~5-fold assayed by filter binding (F423A or Y450A), or reduced Teb1BC DNA binding affinity to near that of Teb1B alone (F603A or K660A). Both Teb1C substitutions also greatly inhibited telomerase catalytic activation.

Bacterial expression and affinity purification of N-terminally tagged full-length Teb1 proteins gave predominantly full-length protein by single-step affinity purification (Figure 3.3B). We used the purified proteins for ssDNA interaction EMSA assays (Figure 3.3C and D). The two substitutions in the Teb1A domain had the greatest impact on DNA binding, decreasing affinity ~20- and ~15-fold for F293A and K300A, respectively. Substitutions in the Teb1B domain decreased DNA binding affinity less severely, by at most ~10-fold. The Teb1C domain substitution F603A did not affect full-length Teb1 DNA binding affinity, while the K660A substitution imposed a loss of DNA binding activity that was variable between replicate assays, suggestive of a loss of overall protein folding stability.

Next we tested the panel of Teb1 proteins for *in vitro* reconstitution of high-RAP telomerase activity assayed by direct primer extension with dTTP and radiolabeled dGTP (Figure 3.3E). The RNP catalytic core containing bacterially expressed p65, *in vitro* transcribed TER, and RRL-expressed C-terminally FLAG-tagged TERT (TERT-F) was assembled in RRL and combined with separately RRL-expressed p50 and p75. Telomerase complexes were affinity purified using FLAG antibody resin and then combined with bacterially expressed Teb1 in the activity assay prior to addition of the DNA primer. Full-length Teb1 with a DNA binding domain F298A, K300A, F423A, or Y450A substitution showed little if any difference from wild-type Teb1 in high-RAP activity reconstitution (Figure 3.3E, lanes 1-6). This is consistent with the previously noted lack of correlation between Teb1 DNA binding affinity and processivity stimulation, an artifact attributed to the excess recombinant Teb1 required to recapitulate high RAP (Min & Collins, 2010). In contrast, full-length Teb1 with a Teb1C F603A or K660A substitution had reduced stimulation of high-RAP DNA product synthesis (Figure 3.3E, lanes 7-8). Thus, as predicted by domain truncation studies (Min & Collins, 2010), Teb1 biochemical roles in DNA binding and telomerase catalytic activation can be separated in full-length protein context.

Distinct surfaces of Teb1C contribute to Teb1BC DNA binding and telomerase catalytic activation

Structural analysis of Teb1C revealed surface features divergent from a canonical OB-fold DNA binding domain (Zeng et al., 2011). Despite distinct structure and lack of high affinity DNA binding, Teb1C could contact ssDNA to guide its threading from the telomerase active site to Teb1AB in the elongating high-RAP holoenzyme conformation. In addition, with or without a role in DNA contact, Teb1C interaction with p50-assembled RNP catalytic core stimulates the rate of high-RAP product synthesis (Hong et al., 2013). Teb1C amino acid substitution can compromise Teb1BC telomerase activation without impact on DNA interaction, and Teb1C alone can stimulate some high-RAP activity despite undetectable DNA binding (Min & Collins, 2010). Thus, we sought to additionally resolve the biochemical activities of Teb1C in order to discern how its properties affect telomerase-telomere interaction. To this end we screened substitutions of bulky side chain residues on the Teb1C surface, informed by the high-resolution Teb1C structure (Zeng et al., 2011) and known determinants of Rpa1 protein-protein and protein-DNA interactions (Bochkareva, Belegu, Korolev, & Bochkarev, 2001; Bochkareva, Korolev, Lees-Miller, & Bochkarev, 2002; Lao, Lee, & Wold, 1999). Based on previous studies (Min & Collins, 2010), we assayed for potential changes in Teb1C contribution to Teb1BC DNA binding affinity and telomerase catalytic activation.

Teb1C sequence changes of interest (Figure 3.4A) were assayed as purified Teb1BC proteins (Figure 3.4B) for DNA binding affinity by EMSA (Figure 3.4C and D) and for high-RAP activity stimulation by direct primer extension (Figure 3.4E). Of particular interest, alanine substitutions of residues F590 and F648 distant from the canonical OB-fold DNA binding surface (Figure 3.4A) did not affect the affinity of Teb1BC DNA binding by EMSA (Figure 3.4C and D) but entirely eliminated telomerase activation (Figure 3.4E). In comparison replacement of the entire zinc-ribbon lobe by a short linker (residues 555-581 to GSGSG) (Zeng et al., 2011) only partially inhibited telomerase activation (Figure 3.4E). A newly constructed replacement of the unstructured loop connecting OB-fold β-strands 4 and 5 (residues 660-666 to AGSSG, ΔL_{45}) on the potential DNA binding surface (Bochkareva et al., 2001) had some influence on the DNA binding affinity of Teb1BC and also partially inhibited telomerase activation (Figure 3.4C, D, and E). As previously noted (Min & Collins, 2010), deletion of the predicted Teb1 C-terminal α-helix (residues 687-701, ΔCTαH) that was disordered in the Teb1C structure (Zeng et al., 2011) but has potentially close proximity to the F590/ F648 surface (Figure 3.4A) had no discernable consequence (Figure 3.4C, D, and E). The lack of requirement for the Teb1 ΔCTαH was proposed to reflect evolutionary divergence from Rpa1 to avoid CTαH-mediated heterotrimer association with other RPA subunits (Min & Collins, 2010). Taken together, the results above suggest that instead of the CTαH, a Teb1C surface involving F590 and F648 could be the major determinant for the association of Teb1C with p50 and thus the entire holoenzyme. However, due to the compromised assembly of recombinant Teb1 with other reconstituted holoenzyme

components *in vitro* (Jiang et al., 2013), it was not possible to test this this hypothesis directly using *in vitro* reconstitution.

In vivo *expression of full-length Teb1 variants reveals structural requirements for Teb1 holoenzyme assembly*

Separation-of-function full-length Teb1 variants provided an opportunity to test the Teb1 biochemical requirements for holoenzyme assembly, catalytic activity, and telomere interaction *in vivo***.** We generated *Tetrahymena* strains expressing full-length Teb1 proteins with different defects for DNA binding and/or telomerase activation *in vitro* (Figures 3.3 and 3.4). For consistent comparison independent of the ability of the Teb1 variant to support cell viability in replacement of endogenous Teb1, we integrated expression transgenes driven by the cadmium-inducible *MTT1* promoter at the *BTU1* locus. Each Teb1 variant or wild-type Teb1 was C-terminally FZZ-tagged. We confirmed by western blot that equivalent levels of each Teb1-FZZ protein were expressed in cells starved and re-fed to initiate cell cycle progression, induced for transgene Teb1 expression and sampled at the post-feeding 4 h time point of macronuclear DNA replication (Figure 3.5A and B). Levels of induced Teb1-FZZ protein overexpression remained constant across the time course of cell cycle analysis (Figure 3.5C).

We first examined the cellular assembly of each tagged Teb1 protein as telomerase holoenzyme. Cell extracts were used to perform an established F-tag affinity purification (Min & Collins, 2009). Purified complexes associated with tagged Teb1 were assayed in parallel for telomerase activity using the direct primer extension assay and for quantification of TER by dot blot hybridization. To control for non-specific purification background, cell extract lacking a tagged protein was used in parallel (Figure 3.5D and E, lanes 1). Each of the Teb1-FZZ proteins with a single-residue substitution on the typical OB-fold domain DNA binding surface assembled telomerase holoenzyme comparably to wild-type Teb1, as judged by co-purification of TER (Figure 3.5D). The Teb1A or Teb1B domain variants also had little difference in the telomerase activity product profile compared to wild-type Teb1 (Figure 3.5D, lanes 2-5), mirroring the *in vitro* reconstitution results (Figure 3.3E). In comparison, *in vivo* assembly of Teb1C domain variants F603A and K660A revealed that these substitutions did affect assembled holoenzyme catalytic activity (Figure 3.5D, lanes 7-8). Product DNAs had a pronounced low-RAP profile as well as some of the high-RAP profile of wild-type enzyme. The Teb1 K660A holoenzyme also had reduced catalytic activity per TER relative to wild-type holoenzyme (Figure 3.5D, compare lanes 2 and 8), which would be consistent with an overall protein folding problem as well as an activity defect incurred by the K660A substitution.

A dramatic difference from wild-type was observed for Teb1-FZZ with the F590A F648A substitutions, which did not recover any associated telomerase activity or TER

(Figure 3.5E, lanes 2-3). Thus these substitutions on a Teb1C surface far from the canonical DNA binding interface abrogated full-length Teb1 holoenzyme assembly *in vivo*. Teb1-FZZ with Teb1C zinc ribbon or L_{45} loop deletion efficiently assembled telomerase holoenzyme based on the level of co-purified TER, but these holoenzymes had compromised catalytic activity (Figure 3.5E, lanes 4-5). Curiously, RAP as well as overall activity was affected for the holoenzyme with Teb1ΔL_{45}-FZZ (Figure 3.5E, lane 5), suggestive of a possible role for the L_{45} loop in clamping product DNA. Intriguingly, Teb1ΔCTαH did not support holoenzyme assembly *in vivo* (Figure 3.5E, lane 6). This finding was surprising given that deletion of the CTαH was inconsequential for robust high-RAP activity reconstitution *in vitro* (Figure 3.4E, lane 6). We suggest that the need for Teb1 CTαH function could be obviated *in vitro* by the high concentration of Teb1 required in the activity assay (see Discussion).

Teb1 DNA binding activity independent of holoenzyme association is sufficient for telomere interaction

We next used the full-length Teb1-FZZ transgene expression strains to determine the biochemical requirements for Teb1-mediated telomerase recruitment to telomeres by ChIP. Overexpressed wild-type Teb1-FZZ gave almost ~20-fold telomeric DNA signal enrichment over background binding assayed using cell extract lacking tagged protein (Figure 3.6A), which is an ~5-fold increase in the amount of telomeric ChIP signal compared to ChIP of Teb1-FZZ tagged at its endogenous locus (Figure 3.1E). From previous data, this increase in telomere association is expected given that overexpression of Teb1 results in telomere loss due to Teb1 binding in the absence of holoenzyme, eventually causing cell-cycle arrest (Min & Collins, 2009). Remarkably, even overexpessed Teb1 retained cell cycle specificity of telomere interaction, evident as the sharp peak of telomere interaction at 4 h after release from starvation (Figure 3.6A). This result highlights the tight regulation of Teb1-telomere interaction during S phase of the cell cycle and suggests that the cell cycle regulation of Teb1-telomere interaction is controlled by a mechanism autonomous to Teb1.

We compared ChIP by the transgene-expressed wild-type Teb1-FZZ and the Teb1-FZZ single-residue substitutions on the canonical OB-fold DNA binding surfaces, which for Teb1 A and B domains compromised full-length Teb1 DNA binding *in vitro* (Figure 3.3C and D). The F293A and K300A substitutions within Teb1A reduced telomere ChIP signal, whereas the F423A and Y450A substitutions in Teb1B and the F603A and K660A substitutions in Teb1C did not substantially change telomere ChIP in comparison to wild-type Teb1 (Figure 3.6A). No single-residue substitution eliminated telomere interaction by full-length Teb1-FZZ *in vivo*, consistent with the results for full-length Teb1 DNA binding *in vitro*. Nonetheless, among the single-residue Teb1 variants, the substitutions that did reduce telomere interaction were those with the greatest impact on Teb1 DNA binding affinity *in vitro*. To extend this connection, we compared ChIP by full-length Teb1-FZZ to ChIP by F-Teb1BC or F-Teb1C similarly expressed from the

MTT1 promoter of a transgene integrated at the *BTU1* locus (Jiang et al., 2013). Compared to full-length Teb1, Teb1BC showed an ~10-fold decrease in telomeric ChIP signal and Teb1C an ~20-fold decrease in telomeric ChIP signal (Figure 3.6A). We conclude that Teb1BC catalytic activation of telomerase to high-RAP product synthesis is insufficient for telomere recruitment, at least under conditions of competition with the coexpressed endogenous Teb1 required for cell viability (Jiang et al., 2013).

Finally we compared ChIP by the transgene-expressed wild-type Teb1-FZZ to that of the Teb1-FZZ proteins with Teb1C deletions or substitutions beyond the canonical OB-fold DNA binding surface. Teb1ΔL_{45} showed a decrease in telomere interaction but retained ChIP signal within ~2-fold of wild-type (Figure 3.6B). Of particular interest were the two Teb1 variants lacking any biochemically detectable holoenzyme assembly. Both the F590A F648A and ΔCTαH Teb1-FZZ proteins gave telomeric ChIP signal equaling or exceeding that of the wild-type Teb1-FZZ (Figure 3.6B). These findings imply that Teb1 can associate with telomeres directly without requirement for the other telomerase holoenzyme subunits. Overall the results above suggest the conclusion that in *Tetrahymena*, an integral subunit of a constitutively assembled telomerase holoenzyme mediates telomerase recruitment to telomeres by direct sequence-specific but cell cycle regulated association with ssDNA (Figure 3.7). These studies of *Tetrahymena* reveal a mechanism for telomerase-telomere interaction that is distinct from telomerase recruitment mechanisms proposed for yeast or mammalian cell model systems.

Discussion

This study provides mechanistic insight into how *Tetrahymena* telomerase is governed in its action at telomeres. We show that Teb1 is necessary for telomerase-telomere interaction and also sufficient for telomere interaction as a holoenzyme subunit dissociated from the RNP catalytic core. Furthermore, using mutagenesis for selective disruption of different Teb1 biochemical properties, we determined that telomere association by Teb1 depends on its high affinity of DNA binding. Together these results support a model in which telomere recruitment of telomerase occurs through direct interaction of Teb1-containing holoenzyme with DNA (Figure 3.7), rather than by telomerase interaction with a telomere-bound protein as in yeasts and mammalian cells (Abreu et al., 2010; Miyoshi et al., 2008; Moser et al., 2011; Tejera et al., 2010; Xin, Liu, Wan, Safari, Kim, Sun, et al., 2007; Yamazaki, Tarumoto, & Ishikawa, 2012). Activity assays here and in previous studies (Hong et al., 2013; Jiang et al., 2013; Min & Collins, 2009; Witkin & Collins, 2004; Witkin et al., 2007) suggest that a *Tetrahymena* telomerase holoenzyme is largely assembled off the telomere, although dynamic exchange of Teb1 and/or 7-1-4 could occur (Figure 3.7). This constitutive assembly of the holoenzyme makes sense in light of *Tetrahymena's* unique nuclear dualism and the resulting extended S-phase required for DNA synthesis. Despite cell extract evidence for apparently constitutive telomerase holoenzyme assembly, the ChIP assays of every

telomerase protein subunit across a synchronized cell cycle demonstrate conclusively that *Tetrahymena* telomerase-telomere interaction is cell cycle regulated. Therefore, after telomere elongation in S-phase is complete, telomerase holoenzyme must be excluded from telomeric DNA interaction until the next cell cycle of DNA synthesis.

We suggest that because a *Tetrahymena* telomerase holoenzyme is recruited to ssDNA, the cell cycle regulation of telomerase-telomere interaction can derive from direct DNA binding competition for the telomere 3′ overhang (Figure 3.7). *Tetrahymena* telomeres are capped by Pot1a in complex with Tpt1, Pat1, and Pat2 (Linger et al., 2011; Premkumar et al., 2014), bound to an overhang of 14-15 or 20-21 nucleotides with TGGGGT-3′OH end permutation (Jacob, Kirk, & Price, 2003; Jacob, Skopp, & Price, 2001). This length of overhang is insufficient for binding both Pot1a and Teb1 (Min & Collins, 2010). Because Pot1a depletion triggers run-away telomere elongation even in non-dividing cells (Jacob et al., 2007), telomerase exclusion from chromosome termini may depend on a low off-rate of Pot1a from bound DNA achieved in part by interactions with other telomere proteins (Linger et al., 2011; Wang et al., 2007). Alternately Teb1 binding to telomeres could be competed by RPA, with subsequent RPA replacement by Pot1a complexes. After Pot1a binding, genome replication or potentially C-strand resection would then be required to displace Pot1a and allow telomerase recruitment (Figure 3.7). However, simple binding competition predicts that the extended ssDNA length of telomeres elongated by telomerase would be a highly favorable substrate for additional elongation, which is not consistent with telomere length homeostasis. Thus we suggest that new repeat synthesis by telomerase is coupled to C-strand synthesis in a Teb1-dependent manner that is disadvantageous to another Teb1 engagement of the same telomere (Figure 3.7). Telomerase synthesis-dependent recruitment of its own displacement factors provides a compelling model for function of an Rpa1-like domain architecture in Teb1, because Rpa1 recruits second-strand synthesis activity by conformational change induced upon DNA binding (Fan & Pavletich, 2012).

The DNA interaction affinity of Teb1 derives from the central Teb1 A and B domains, which combined have higher affinity for telomeric repeat sequence than does full-length *Tetrahymena* Rpa1 (Min & Collins, 2010). While loss of the Teb1 N and A domains results in a notable decrease in telomeric ChIP signal, comparison to the signal derived from ChIP using the Teb1A domain substitutions is difficult given the difference in the overall size of the DNA binding site. Teb1C interaction with DNA is not detectable directly by EMSA, but a contribution of Teb1C to DNA interaction would be consistent with the reduced telomerase RAP and telomere interaction imposed by the Teb1C ΔL_{45} substitution. In crystallography studies the predicted Teb1C terminal α-helix peptide was not ordered in position relative to the Teb1C OB-fold. However, based on the position of the C-terminal residue of the OB fold, the peptide extension could be near the F590/F648 protein face away from the canonical DNA binding cleft (Figure 3.4A). The importance of F590 and F648 for Teb1 assembly with the p50 RNP catalytic core is

supported by both *in vitro* and *in vivo* telomerase reconstitutions, whereas the significance of the α-helix at the C-terminus was evident only with *in vivo* reconstitution. This terminal α-helix could interact with as-yet unidentified Rpa2 and Rpa3 homologs that chaperone telomerase holoenzyme assembly *in vivo*. Or, a more likely explanation lies in the failure of recombinant versus endogenous Teb1 to support high-affinity p50 interaction, compensated by the use of a high concentration of Teb1 in the reconstituted enzyme activity assays. The biochemical challenge to *in vitro* folding of a physiological *Tetrahymena* Teb1-p50-RNP catalytic core holoenzyme conformation is paralleled by the inefficient reconstitution of purified human TPP1 with recombinant human telomerase RNP *in vitro* (Sexton et al., 2012). Studies of *Tetrahymena* telomerase holoenzyme conformational change upon ssDNA binding, elongation, and termination (Figure 3.7) will provide informative comparison for general insights about telomerase mechanism and regulation at telomeres.

Acknowledgements

Funding for this work was provided by an NSF Graduate Research Fellowship under grant DGE-11064400 to H.U. and NIH R01 GM54198 to K.C. Molecular graphics and analyses were performed with the UCSF Chimera package. Chimera is developed by the Resource for Biocomputing, Visualization, and Informatics at the University of California, San Francisco (supported by NIGMS P41-GM103311).

Figure 3.1

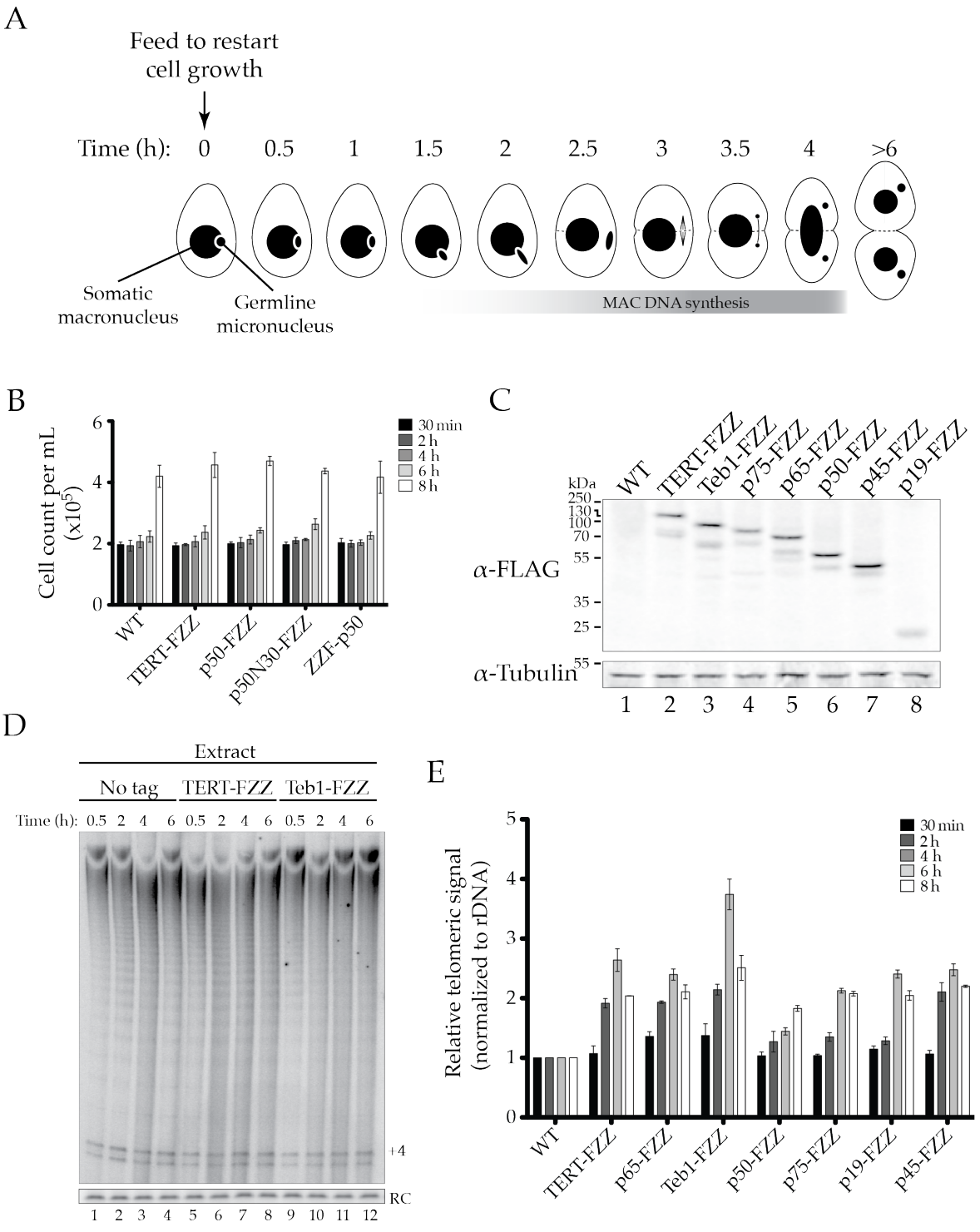

***Tetrahymena* telomerase holoenzyme components have cell cycle regulated telomere association.** (A) Vegetative growth of *Tetrahymena* schematized to highlight nuclear events starting from starvation-synchronized G_1 to the formation of daughter cells. The

Figure 3.1 (cont.)

diploid micronucleus (containing 20 telomeres) duplicates and divides by mitosis, following which the somatic macronucleus (containing ~30,000 telomeres) replicates and is partitioned by amitotic fission. (B) Cell counts performed after release from starvation to monitor cell division synchronization. A representative cell count is shown from growth of the parental CU522 strain without tagged protein and strains expressing TERT-FZZ, p50-FZZ, p50N30-FZZ, and ZZF-p50 counted in triplicate as independent cultures. Cell cultures for the other expression strains were counted similarly with no difference from the parental strain. (C) Western blot of cell extracts from strains with each holoenzyme component tagged at its endogenous locus by C-terminal fusion to FZZ. (D) Representative activity assays of extracts from wild-type and tagged-subunit strains following release from synchronization. (E) ChIP of each FZZ-tagged telomerase protein expressed from its endogenous locus following release from synchronization. Error bars correspond to the standard error of the mean from multiple independent experiments.

Figure 3.2

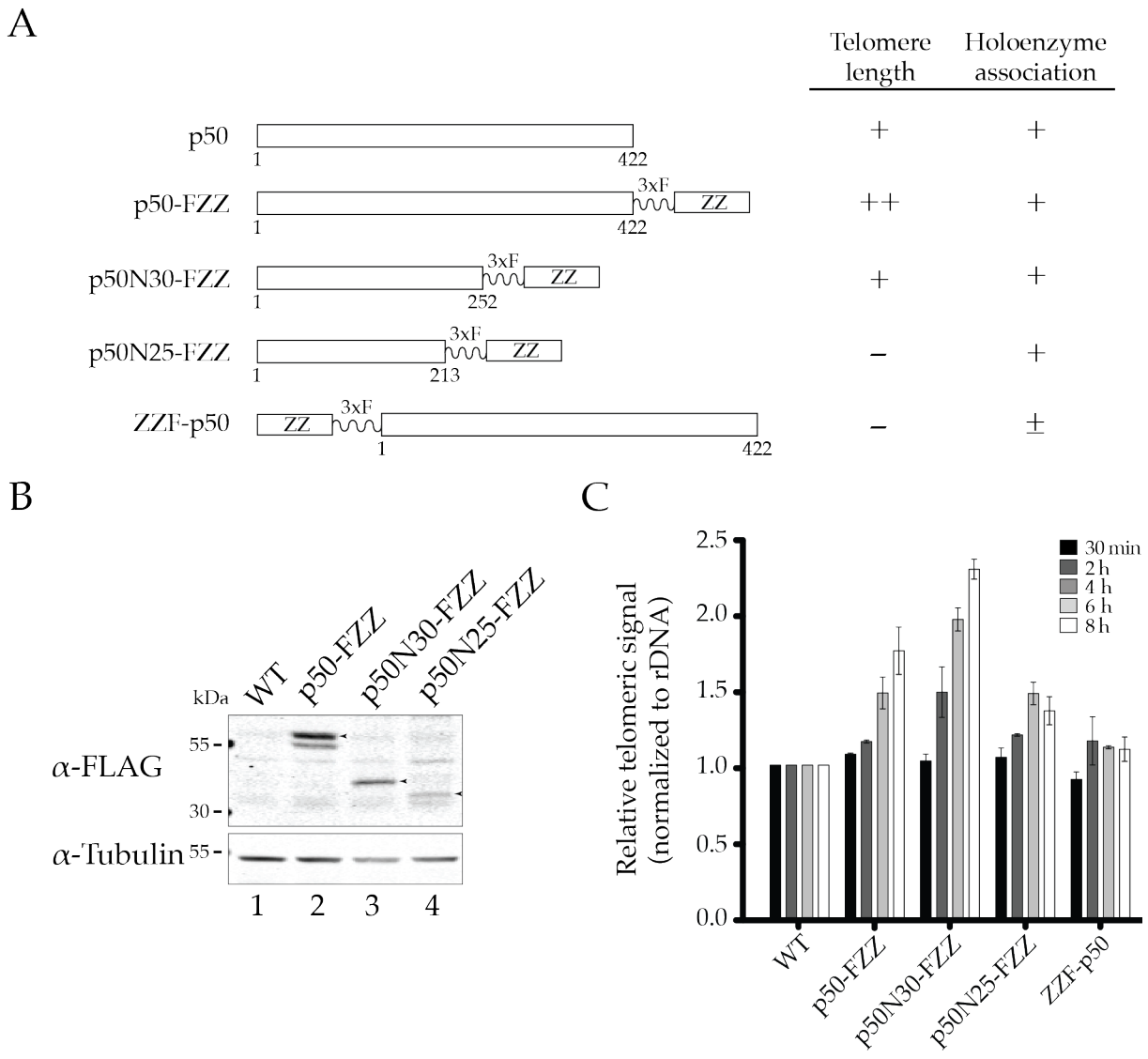

Sites of p50 tagging and truncation influence holoenzyme assembly and telomere association. (A) Schematic representation of the tagged p50 proteins used in this study with a summary of their relative function for telomere maintenance and holoenzyme association *in vivo* (Hong et al., 2013; Min & Collins, 2009). (B) Western blot of tagged p50 proteins in cell extract. The positions of the p50 proteins are indicated by the arrowhead to the right of the lane. Minor bands at ~60 kDa, ~50 kDa, and ~35 kDa are co-purifying contaminants as seen in lane 1; secondary band at ~50 kDa appearing in lane 2 is a proteolysis product of p50. (C) ChIP performed for p50 proteins as described in the legend of Figure 3.1.

Figure 3.3

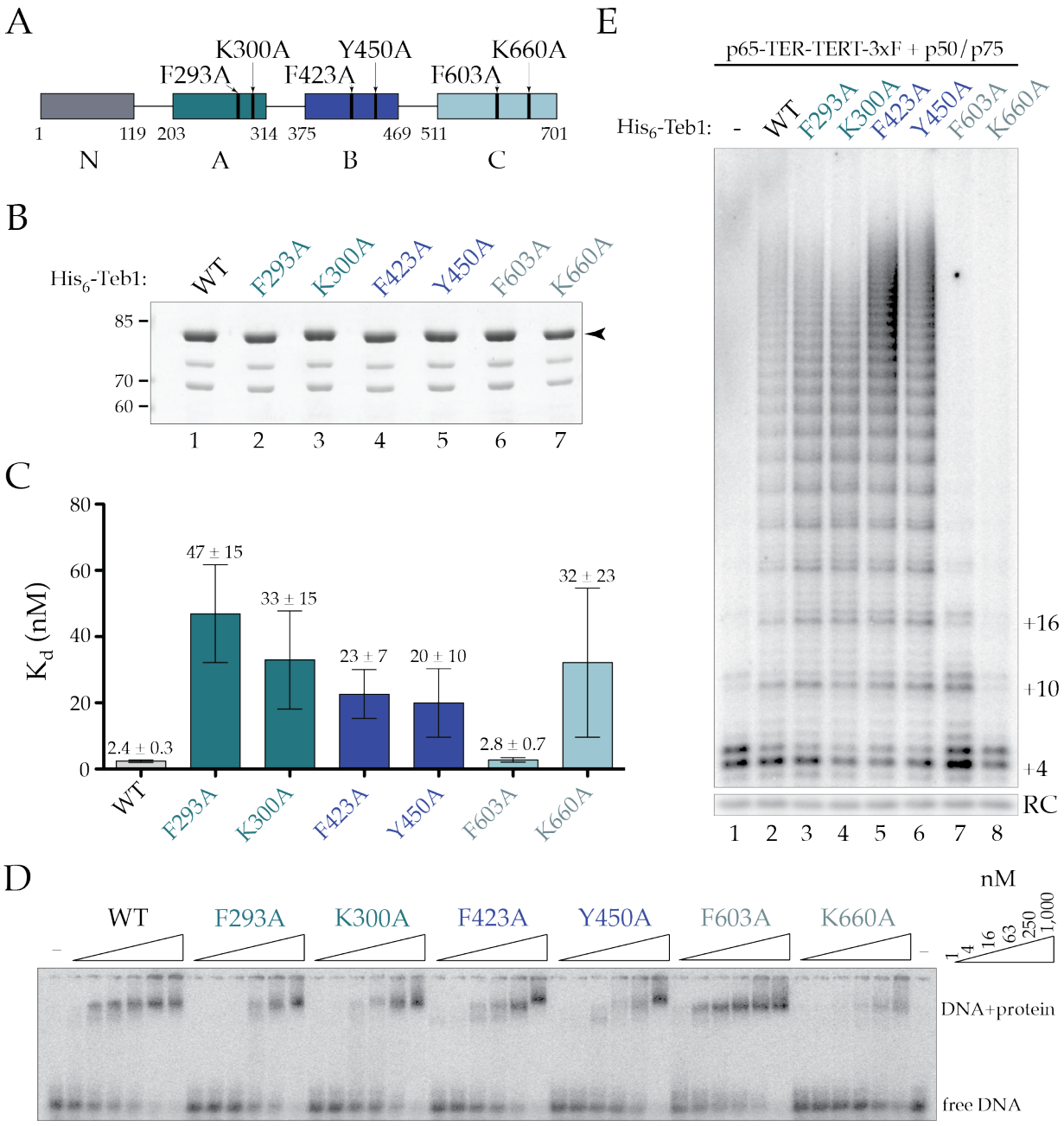

Substitutions of canonical DNA binding surfaces of the A, B, and C domains of full-length Teb1 alter DNA binding or telomerase activity *in vitro*. (A) Schematic of full-length Teb1single-residue substitutions used in this study. (B) SDS-PAGE of bacterially expressed and purified His_6-Teb1 proteins. The arrow to the right of the gel indicates full-length Teb1; minor amounts of ~75 and ~65 kDa protein are a co-purifying contaminant and Teb1 truncated by proteolysis of the linker between Teb1 B and C domains, respectively. (C,D) Calculated K_d for each of the Teb1 proteins as determined

Figure 3.3 (cont.)

by EMSA in triplicate (C), with a representative EMSA shown in (D). (E) Activity assay of recombinant full-length Teb1 reconstitution of holoenzyme catalytic activity.

Figure 3.4

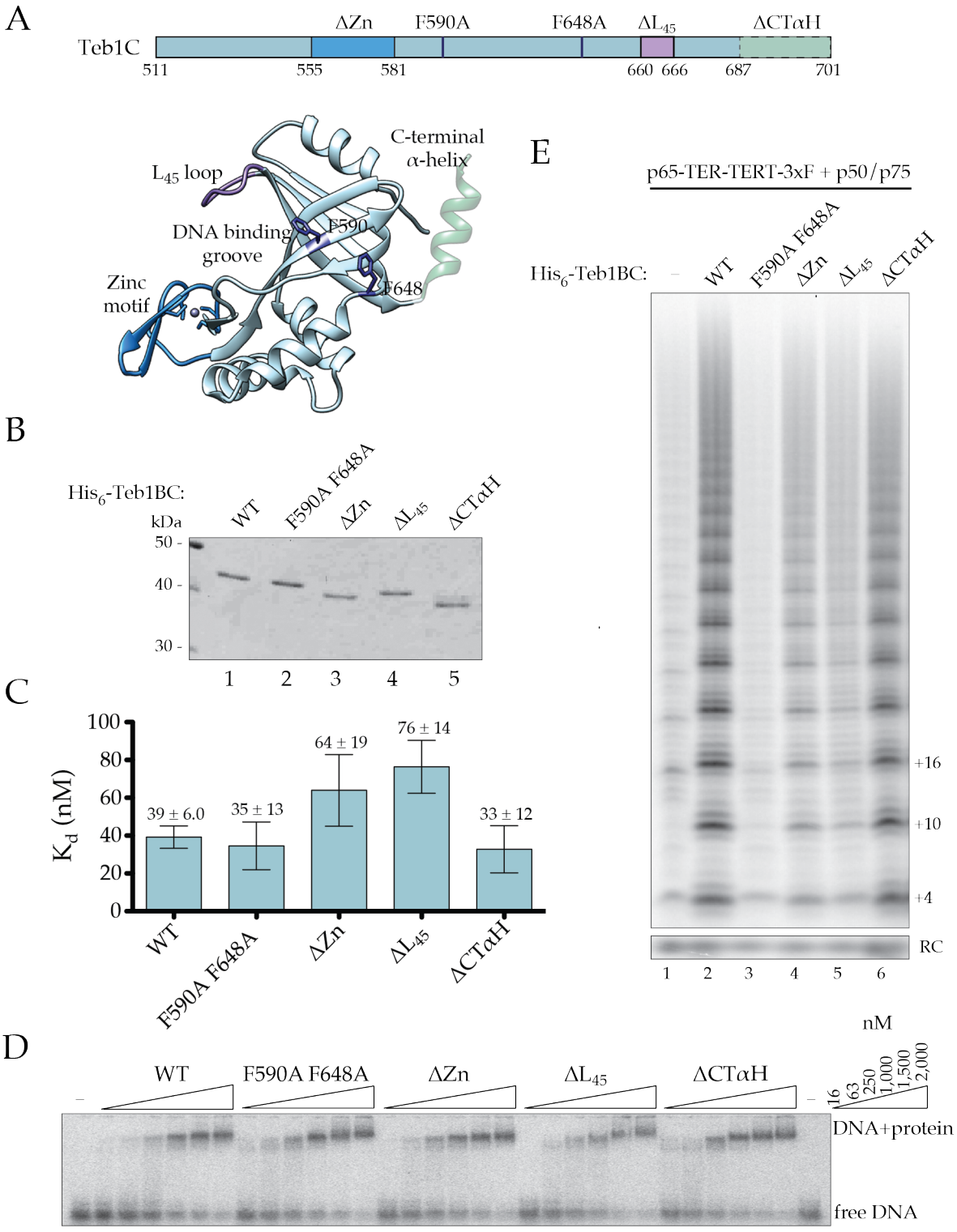

Teb1C requirements for DNA binding and telomerase activation involve distinct domain surfaces. (A) Schematic of Teb1C variants used in this study. The L_{45} loop and

Figure 3.4 (cont.)

α-helix at the C-terminus were added to the crystal structure (Zeng et al., 2011) by modeling using Chimera (Pettersen et al., 2004). (B) SDS-PAGE of bacterially expressed and purified His_6-Teb1BC proteins. (C,D) Calculated K_d for each of the Teb1BC proteins as determined by EMSA in triplicate (C), with a representative EMSA shown in (D). (E) Activity assay of recombinant Teb1BC reconstitution of holoenzyme catalytic activity.

Figure 3.5

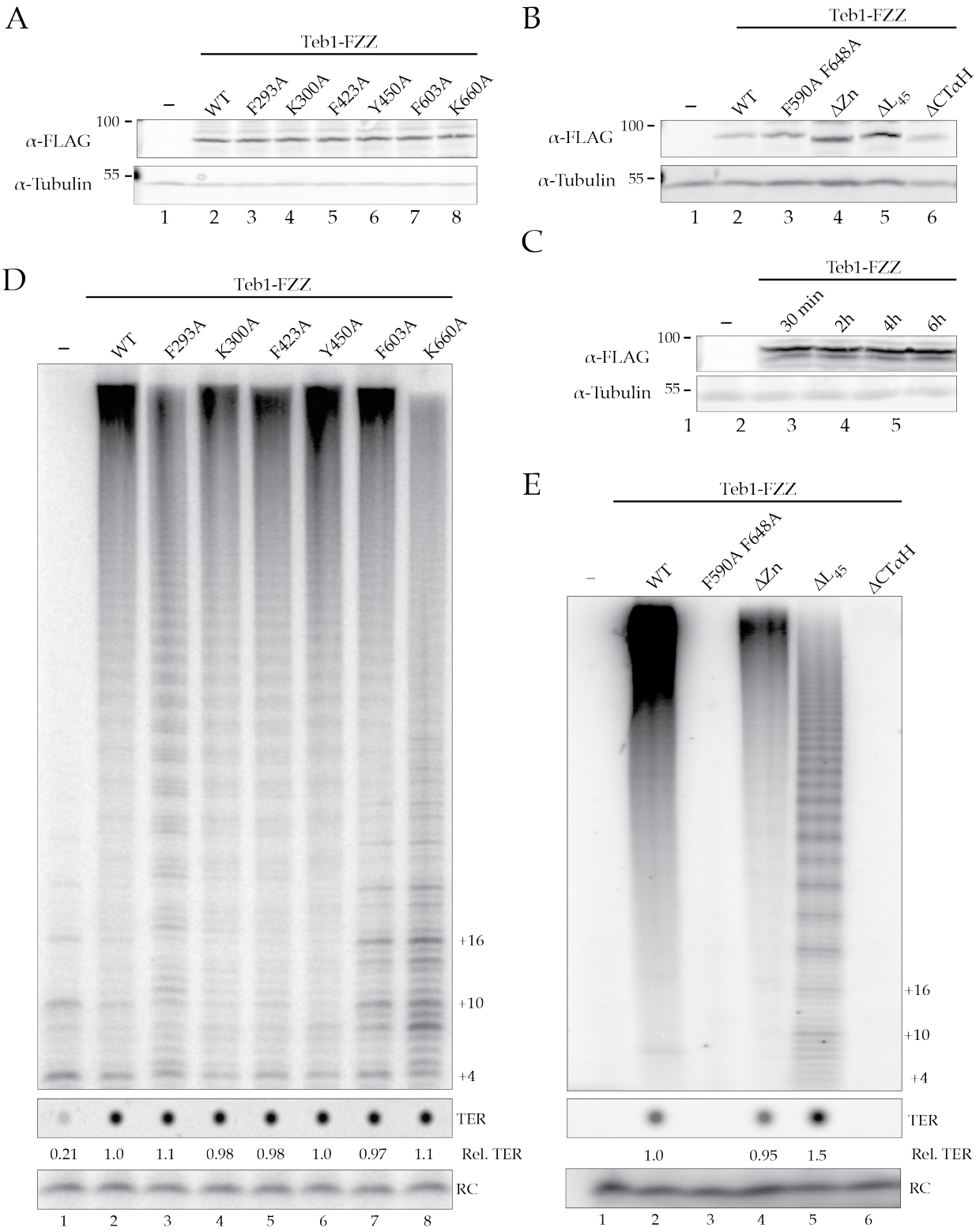
A
Teb1-FZZ
–
WT
F293A
K300A
F423A
Y450A
F603A
K660A
100
α-FLAG
55
α-Tubulin
1 2 3 4 5 6 7 8
B
Teb1-FZZ
–
WT
F590A F648A
ΔZn
ΔL45
ΔCTdH
100
α-FLAG
55
α-Tubulin
1 2 3 4 5 6
C
Teb1-FZZ
–
30 min
2h
4h
6h
100
α-FLAG
55
α-Tubulin
1 2 3 4 5
D
Teb1-FZZ
–
WT
F293A
K300A
F423A
Y450A
F603A
K660A
+16
+10
+4
TER
0.21 1.0 1.1 0.98 0.98 1.0 0.97 1.1
Rel. TER
RC
1 2 3 4 5 6 7 8
E
Teb1-FZZ
–
WT
F590A F648A
ΔZn
ΔL45
ΔCTdH
+16
+10
+4
TER
1.0 0.95 1.5
Rel. TER
RC
1 2 3 4 5 6

Figure 3.5 (cont.)

Inducible expression and holoenzyme assembly of FZZ-tagged Teb1 variants reveal requirements for Teb1 holoenzyme assembly. (A,B) Western blots of cell extracts from full-length Teb1-FZZ transgene expression strains with single-residue substitutions of the A, B, or C domain (A) or other Teb1C domain substitutions or deletions (B). (C) Western blot of representative Teb1-FZZ expression across the time course of cell cycle analysis. (D,E) Telomerase activity assay following FLAG antibody purification of Teb1-FZZ complexes from cell extracts.

Figure 3.6

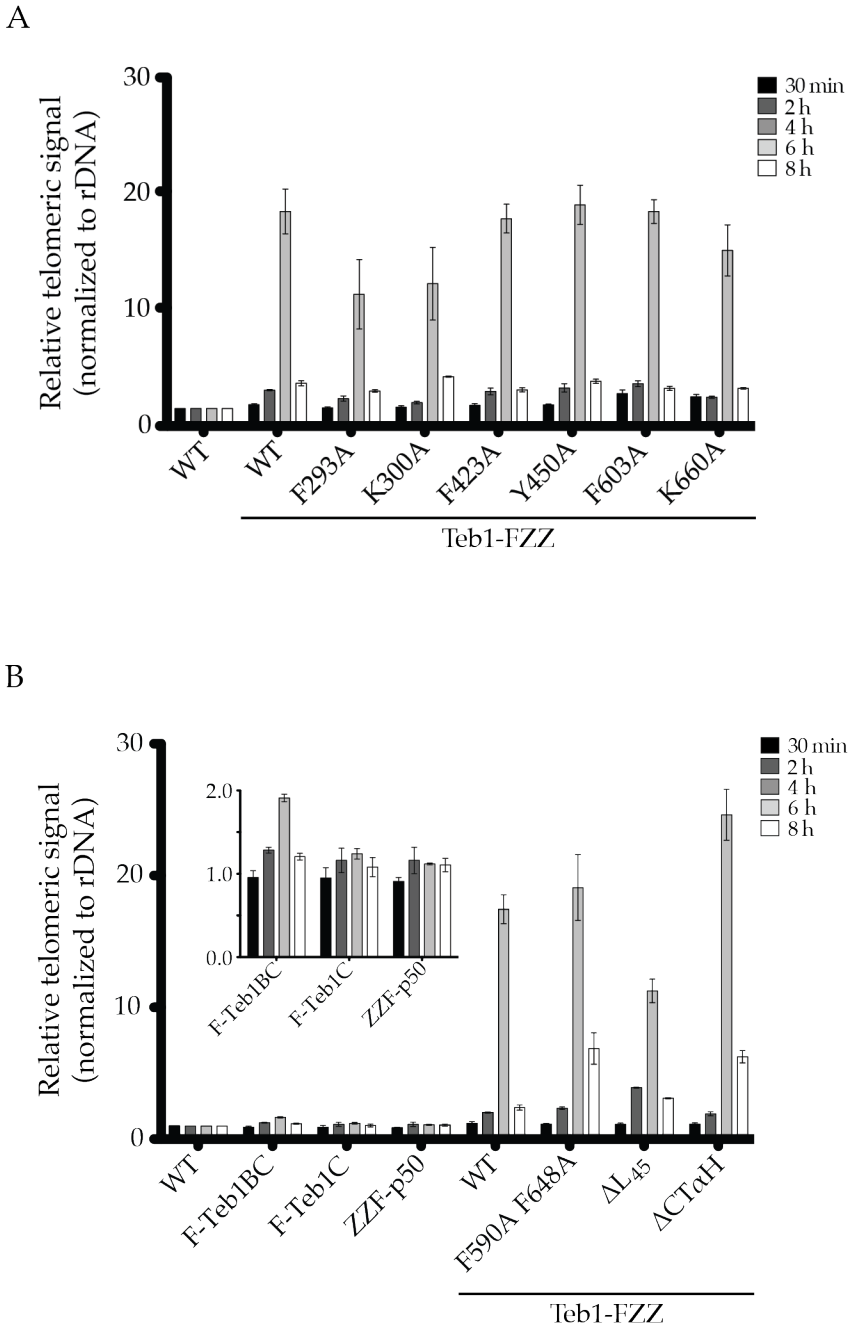

DNA binding mediates Teb1-telomere interaction. ChIP was performed as described in the legend of Figure 3.1 for the Teb1 transgene expression strains containing (A) single residue amino acid substitutions in the A, B, or C domains or (B) domain deletions and C domain substitutions and variants. Inset shows ChIP signal for Teb1BC-FZZ, TEB1C-FZZ, and FZZ-p50.

Figure 3.7

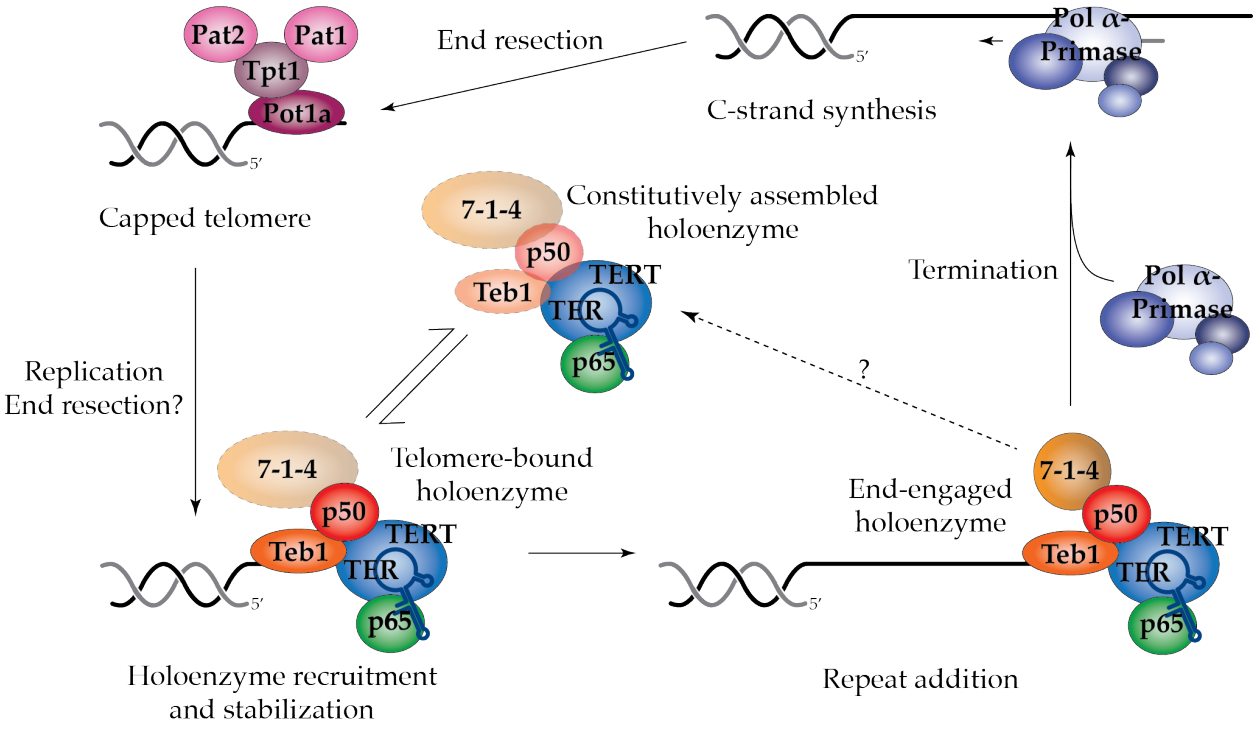

A working model of *Tetrahymena* telomerase recruitment to and regulation at telomeres. During G1 telomeres are capped by the four-protein complex consisting of Pot1a, Tpt1, Pat1, and Pat2. S phase marks the start of DNA replication and synthesis, which initiates a series of events to orchestrate a handoff between Pot1a and Teb1. After holoenzyme recruitment to the telomeres, telomerase engages in productive repeat addition. Termination of this step may be coupled to disassembly and/or displacement by Polα-primase to extend the C-strand and favor re-establishment of the *Tetrahymena* telomere protein complex.

CHAPTER FOUR

Concluding Remarks

Throughout the eukaryotic cell cycle, telomere proteins and telomerase complexes are an integral part of protecting the chromosome terminus. Assemblages characterized to date range from two-component protein-nucleic acid and protein-protein complexes to much larger multi-component, macromolecular complexes. The high-resolution structures and biochemical characterizations for these complexes has provided insight into strategies for the treatment of telomeropathies such as dyskaratosis congenita and idiopathic pulmonary fibrosis. However, obtaining such information has been limited in part because telomerase and many telomerase- and telomere-associated proteins are 'poorly behaved' biochemically, act in concert with a multitude of other proteins, and often are found at low cellular levels or are subject to cell cycle regulation.

Inherent properties of the *T. thermophila* holoenzyme have enabled detailed structural, functional, and genetic studies of recombinantly or physiologically assembled telomerase to answer several of the outstanding questions in the field of telomerase biology. By taking advantage of these properties and several fruitful collaborations, I have made immense strides in our understanding of telomerase mechanism and holoenzyme function. In Chapter 2, I dissect the importance of p50 to holoenzyme assembly and function, highlighting its vital role as an interaction hub for three separate ternary complexes (TERT-TER-p65 [the catalytic core], Teb1-Teb2-Teb3 [TEB], and p75-p45-p19 [CST]). In Chapter 3, I use a variety of *in vivo* and *in vitro* assays to show that Teb1 directly recruits *Tetrahymena* telomerase to the telomere. This is in stark contrast to all other model organisms where telomere bound proteins indirectly recruit telomerase to the end of the chromosome (see Figure 1.3). The findings here and in ongoing research demonstrate that the seemingly ciliate-specific proteins of the telomerase holoenzyme are in fact highly specialized homologs of telomerase- and telomere-associated proteins found in yeast, plant, and human systems.

Efforts by our longstanding collaborators the Feigon and Zhou Labs have resulted in vast improvements in resolution of the holoenzyme EM map, giving us new insight into the near universality of *Tetrahymena* telomerase holoenzyme protein components. The most recent holoenzyme structure revealed density for p50 that clearly resembles an OB-fold β-barrel interacting with the TEN domain of TERT (Jiang et al., 2015). Structure informed mutations at the p50-TEN interface disrupt p50 binding and abrogate the increased stability of product interaction typically conferred by p50 to the catalytic core. This is similar to our current understanding of TPP1-TERT TEN domain interaction and lends weight to the proposal that p50 and TPP1 are in fact structural and functional orthologs (Wang et al., 2007). Furthermore, density ascribed to the *Tetrahymena* TERT IFD hints at an interaction between this domain, p50, and the TEN domain. We know

from studies of human telomerase that the IFD may be involved in telomerase-telomere recruitment through TPP1, which lends weight to this predicted TEN-IFD-p50 network (Chu, D'Souza, & Autexier, 2015; Jiang et al., 2015). Future studies directed at identifying key residues along these interfaces would prove invaluable when examining telomerase regulation and recruitment in human cells.

Addition of TEB to the p50-RNP *in vitro* dramatically stimulates the product synthesis rate (Hong et al., 2013). Arguably, this same stimulation can be seen in the effect of the human POT1-TPP1 shelterin complex on telomerase activity albeit to a lesser extent (Wang et al., 2007). Extensive research has identified a TPP1-POT1-like complex at the telomere in *Tetrahymena* (Tpt1-Pot1a) in addition to the p50-Teb1 interaction of the holoenzyme (Linger, Morin, & Price, 2011; Premkumar et al., 2014). Given the distinct roles that Tpt1-Pot1a and p50-Teb1 play during the cell cycle in telomere protection and telomerase activation, respectively, it is possible that *Tetrahymena* evolved two unique complexes to take the place of vertebrate TPP1-POT1. This evolved separation of function allowed Teb1 to become a holoenzyme protein specialized for high affinity telomeric single stranded DNA binding and telomerase-telomere recruitment (discussed in Chapter 3).

Until recently, no biological function, predicted domains, or eukaryotic homologs had been identified within the genetically essential p75-p45-p19 subcomplex in the *Tetrahymena* telomerase holoenzyme. Biochemically, I determined that p75 stimulates catalytic activity of the p50-assembled RNP with no apparent role for p45 or p19 (discussed in Chapter 2). The high-resolution EM map and crystal structures of the p45N-p19 dimer revealed structural similarities to the Ctc1/Cdc13-Stn1-Ten1 (CST) complex in budding yeast (Hong et al., 2013; Jiang et al., 2015; Wan et al., 2015). Disruption of the p45-p19 interface *in vivo* resulted in longer than wild-type G-strand telomeres and shorter than wild-type C-strand telomeres providing functional evidence that the *Tetrahymena* telomerase p75-p45-p19 subcomplex is a species-specific CST (Wan et al., 2015). In humans, CST is known to interact with TPP1-POT1 during S phase of the cell cycle and was suggested to inhibit telomerase activity through this interaction and telomere G-strand binding (Chen, Redon, & Lingner, 2012). Once bound to single-stranded DNA, CST is responsible for recruiting DNA polymerase α-primase thereby coordinating G-strand and C-strand synthesis. While only future experiments will highlight this dynamic, our current hypothesis is that *Tetrahymena* CST will maintain a similar biological role despite its presence in the holoenzyme.

REFERENCES

Abreu, E., Aritonovska, E., Reichenbach, P., Cristofari, G., Culp, B., Terns, R. M., . . . Terns, M. P. (2010). TIN2-tethered TPP1 recruits human telomerase to telomeres *in vivo*. *Molecular and Cellular Biology , 30*, 2971-2982.

Armanios, M., & Blackburn, E. H. (2012). The telomere syndromes. *Nature Reviews Genetics, 13*(10), 693-704. doi: 10.1038/nrg3246

Baumann, P., & Cech, T. R. (2001). Pot1, the putative telomere end-binding protein in fission yeast and humans. *Science, 292*, 1171-1175.

Blackburn, E. H., & Collins, K. (2011). Telomerase: an RNP enzyme synthesizes DNA. *Cold Spring Harbor Perspectives in Biology, 3*(5), 205-213.

Blackburn, E. H., & Gall, J. G. (1978). A tandemly repeated sequence at the termini of the extrachromosomal ribosomal RNA genes in *Tetrahymena*. *Journal of Molecular Biology, 120*, 33-53.

Blackburn, E. H., Greider, C. W., & Szostak, J. W. (2006). Telomeres and telomerase: the path from maize, *Tetrahymena* and yeast to human cancer and aging. *Nature Medicine, 12*, 1133-1138.

Bley, C. J., Qi, X., Rand, D. P., Borges, C. R., Nelson, R. W., & Chen, J. J.-L. (2011). RNA-protein binding interface in the telomerase ribonucleoprotein. *Proceedings of the National Academy of Sciences USA, 108*(51), 20333-20338. doi: 10.1073/pnas.1100270108

Bochkareva, E., Belegu, V., Korolev, S., & Bochkarev, A. (2001). Structure of the major single-stranded DNA-binding domain of replication protein A suggests a dynamic mechanism for DNA binding. *EMBO Journal, 20*, 612-618.

Bochkareva, E., Korolev, S., Lees-Miller, S. P., & Bochkarev, A. (2002). Structure of the RPA trimerization core and its role in the multistep DNA-binding mechanism of RPA. *EMBO Journal, 21*(7), 1855-1863. doi: 10.1093/emboj/21.7.1855

Brown, A. F., Podlevsky, J. D., & Chen, J. J.-L. (2014). Telomerase: A eukaryotic DNA polymerase specialized in telomeric repeat synthesis. *Nucleic Acid Polymerases* (Vol. 30, pp. 215-235). Verlag Berlin Heidelberg: Springer.

Cavalier-Smith, T. (1974). Palindromic Base Sequences and Replication of Eukaryotic Chromosome Ends. *Nature, 250*, 467-470.

Chakhparonian, M., & Wellinger, R. J. (2003). Telomere maintenance and DNA replication: how closely are these two connected? *Trends in Genetics, 19*(8), 439-446.

Chalker, D. L. (2012). Transformation and strain engineering of *Tetrahymena*. *Methods in Cell Biology, 109*, 327-345. doi: 10.1016/B978-0-12-385967-9.00011-6

Chen, L. Y., Redon, S., & Lingner, J. (2012). The human CST complex is a terminator of telomerase activity. *Nature, 488*, 540-544.

Chu, T. W., D'Souza, Y., & Autexier, C. (2015). The human telomerase 'Insertion in Fingers Domain' can mediate enzyme processivity and telomerase recruitment to telomeres in a TPP1-dependent manner. *Molecular and Cellular Biology, 36*(1), 210-222. doi: 10.1128/MCB.00746-15

Collins, K. (2011). Single-stranded DNA repeat synthesis by telomerase. *Current Opinion in Chemical Biology, 15*(5), 643-648.

Collins, K. (2012). *Tetrahymena thermophila* (Vol. 109): Elsevier Inc.

Couvillion, M. T., & Collins, K. (2012). Biochemical approaches including the design and use of strains expressing epitope-tagged proteins. *Methods in Cell Biology, 109*, 347-355. doi: 10.1016/B978-0-12-385967-9.00012-8

de Lange, T. (2009). How telomeres solve the end-protection problem. *Science, 326*, 948-952.

Egan, E. D., & Collins, K. (2010). Specificity and stoichiometry of subunit interactions in the human telomerase holoenzyme assembled *in vivo*. *Molecular and Cellular Biology, 30*, 2775-2786

Egan, E. D., & Collins, K. (2012). Biogenesis of telomerase ribonucleoproteins. *RNA, 18*, 1747-1759.

Fan, J., & Pavletich, N. P. (2012). Structure and conformational change of a replication protein A heterotrimer bound to ssDNA. *Genes and Development, 26*(20), 2337-2347.

Fu, D., & Collins, K. (2003). Distinct biogenesis pathways for human telomerase RNA and H/ACA small nucleolar RNAs. *Molecular Cell, 11*(5), 1361-1372.

Gillis, A. J., Schuller, A. P., & Skordalakes, E. (2008). Structure of the *Tribolium castaneum* telomerase catalytic subunit TERT. *Nature, 455*(7213), 633-637. doi: 10.1038/nature07283

Gilson, E., & Geli, V. (2007). How telomeres are replicated. *Nature Reviews Molecular Cell Biology, 8*, 825-838.

Greider, C. W. (1991). Telomerase is processive. *Molecular and Cellular Biology, 11*, 4572-4580.

Greider, C. W. (1996). Telomere length regulation. *Annual Review of Biochemistry, 66*, 337-365.

Greider, C. W., & Blackburn, E. H. (1985). Identification of a specific telomere terminal transferase activity in *Tetrahymena* extracts. *Cell, 43*, 405-413.

Greider, C. W., & Blackburn, E. H. (1987). The telomere terminal transferase of *Tetrahymena* is a ribonucleoprotein enzyme with two kinds of primer specificity. *Cell, 51*, 887-898.

Greider, C. W., & Blackburn, E. H. (1989). A telomeric sequence in the RNA of *Tetrahymena* telomerase required for telomere repeat synthesis. *Nature, 337*, 331-337.

Hardy, C. D., Schultz, C. S., & Collins, K. (2001). Requirements for the dGTP-dependent repeat addition processivity of recombinant *Tetrahymena* telomerase. *The Journal of Biological Chemistry, 276*, 4863-4871.

Hengesbach, M., Akiyama, B. M., & Stone, M. D. (2011). Single-molecule analysis of telomerase structure and function. *Current Opinion in Chemical Biology, 15*(6), 845-852. doi: 10.1016/j.cbpa.2011.10.008

Holohan, B., Wright, W. E., & Shay, J. W. (2014). Telomeropathies: An emerging spectrum disorder. *The Journal of Cell Biology, 205*(3), 289-299. doi: 10.1083/jcb.201401012

Hong, K., Upton, H., Miracco, E. J., Jiang, J., Zhou, Z. H., Feigon, J., & Collins, K. (2013). *Tetrahymena* telomerase holoenzyme assembly, activation, and inhibition by domains of the p50 central hub. *Molecular and Cellular Biology, 33*(19), 3962-3971. doi: 10.1128/MCB.00792-13

Hossain, S., Singh, S., & Lue, N. F. (2002). Functional analysis of the C-terminal extension of telomerase reverse transcriptase. *The Journal of Biological Chemistry, 277*, 36174-36180.

Huard, S., Moriarty, T. J., & Autexier, C. (2003). The C terminus of the human telomerase reverse transcriptase is a determinant of enzyme processivity. *Nucleic Acids Research, 31*(14), 4059-4070. doi: 10.1093/nar/gkg437

Jacob, N. K., Kirk, K. E., & Price, C. M. (2003). Generation of telomeric G strand overhangs involves both G and C strand cleavage. *Molecular Cell, 11*(4), 1021-1032.

Jacob, N. K., Lescasse, R., Linger, B. R., & Price, C. M. (2007). *Tetrahymena* POT1a regulates telomere length and prevents activation of a cell cycle checkpoint. *Molecular and Cellular Biology, 27*, 1592-1601.

Jacob, N. K., Skopp, R., & Price, C. M. (2001). G-overhang dynamics at *Tetrahymena* telomeres. *EMBO Journal, 20*, 4299-4308.

Jacob, N. K., Stout, A. R., & Price, C. M. (2004). Modulation of telomere length dynamics by the subtelomeric region of *Tetrahymena* telomeres. *Molecular Biology of the Cell, 15*(8), 3719-3728.

Jahn, C. L., & Klobutcher, L. A. (2002). Genome remodeling in ciliated protozoa. *Annual Review of Microbiology, 56*, 489-520.

Jiang, J., Chan, H., Cash, D. D., Miracco, E. J., Ogorzalek Loo, R. R., Upton, H. E., . . . Feigon, J. (2015). Structure of *Tetrahymena* telomerase reveals previously unknown subunits, functions, and interactions. *Science, 350*(6260), 529-539.

Jiang, J., Miracco, E. J., Hong, K., Eckert, B., Chan, H., Cash, D. D., . . . Feigon, J. (2013). The architecture of *Tetrahymena* telomerase holoenzyme. *Nature, 496*(7444), 187-192. doi: 10.1038/nature12062

Kiss, T., Fayet-Lebaron, E., & Jady, B. E. (2010). Box H/ACA small ribonucleoproteins. *Molecular Cell, 37*(5), 597-606. doi: 10.1016/j.molcel.2010.01.032

Lao, Y., Lee, C. G., & Wold, M. S. (1999). Replication protein A interactions with DNA. 2. Characterization of double-stranded DNA-binding/helix-destabilization activities and the role of the zinc-finger domain in DNA interactions. *Biochemistry, 38*, 3974-3984.

Levy, M. Z., Allsopp, R. C., Futcher, A. B., Greider, C. W., & Harley, C. B. (1992). Telomere end-replication problem and cell aging. *Journal of Molecular Biology, 225*, 951-960.

Linger, B. R., Morin, G. B., & Price, C. M. (2011). The Pot1a-associated proteins Tpt1 and Pat1 coordinate telomere protection and length regulation in *Tetrahymena*. *Molecular Biology of the Cell, 22*(21), 4161-4170. doi: 10.1091/mbc.E11-06-0551

Linger, B. R., & Price, C. M. (2009). Conservation of telomere protein complexes: shuffling through evolution. *Critical Reviews in Biochemistry and Molecular Biology, 44*, 434-446.

Lingner, J., Hughes, T. R., Shevchenko, A., Mann, M., Lundblad, V., & Cech, T. R. (1997). Reverse transcriptase motifs in the catalytic subunit of telomerase. *Science, 276*, 561-567.

Loayza, D., & De Lange, T. (2003). POT1 as a terminal transducer of TRF1 telomere length control. *Nature, 423*, 1013-1018.

Londono-Vallejo, J. A., & Wellinger, R. J. (2012). Telomeres and telomerase dance to the rhythm of the cell cycle. *Trends in Biochemical Sciences, 37*(9), 391-399. doi: 10.1016/j.tibs.2012.05.004

Lue, N. F., Lin, Y.-C., & Mian, S. (2003). A conserved telomerase motif within the catalytic domain of telomerase reverse transcriptase is specifically required for repeat addition processivity. *Molecular and Cellular Biology, 23*(23), 8440-8449. doi: 10.1128/MCB.23.23.8440-8449.2003

McClintock, B. (1931). Cytological observations of deficiencies involving known genes, translocations and an inversion in *Zea mays*. *Missouri Agricultural Experiment Station Publication Research Bulletin, 163*, 1-48.

McClintock, B. (1939). The Behavior in successive nuclear divisions of a chromosome broken at meiosis. *Proceedings of the National Academy of Sciences USA, 25*, 405-416.

Miller, M. C., & Collins, K. (2000). The *Tetrahymena* p80/p95 complex is required for proper telomere length maintenance and micronuclear genome stability. *Molecular Cell, 6*(4), 827-837. doi: 10.1016/S1097-2765(05)00078-X

Miller, M. C., & Collins, K. (2000). The *Tetrahymena* p80/p95 complex is required for proper telomere length maintenance and micronuclear genome stability. *Molecular Cell, 6*, 827-837.

Min, B., & Collins, K. (2009). An RPA-related sequence-specific DNA-binding subunit of telomerase holoenzyme is required for elongation processivity and telomere maintenance. *Molecular Cell, 36*, 609-619.

Min, B., & Collins, K. (2010). Multiple mechanisms for elongation processivity within the reconstituted *Tetrahymena* telomerase holoenzyme. *The Journal of Biological Chemistry, 285*, 16434-16443.

Miyoshi, T., Kanoh, J., Saito, M., & Ishikawa, F. (2008). Fission yeast Pot1-Tpp1 protects telomeres and regulates telomere length. *Science, 320*, 1341-1344.

Moriarty, T. J., Marie-Egyptienne, D. T., & Autexier, C. (2004). Functional organization of repeat addition processivity and DNA synthesis determinants in the human telomerase multimer. *Molecular and Cellular Biology, 24*, 3720-3733.

Moser, B. A., Chang, Y. T., Kosti, J., & Nakamura, T. M. (2011). Tel1^{ATM} and Rad3^{ATR} kinases promote Ccq1-Est1 interaction to maintain telomeres in fission yeast. *Nature Structural and Molecular Biology, 18*(12), 1408-1413. doi: 10.1038/nsmb.2187

Moser, B. A., & Nakamura, T. M. (2009). Protection and replication of telomeres in fission yeast. *Biochemistry and Cell Biology, 87*(5), 747-758. doi: 10.1139/O09-037

Moyzis, R. K., Buckingham, J. M., Cram, L. S., Dani, M., Deaven, L. L., Jones, M. D., . . . Wu, J.-R. (1988). A highly conserved repetitive DNA sequence, (TTAGGG)n, present at the telomeres of human chromosomes. *Proceedings of the National Academy of Sciences USA, 85*, 6622-6626.

Müller, H. J. (1938). The remaking of chromosomes. *The Collecting Net, 13*, 181-198.

Nandakumar, J., Bell, C. F., Weidenfeld, I., Zaug, A. J., Leinwand, L. A., & Cech, T. R. (2012). The TEL patch of telomere protein TPP1 mediates telomerase recruitment and processivity. *Nature, 492*(7428), 285-289. doi: 10.1038/nature11648

Nandakumar, J., & Cech, T. R. (2013). Finding the end: recruitment of telomerase to telomeres. *Nature Reviews Molecular Cell Biology, 14*(2), 69-82. doi: 10.1038/nrm3505

O'Sullivan, R. J., & Karlseder, J. (2010). Telomeres: protecting chromosomes against genome instability. *Nature Reviews Molecular Cell Biology, 11*, 171-181.

Palm, W., & de Lange, T. (2008). How shelterin protects mammalian telomeres. *Annual Review of Genetics, 42*, 301-334.

Pettersen, E. F., Goddard, T. D., Huang, C. C., Couch, G. S., Greenblatt, D. M., Meng, E. C., & Ferrin, T. E. (2004). UCSF Chimera--a visualization system for exploratory research and analysis. *Journal of Computational Chemistry, 25*(13), 1605-1612. doi: 10.1002/jcc.20084

Pfeiffer, V., & Lingner, J. (2013). Replication of telomeres and the regulation of telomerase. *Cold Spring Harbor Perspectives in Biology.* doi: 10.1101/cshperspect.a010405

Podlevsky, J. D., & Chen, J. J. (2012). It all comes together at the ends: Telomerase structure, function, and biogenesis. *Mutation Research, 730*(1-2), 3-11. doi: 10.1016/j.mrfmmm.2011.11.002

Premkumar, V. L., Cranert, S., Linger, B. R., Morin, G. B., Minium, S., & Price, C. (2014). The 3' overhangs at *Tetrahymena thermophila* telomeres are packaged by four proteins, Pot1a, Tpt1, Pat1, and Pat2. *Eukaryotic Cell, 13*, 240-245.

Radermacher, M., Wagenknecht, T., Verschoor, A., & Frank, J. (1987). Three-dimensional reconstruction from a single-exposure, random conical tilt series applied to the 50S ribosomal subunit of *Escherichia coli*. *Journal of Advanced Microscopy Research, 146*(Pt 2), 113-136.

Robart, A. R., & Collins, K. (2011). Human telomerase domain interactions capture DNA for TEN domain-dependent processive elongation. *Molecular Cell, 42*(3), 308-318.

Sampathi, S., & Chai, W. (2011). Telomere replication: poised but puzzling. *Journal of Cellular and Molecular Medicine, 15*(1), 3-13. doi: 10.1111/j.1582-4934.2010.01220.x

Sexton, A. N., Youmans, D. T., & Collins, K. (2012). Specificity requirements for human telomere protein interaction with telomerase holoenzyme. *Journal of Biological Chemistry, 287*(41), 34455-34464. doi: 10.1074/jbc.M112.394767

Shampay, J., Szostak, J. W., & Blackburn, E. H. (1984). DNA sequences of telomeres maintained in yeast. *Nature, 310*, 154-157.

Shay, J. W., & Wright, W. E. (2011). Role of telomeres and telomerase in cancer. *Seminars in Cancer Biology, 21*(6), 349-353. doi: 10.1016/j.semcancer.2011.10.001

Singh, M., Wang, Z., Koo, B. K., Patel, A., Cascio, D., Collins, K., & Feigon, J. (2012). Structural basis for telomerase RNA recognition and RNP assembly by the holoenzyme La family protein p65. *Molecular Cell*. doi: 10.1016/j.molcel.2012.05.018

Soudet, J., Jolivet, P., & Teixeira, M. T. (2014). Elucidation of the DNA End-Replication Problem in *Saccharomyces cerevisiae*. *Molecular Cell, 53*(6), 954-964. doi: doi:10.1016/j.molcel.2014.02.030

Stewart, J. A., Chaiken, M. F., Wang, F., & Price, C. M. (2012). Maintaining the end: roles of telomere proteins in end-protection, telomere replication and length regulation. *Mutation Research, 730*, 12-19.

Szostak, J. W., & Blackburn, E. H. (1982). Cloning yeast telomeres on linear plasmid vectors. *Cell, 29*, 245-255.

Tejera, A. M., Stagno d'Alcontres, M., Thanasoula, M., Marion, R. M., Martinez, P., Liao, C., . . . Blasco, M. A. (2010). TPP1 is required for TERT recruitment, telomere elongation during nuclear reprogramming, and normal skin development in mice. *Developmental Cell, 18*(5), 775-789. doi: 10.1016/j.devcel.2010.03.011

Tomita, K., & Cooper, J. P. (2008). Fission yeast Ccq1 is telomerase recruiter and local checkpoint controller. *Genes and Development, 22*(24), 3461-3474. doi: 10.1101/gad.498608

van Steensel, B., & de Lange, T. (1997). Control of telomere length by the human telomeric protein TRF1. *Nature, 385*, 740-743.

Venteicher, A. S., Abreu, E. B., Meng, Z., McCann, K. E., Terns, R. M., Veenstra, T. D., . . . Artandi, S. E. (2009). A human telomerase holoenzyme protein required for Cajal body localization and telomere synthesis. *Science, 323*, 644-648.

Verdun, R. E., & Karlseder, J. (2007). Replication and protection of telomeres. *Nature, 447*, 924-931.

Waga, S., & Stillman, B. (1998). The DNA replication fork in eukaryotic cells. *Annual Review of Biochemistry, 67*, 721-751. doi: 10.1146/annurev.biochem.67.1.721

Wan, B., Tang, T., Upton, H. E., Shuai, J., Zhou, Y., Li, S., . . . Lei, M. (2015). The *Tetrahymena* telomerase p75–p45–p19 subcomplex is a unique CST complex. *Nature Structural and Molecular Biology, 22*, 1023–1026. doi: doi:10.1038/nsmb.3126

Wang, F., Podell, E. R., Zaug, A. J., Yang, Y., Baciu, P., Cech, T. R., & Lei, M. (2007). The POT1-TPP1 telomere complex is a telomerase processivity factor. *Nature, 445*, 506-510.

Watson, J. D. (1972). Origin of concatameric T4 DNA. *Nature New Biology, 239*, 197-201.

Witkin, K. L., & Collins, K. (2004). Holoenzyme proteins required for the physiological assembly and activity of telomerase. *Genes and Development, 18*(10), 1107-1118.

Witkin, K. L., Prathapam, R., & Collins, K. (2007). Positive and negative regulation of *Tetrahymena* telomerase holoenzyme. *Molecular and Cellular Biology, 27*(6), 2074-2083.

Wold, M. S. (1997). Replication protein A: a heterotrimeric, single-stranded DNA-binding protein required for eukaryotic DNA metabolism. *Annual Review of Biochemistry, 66*, 61-92.

Wu, P., Takai, H., & de Lange, T. (2012). Telomeric 3' overhangs derive from resection by Exo1 and Apollo and fill-in by POT1b-associated CST. *Cell, 150*(1), 39-52. doi: 10.1016/j.cell.2012.05.026

Wu, R. A., & Collins, K. (2014). Human telomerase specialization for repeat synthesis by unique handling of primer‐template duplex. *EMBO Journal, 33*(8), 921-935. doi: 10.1002/embj.201387205

Xie, M., Podlevsky, J. D., Qi, X., Bley, C. J., & Chen, J. J. (2010). A novel motif in telomerase reverse transcriptase regulates telomere repeat addition rate and processivity. *Nucleic Acids Research, 38*, 1982-1996. doi: 10.1093/nar/gkp1198

Xin, H., Liu, D., Wan, M., Safari, A., Kim, H., O'Connor, M. S., & Songyang, Z. (2007). TPP1 is a homologue of ciliate TEBP-beta and interacts with POT1 to recruit telomerase. *Nature, 445*(7127), 559-562.

Xin, H., Liu, D., Wan, M., Safari, A., Kim, H., Sun, W., . . . Songyang, Z. (2007). TPP1 is a homologue of ciliate TEBP-beta and interacts with POT1 to recruit telomerase. *Nature, 445*, 559-562.

Yamazaki, H., Tarumoto, Y., & Ishikawa, F. (2012). Tel1(ATM) and Rad3(ATR) phosphorylate the telomere protein Ccq1 to recruit telomerase and elongate telomeres in fission yeast. *Genes and Development, 26*(3), 241-246. doi: 10.1101/gad.177873.111

Ye, J. Z., Hockemeyer, D., Krutchinsky, A. N., Loayza, D., Hooper, S. M., Chait, B. T., & de Lange, T. (2004). POT1-interacting protein PIP1: a telomere length regulator that recruits POT1 to the TIN2/TRF1 complex. *Genes and Development, 18*(14), 1649-1654. doi: 10.1101/gad.1215404

Zaug, A. J., Podell, E. R., Nandakumar, J., & Cech, T. R. (2010). Functional interaction between telomere protein TPP1 and telomerase. *Genes and Development, 24*, 613-622.

Zeng, Z., Min, B., Huang, J., Hong, K., Yang, Y., Collins, K., & Lei, M. (2011). Structural basis for *Tetrahymena* telomerase processivity factor Teb1 binding to single-stranded telomeric-repeat DNA. *Proceedings of the National Academy of Sciences USA, 108*(51), 20357-20361.

Zhang, Y., Chen, L. Y., Han, X., Xie, W., Kim, H., Yang, D., . . . Songyang, Z. (2013). Phosphorylation of TPP1 regulates cell cycle-dependent telomerase recruitment. *Proceedings of the National Academy of Sciences USA, 110*(14), 5457-5462. doi: 10.1073/pnas.1217733110

Zhong, F. L., Batista, L. F., Freund, A., Pech, M. F., Venteicher, A. S., & Artandi, S. E. (2012). TPP1 OB-fold domain controls telomere maintenance by recruiting telomerase to chromosome ends. *Cell, 150*(3), 481-494. doi: 10.1016/j.cell.2012.07.012